计算光学成像与光信息处理技术前沿

（第9讲）

左 超

南京理工大学电光学院光电技术系

Jiangsu Key Laboratory of Spectral Imaging & Intelligent Sense (SIIS)
Nanjing University of Science and Technology,
Nanjing, Jiangsu Province 210094, China

南京理工大学
NANJING UNIVERSITY OF SCIENCE & TECHNOLOGY

光学前沿在线 2020
光学成像与显示
2020年6月19-20日

光学衍射层析与强度衍射层析成像

Optical diffraction tomographic imaging and intensity diffraction tomographic imaging

Chao Zuo（左超）

Smart Computational Imaging Laboratory (SCILab)
Jiangsu Key Laboratory of Spectral Imaging & Intelligent Sense (SIIS)
Nanjing University of Science and Technology,
Nanjing, Jiangsu Province 210094, China

Smart Computational Imaging

Computational microscopy

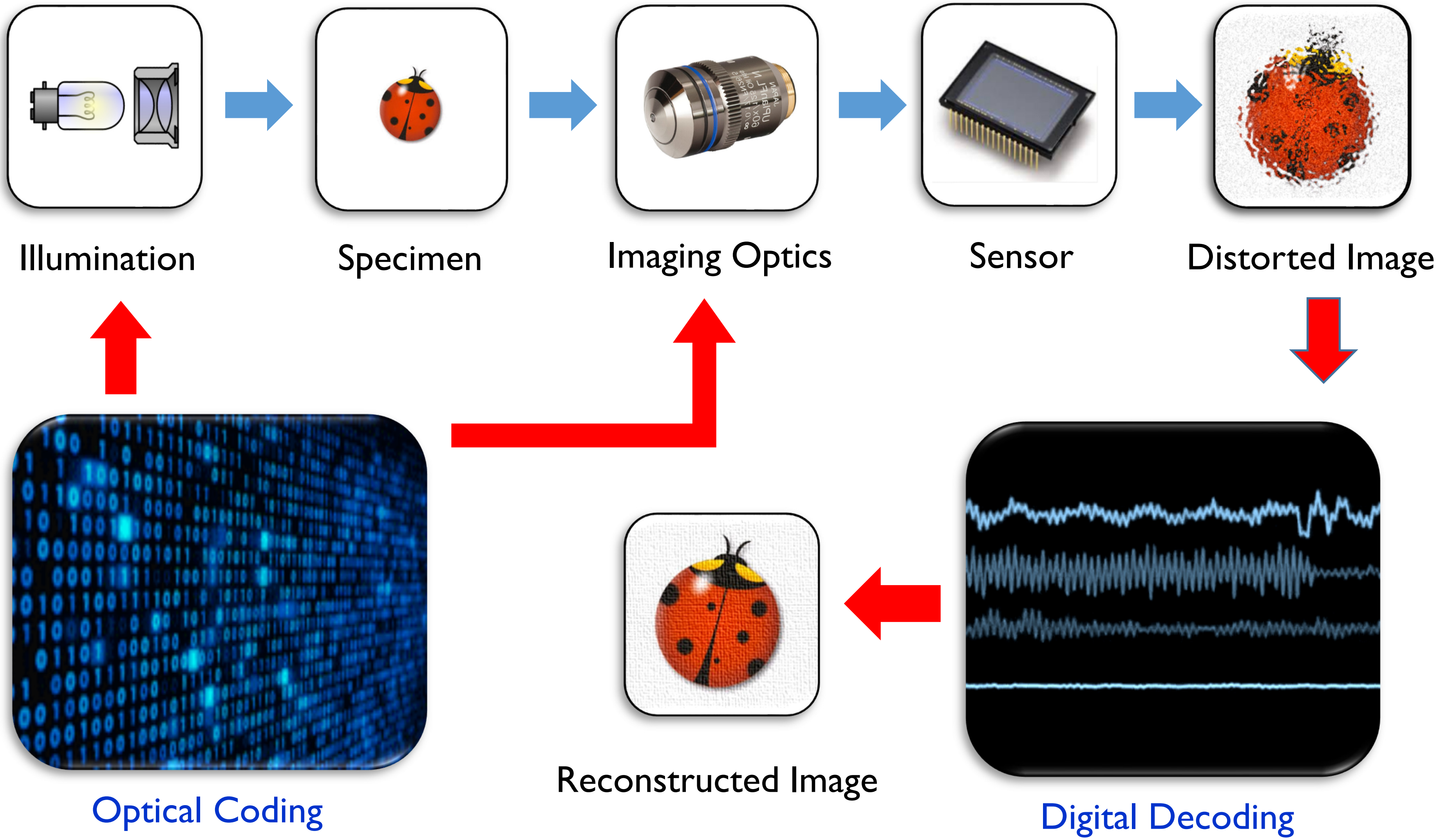

Phase of a image

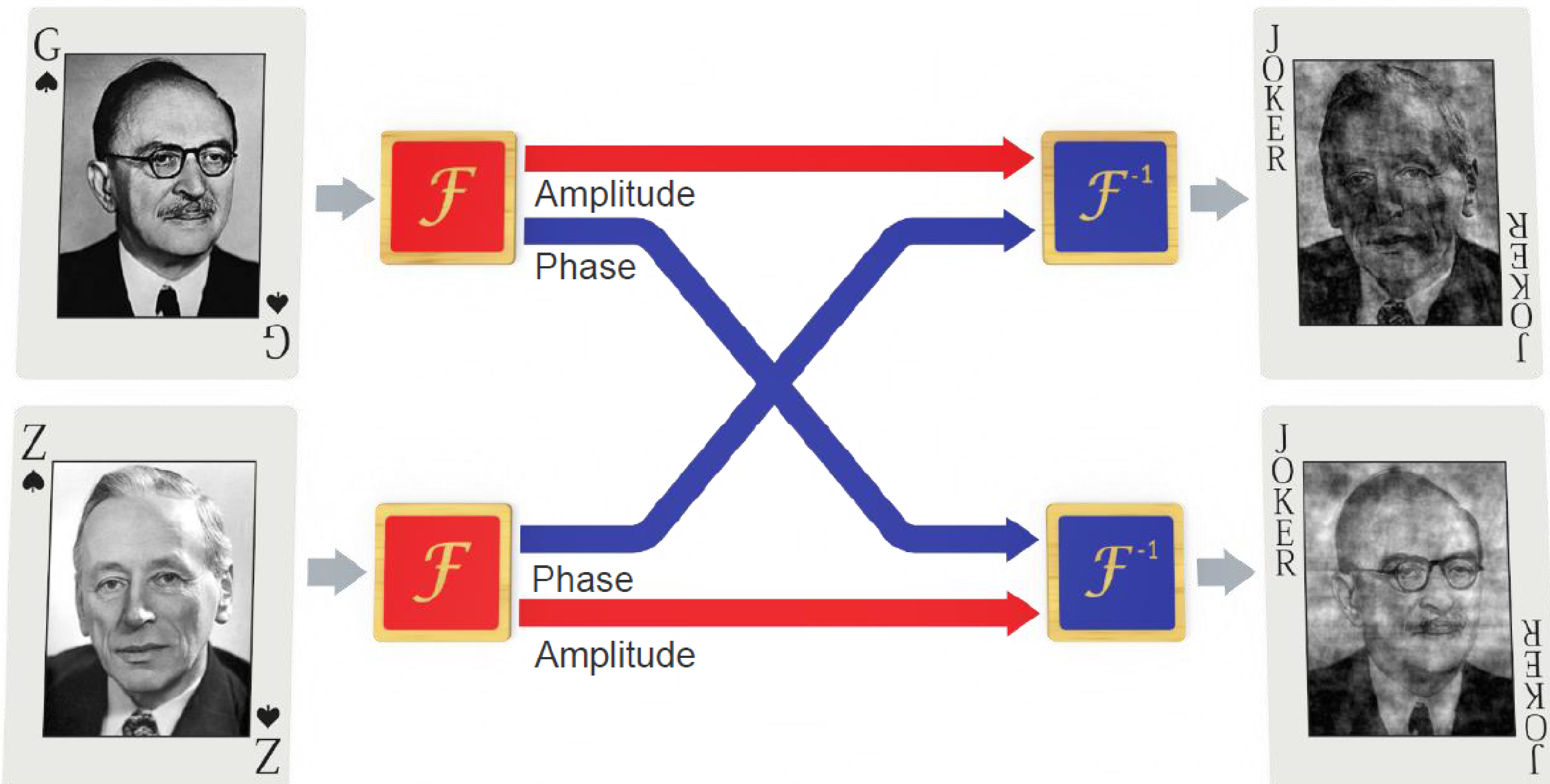

Phase of a object

$$\underbrace{U(x,y)}_{\text{Complex Amplitude}} = \underbrace{A(x,y)}_{\text{Amplitude}}\, e^{\underbrace{j\phi(x,y)}_{\text{Phase}}}$$

$$A(x,y) = \sqrt{\underbrace{I(x,y)}_{\text{Intensity}}}$$

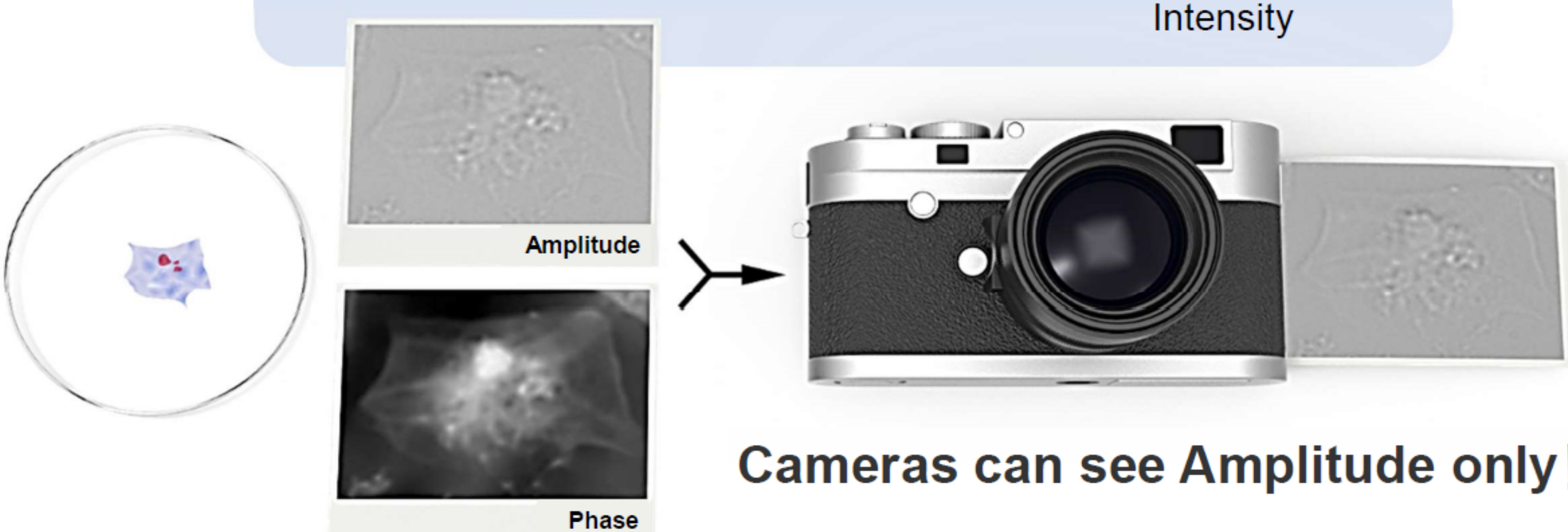

Cameras can see Amplitude only!

3D phase imaging ?

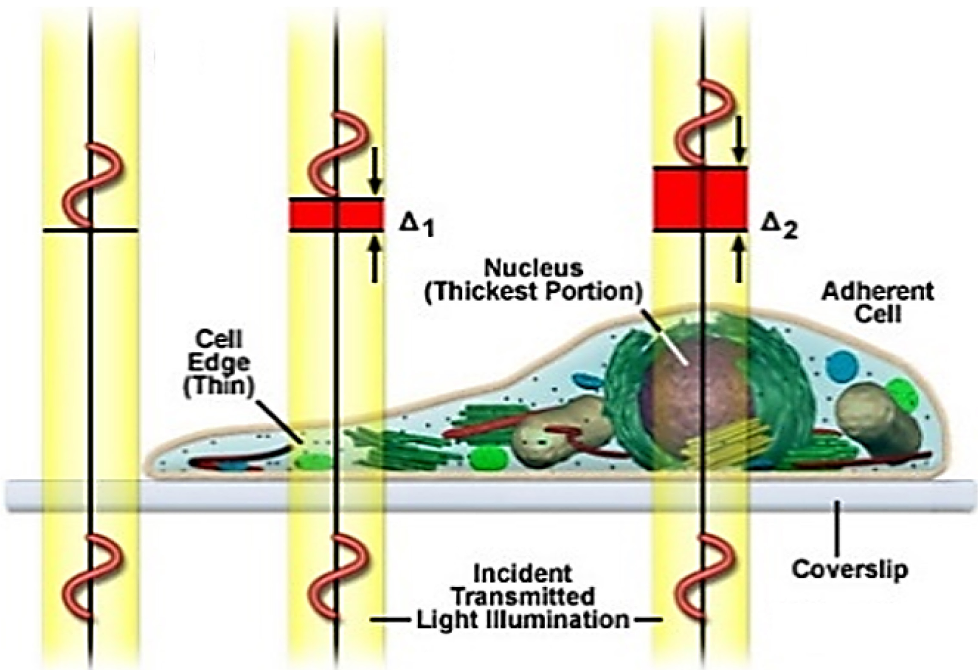

QPI vs ODT（optical diffraction tomography）

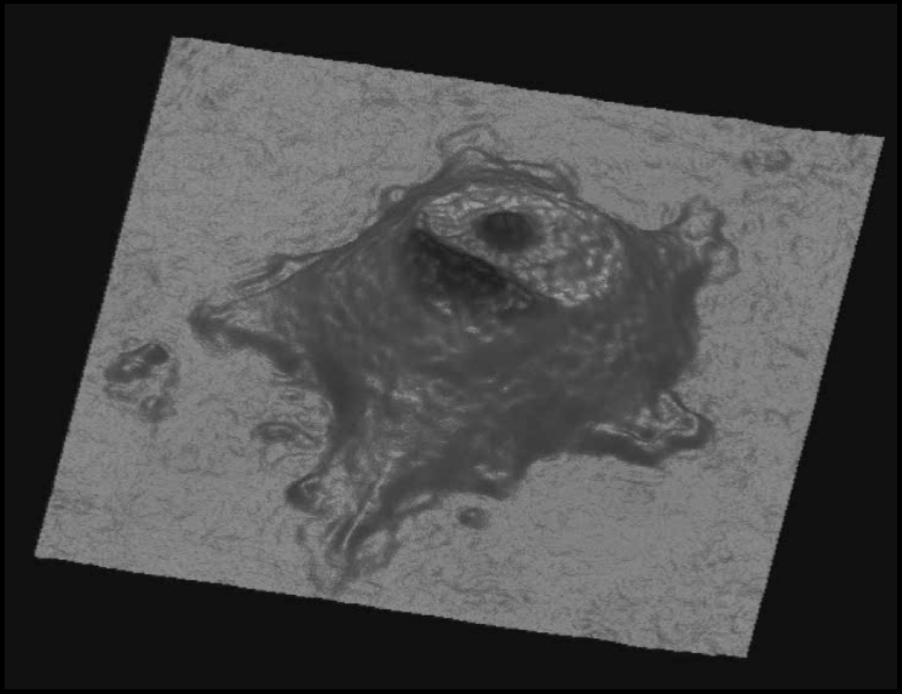

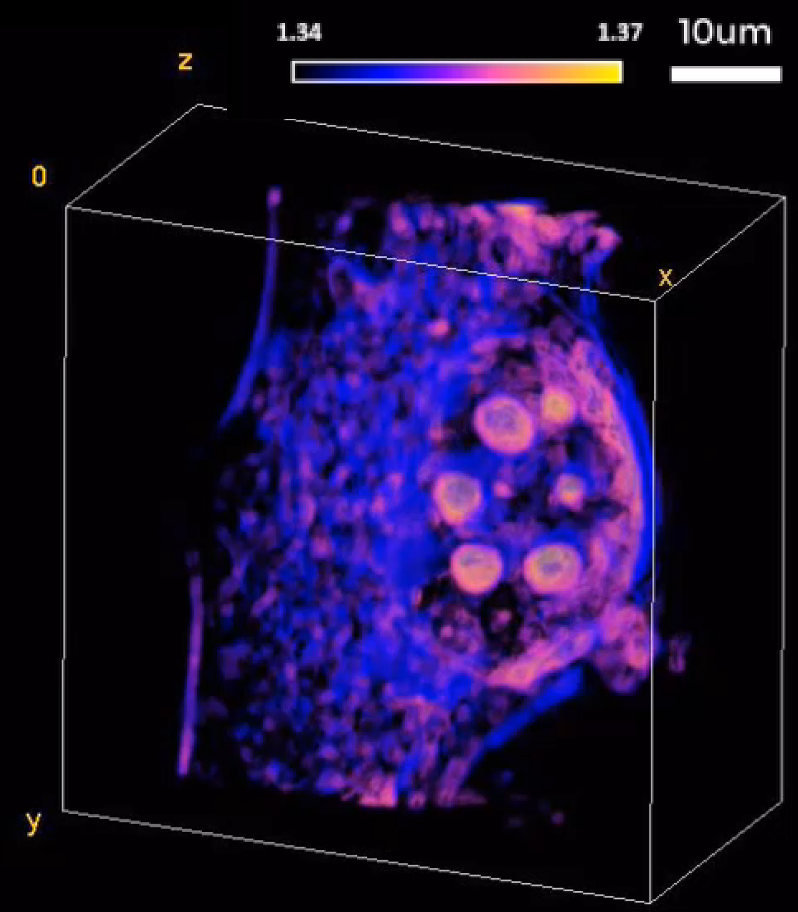

QPI: 2.5D optical path length

Profile

C. Zuo, et. al. , Opt Express, 21 24060-24075 (2013) .

ODT: true 3D refractive index

Volume

J Li, et. al. Biomed. Opt. Express 9, 2526-2542 (2018)

X-ray in biomedical imaging

1895 X-rays and Uranium Rays,
wedding ring

Marie Curie and the Discovery of Radioactivity

Brief review of optical diffraction tomography(ODT)

X-ray computed tomography(CT) & Application

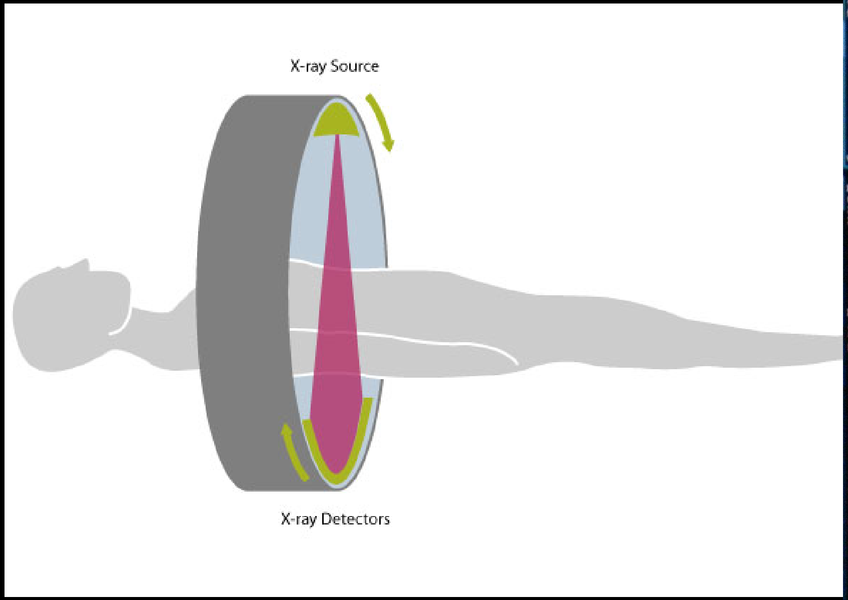

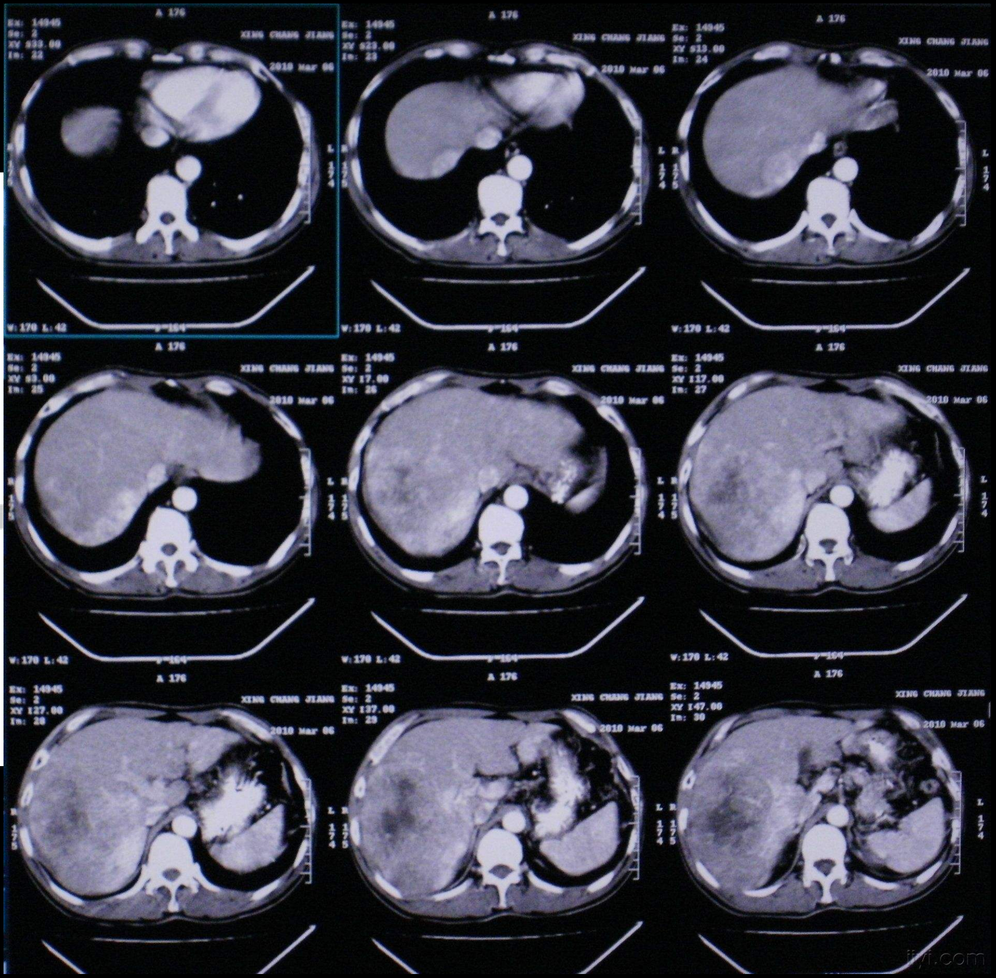

Computed tomography (CT)

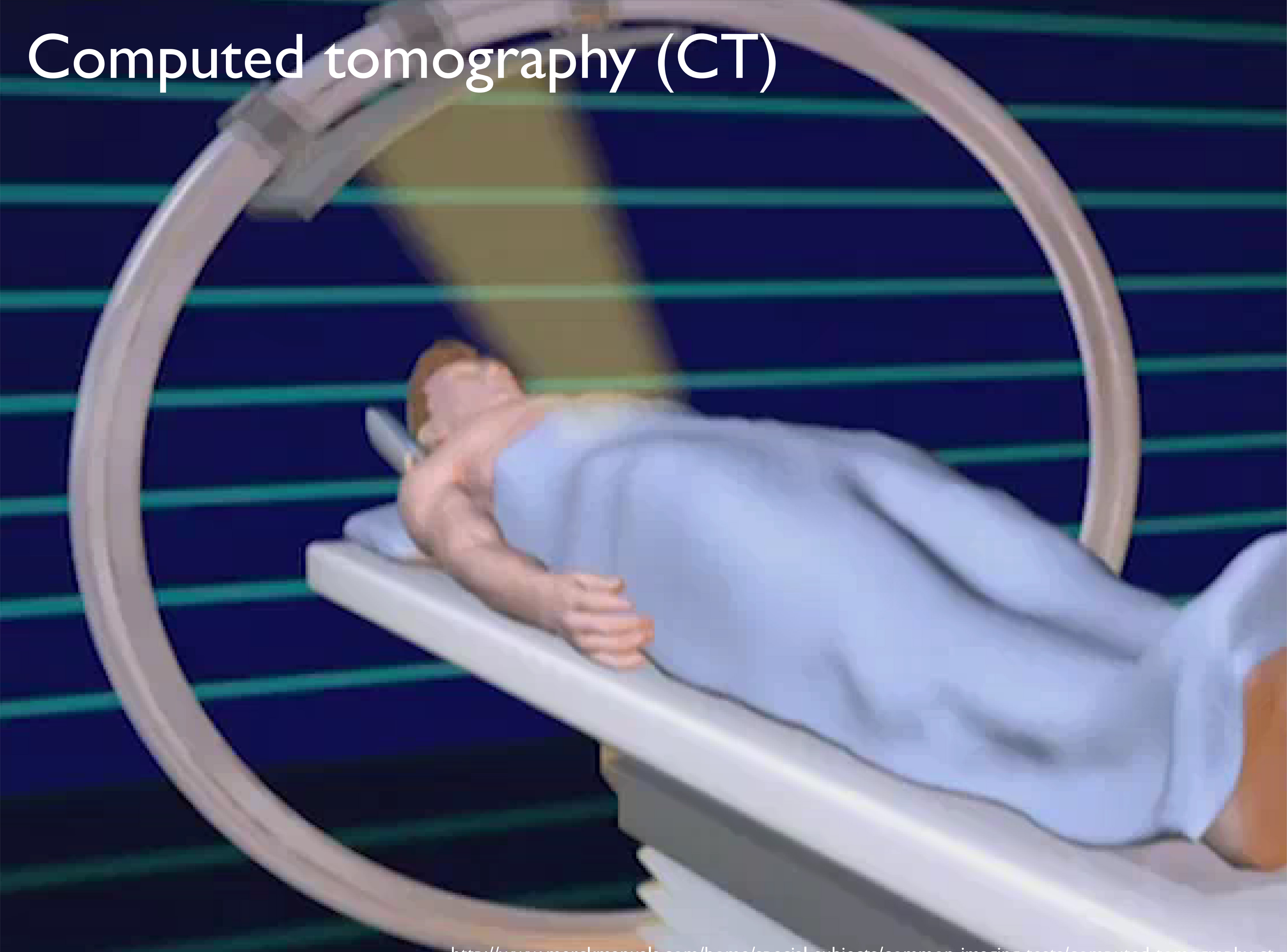

http://www.merckmanuals.com/home/special-subjects/common-imaging-tests/computed-tomography-ct

Integration projection & Radon transform

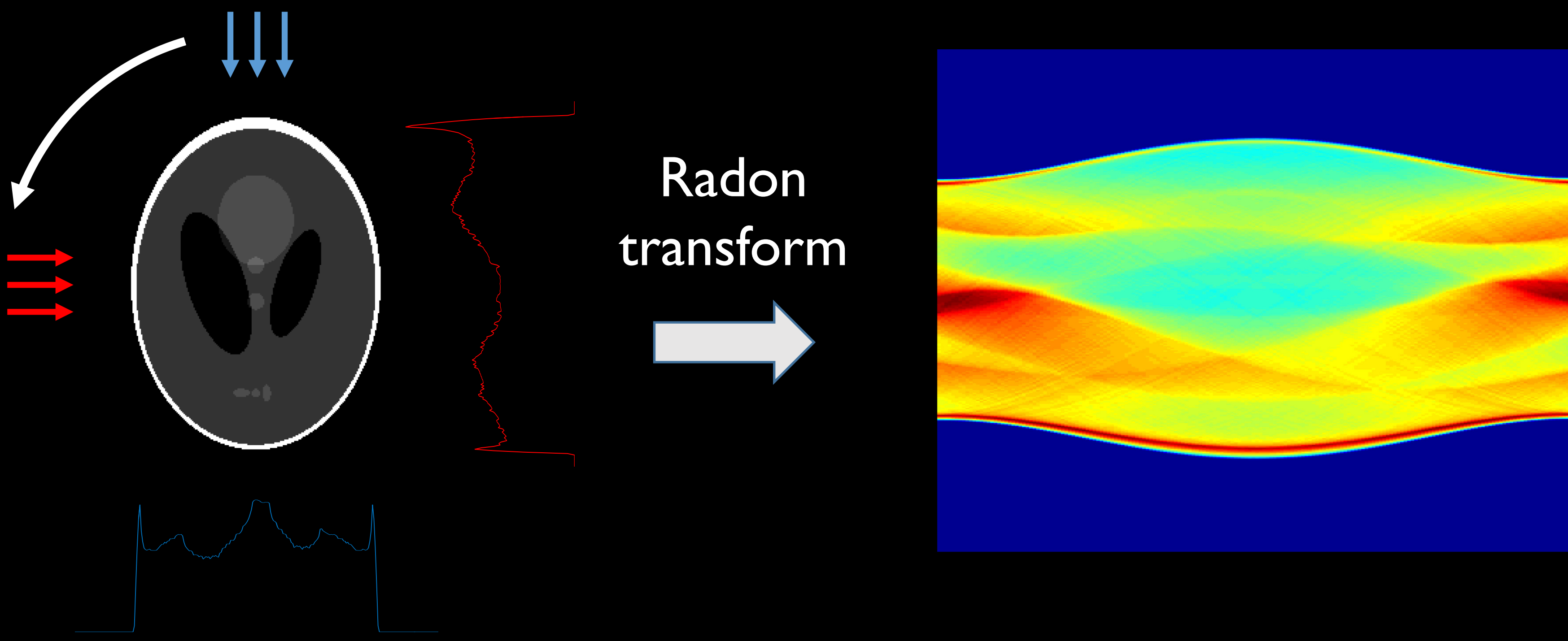

Fourier central slice theorem & back projection

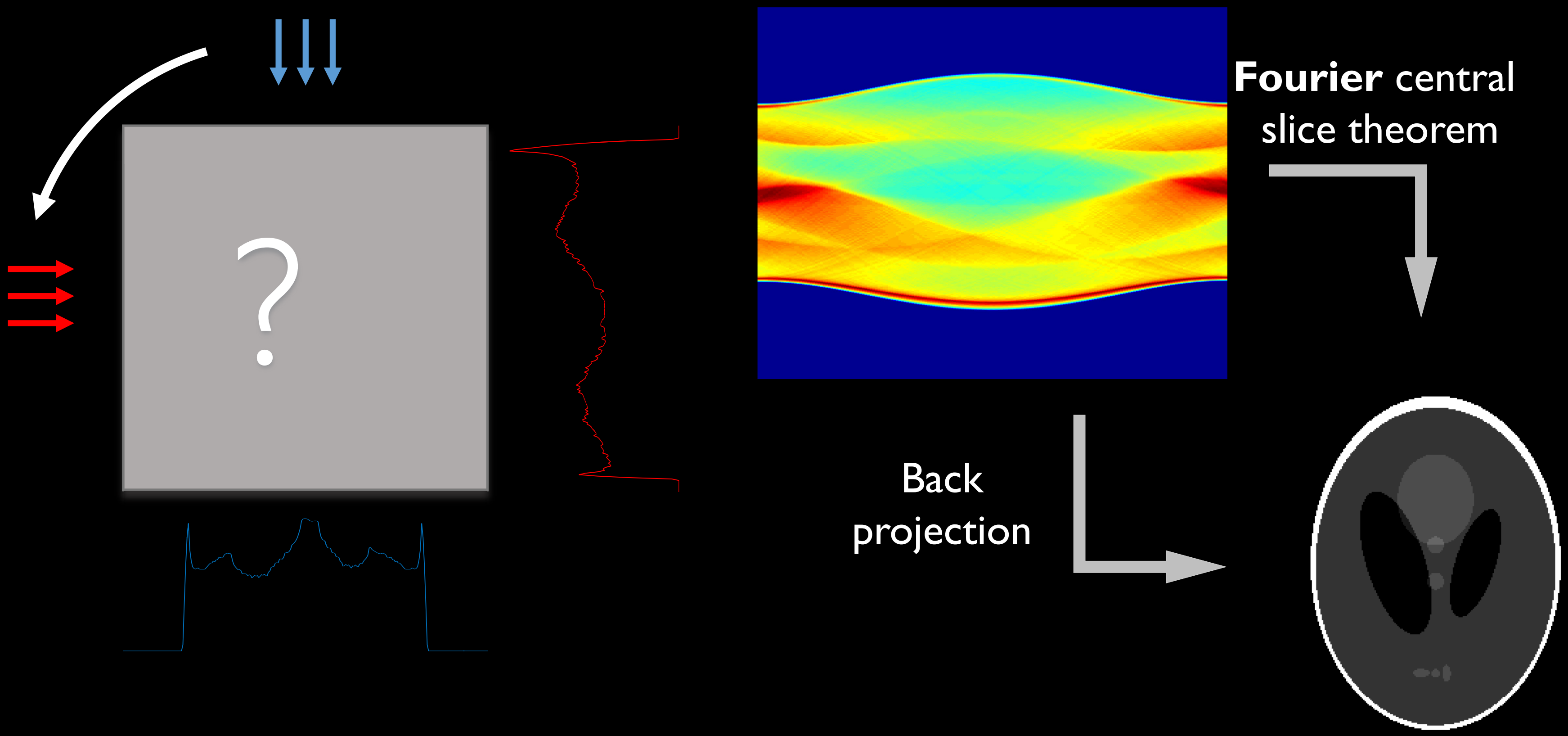

Fourier central slice theorem

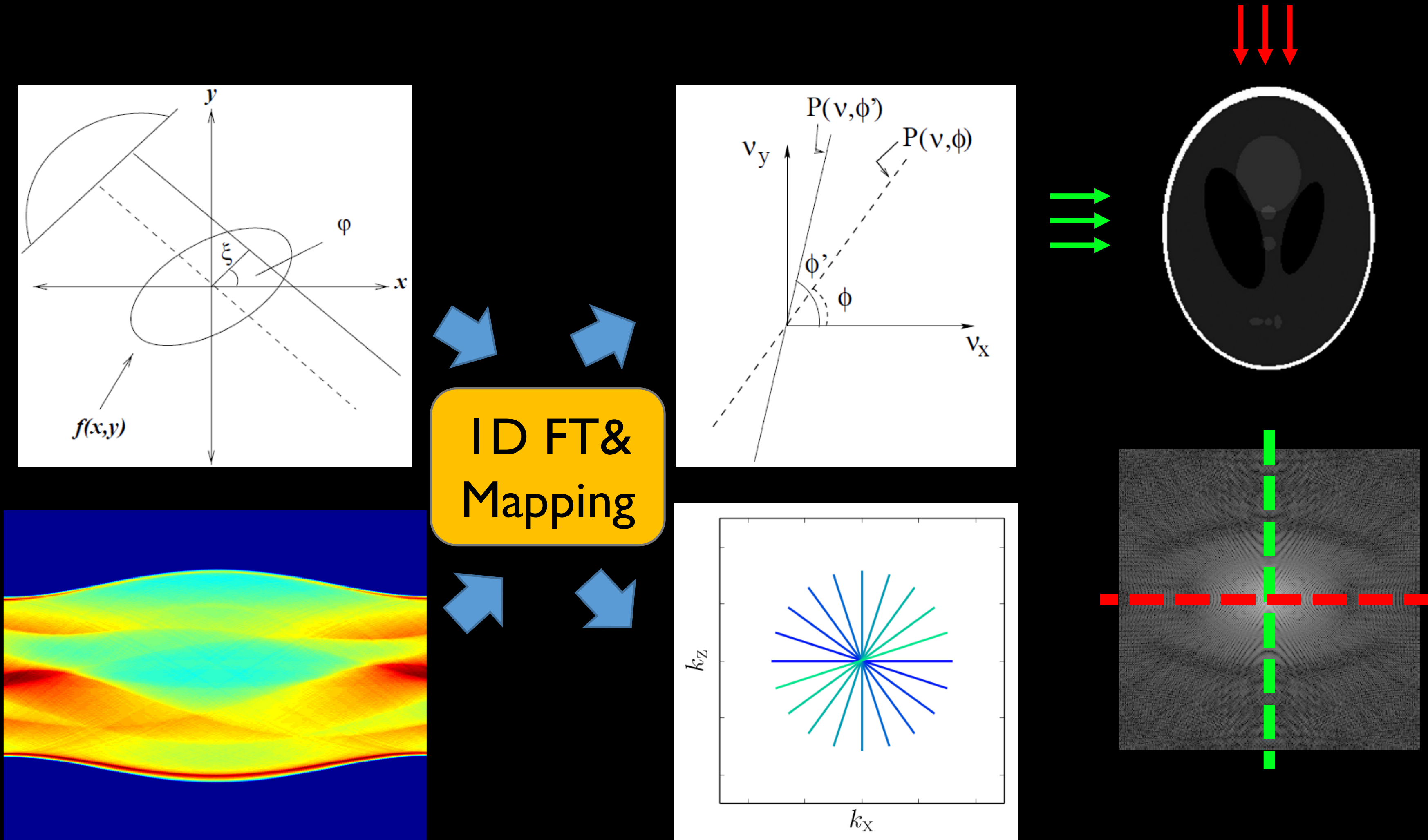

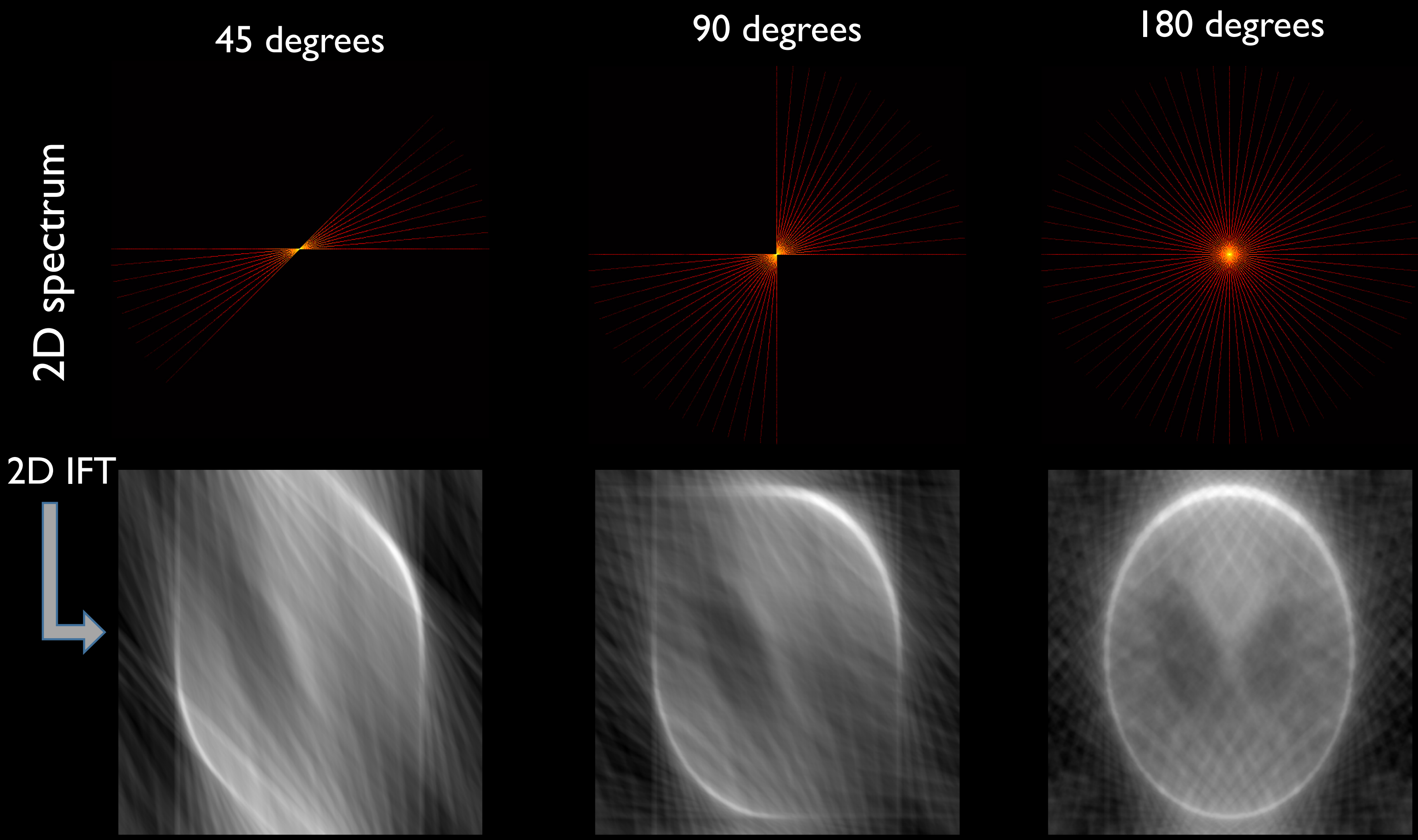
45 degrees
90 degrees
180 degrees
2D spectrum
2D IFT

Back projection algorithm

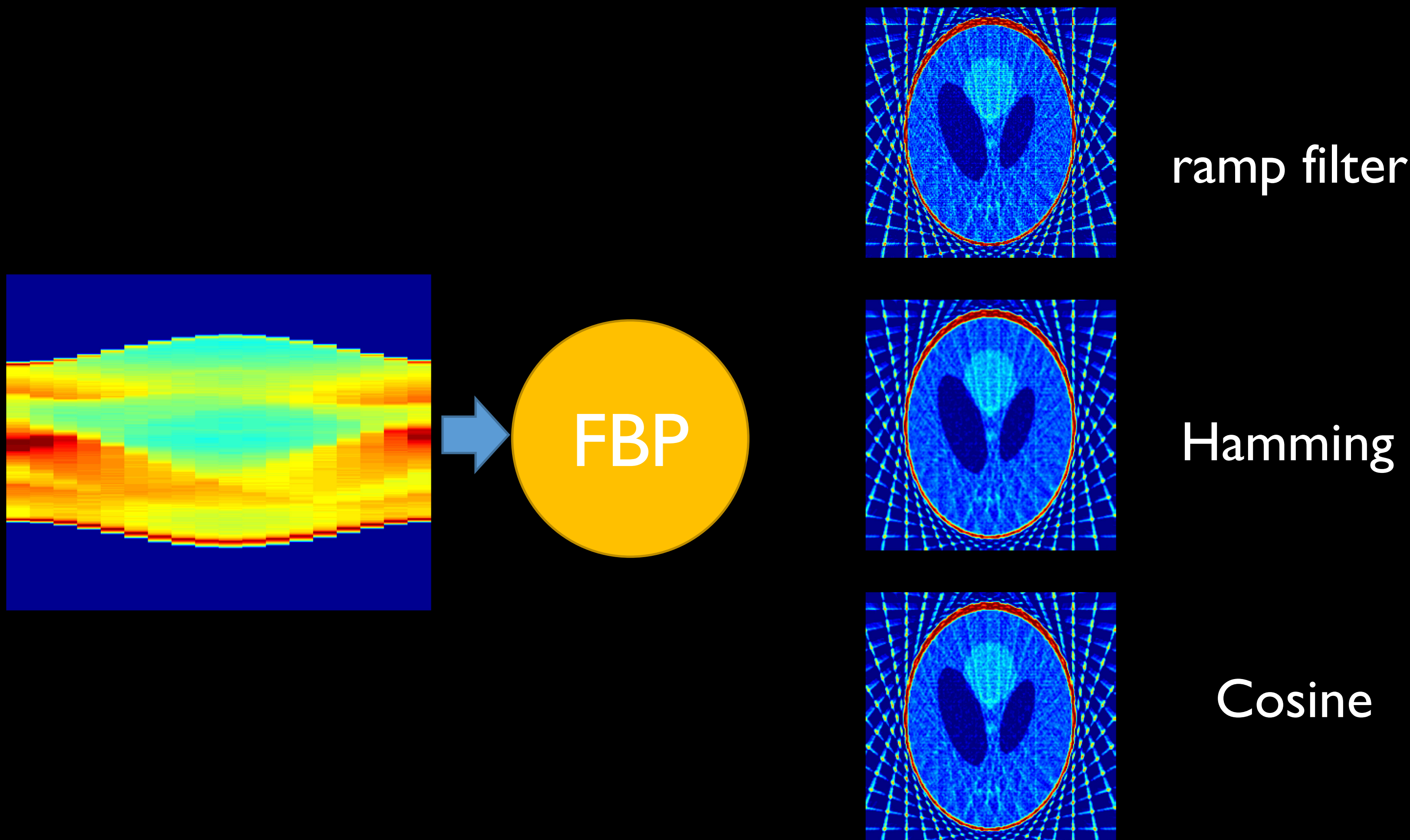

Optical diffraction tomography

	X-ray Computed Tomography	Optical Diffraction Tomography
Experimental schematic	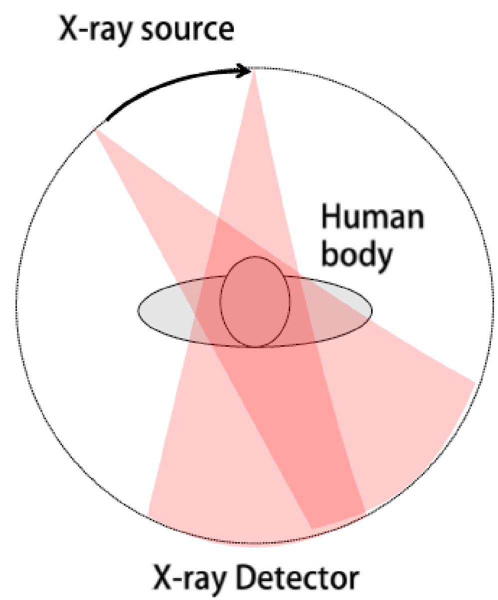	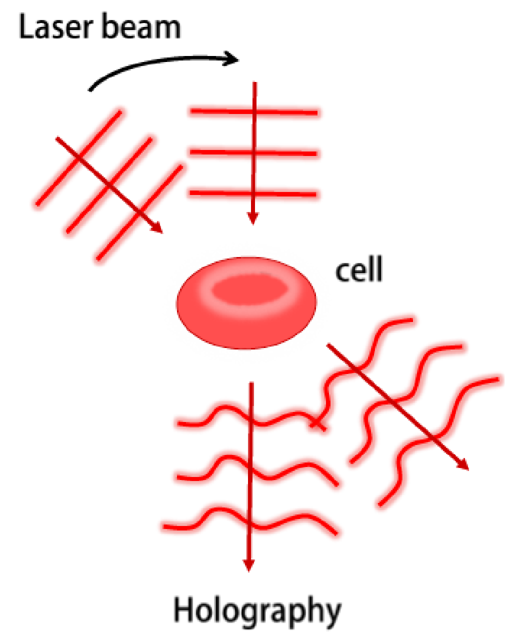
Illumination	Incoherent X-ray	Coherent Laser
Detector	X-ray image sensor	Optical image sensor
Raw images	2-D X-ray Intensity images	2-D Optical Holograms
Governing Equation	Helmholtz Equation	
Reconstructed result	3D tissue image	3D cell image
Imaging contract	Absorptivity	Refractive Index

Diffraction tomography

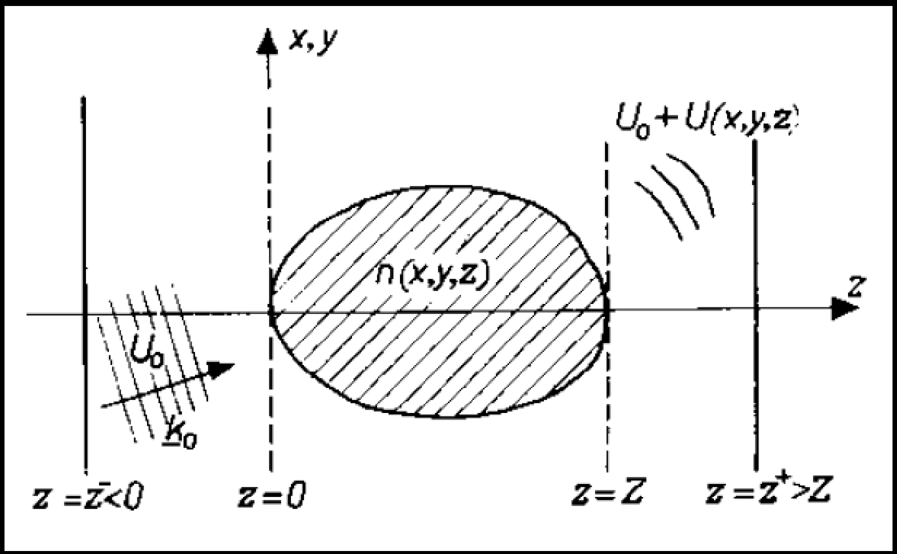

$$U^{(i)}\left(\vec{R}\right) = \exp(ik_0 s_0 \bullet \vec{R})$$

$$U\left(\vec{R}\right) = U^{(i)}\left(\vec{R}\right) + U^{(s)}\left(\vec{R}\right)$$

$$\nabla^2 U(\vec{R}) + k_0^2\, n(\vec{R})^2 U(\vec{R}) = 0$$

$$\nabla^2 U^{(i)}(\vec{R}) + k_0^2\, n(\vec{R})^2 U^{(i)}(\vec{R}) = 0$$

$$(\nabla^2 + k_0^2) U^{(i)}(\vec{R}) = 0$$

$$(\nabla^2 + k_0^2) U^{(s)}(\vec{R}) = F(\vec{R}) U(\vec{R})$$

$$F(\vec{R}) = -k_0^2 [n(\vec{R})^2 - 1]$$

$F(\vec{R})$ **Scattering potential**

Born approximation

$$U^{(s)}(\vec{R}) \ll U^{(i)}(\vec{R})$$

$$U(\vec{R}) \approx U^{(i)}(\vec{R})$$

Rytov approximation

$$U^{(s)} \approx U^{(i)}(\vec{R}) \ln\left(\frac{U(\vec{R})}{U^{(i)}(\vec{R})}\right)$$

Fourier diffraction theorem

$$\widehat{F}(U,V,W)=\frac{ik_z}{\pi}\widehat{U}^{(s)}(u,v;z^{+}=0)$$

In words eq. (15) shows that some of the *three-dimensional Fourier components of the scattering potential* may be immediately determined from the knowledge of the *two-dimensional Fourier components of the scattered field* in the two planes $z = z^{+} > Z$ and $z = z^{-} < 0$. It is now

where

$$\left.\begin{aligned} U &= u - k_0 p_0 , \\ V &= v - k_0 q_0 , \\ W^{\pm} &= \pm w - k_0 m_0 , \end{aligned}\right\}$$

and

$$w = (k_0^2 - u^2 - v^2)^{\frac{1}{2}} .$$

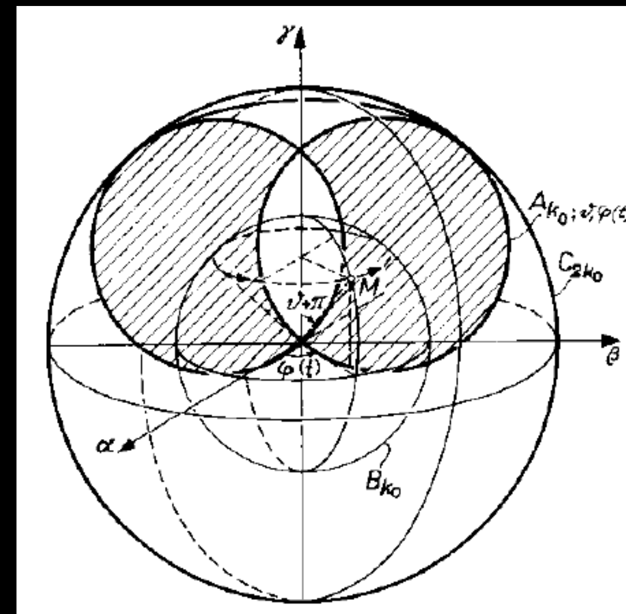

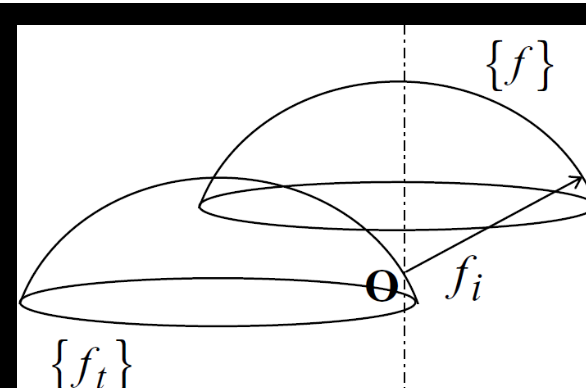

3D K-space of Scattering potential

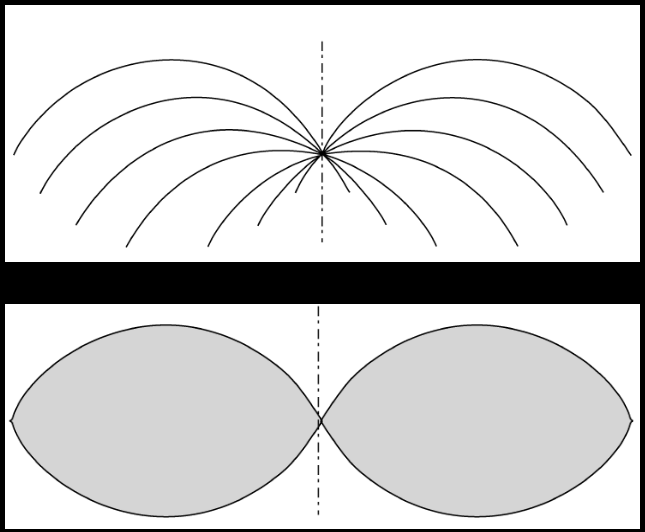

3D OTF for transmission microscope

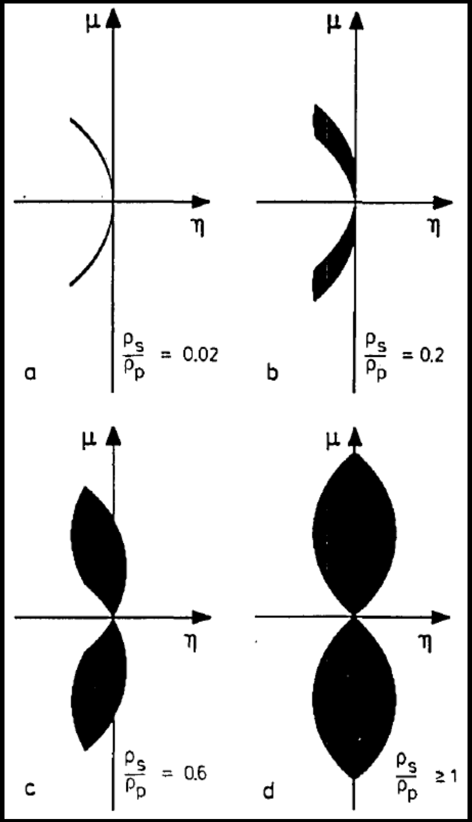

N. Streibl, "Three-dimensional imaging by a microscope," JOSA A **2, 121-127 (1985).**

Optical diffraction tomography

$$\widehat{F}_{\phi_0}(k_x, k_z) = A \cdot \sqrt{\frac{1}{2\pi}}\,\widehat{P}_{\phi_0}(k_{Dx})$$

	Fourier Slice Theorem (equation 1.10)	**Fourier Diffraction Theorem** (equation 4.24)
Sinogram $\widehat{P}_{\phi_0}(k_{Dx})$	Fourier transform of projections $\widehat{P}_{\phi_0}(k_{Dx})$	Fourier transform of complex scattered waves $\widehat{U}_{B,\phi_0}(k_{Dx})$
Factor A	$A = 1$	$A = -\frac{2ik_m M}{a_0}\exp(-ik_m M l_D)$
Coordinates (k_x, k_z) sliced at ϕ_0	$k_x = k_{Dx}$ $k_z = k_t = 0$ (straight line)	$k_x = k_{Dx}$ $k_z = \sqrt{k_m^2 - k_{Dx}^2} - k_m$ (semicircular arc)
Fourier space $\widehat{F}(\mathbf{k})$ coverage (180°)	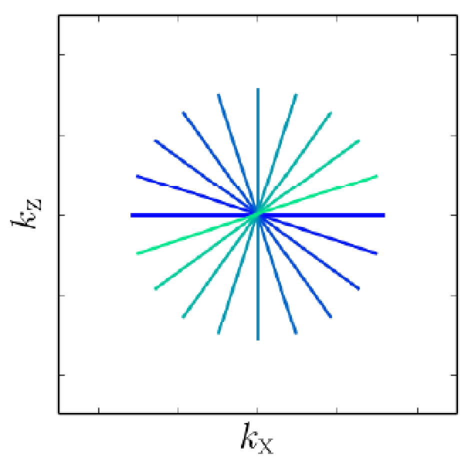	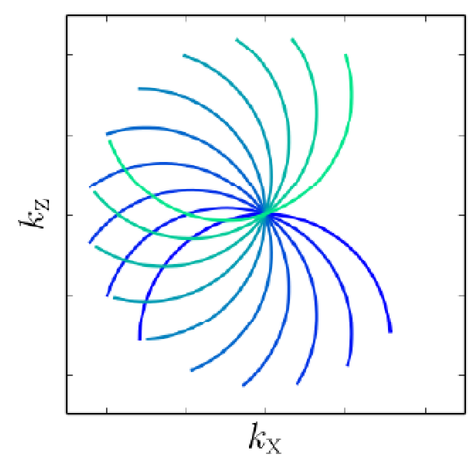

Diffraction tomography setup

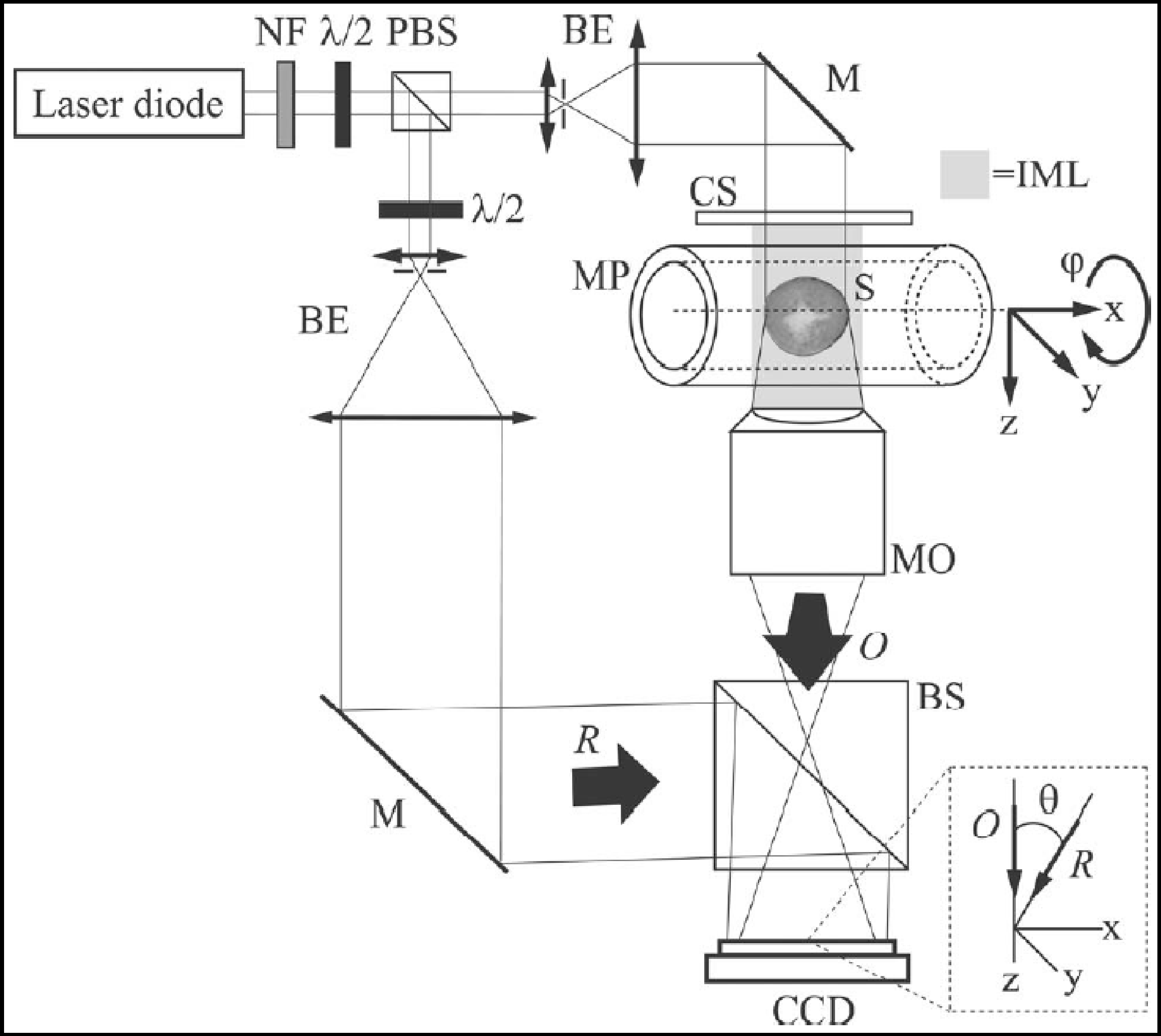

Sample rotation

Diffraction tomography setup

Sample rotation

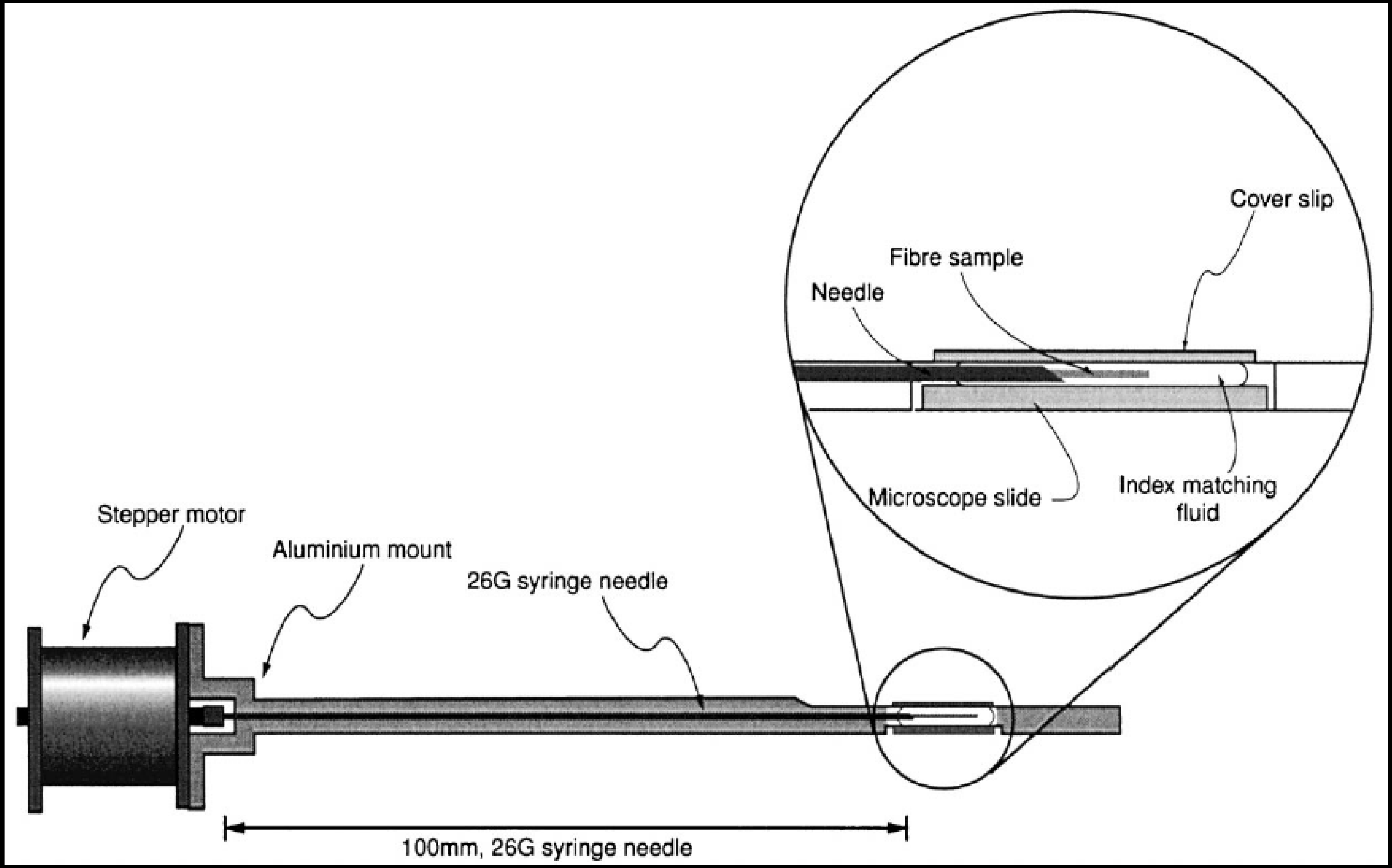

Diffraction tomography setup

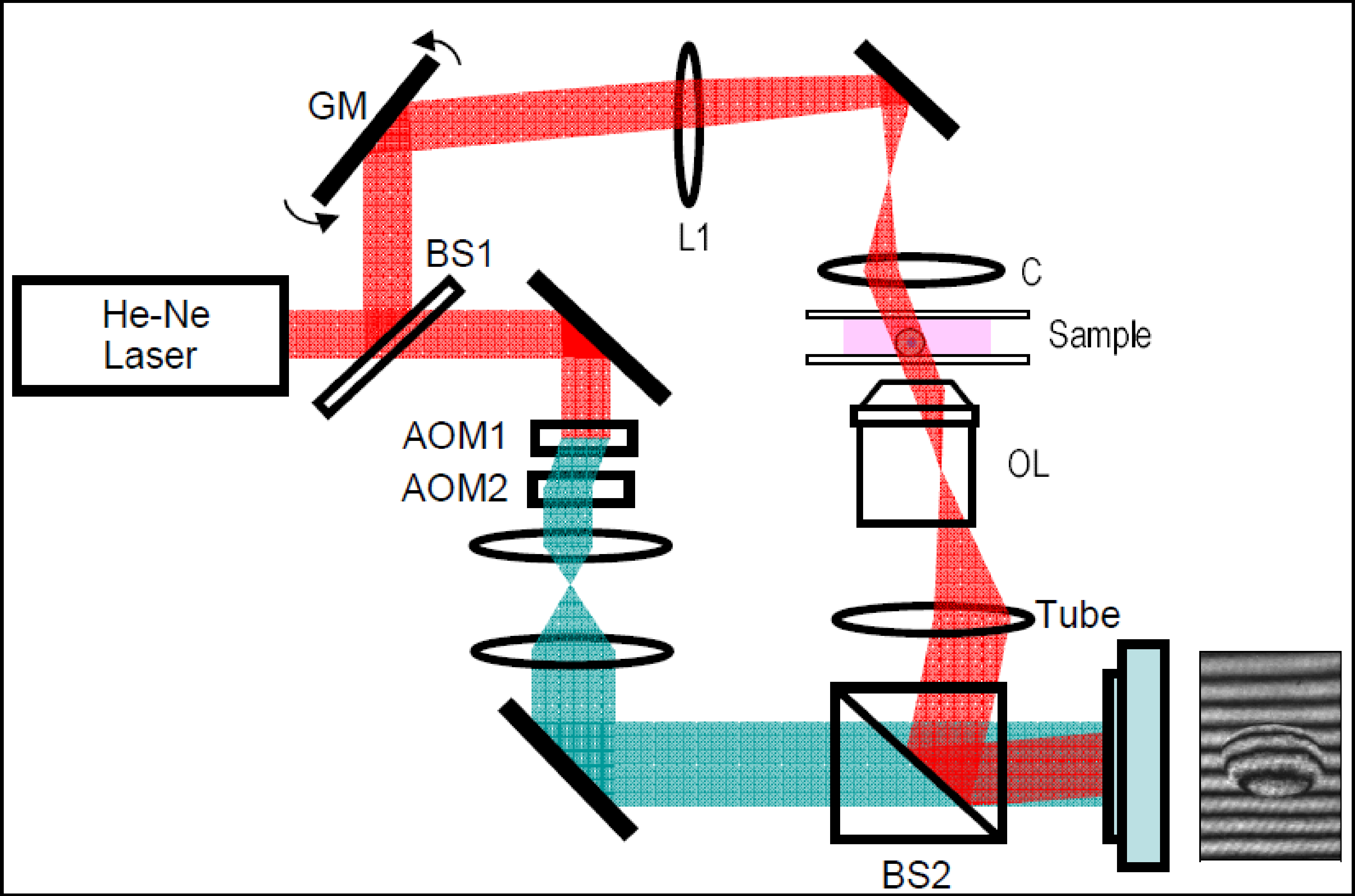

Beam scanning

Diffraction tomography setup

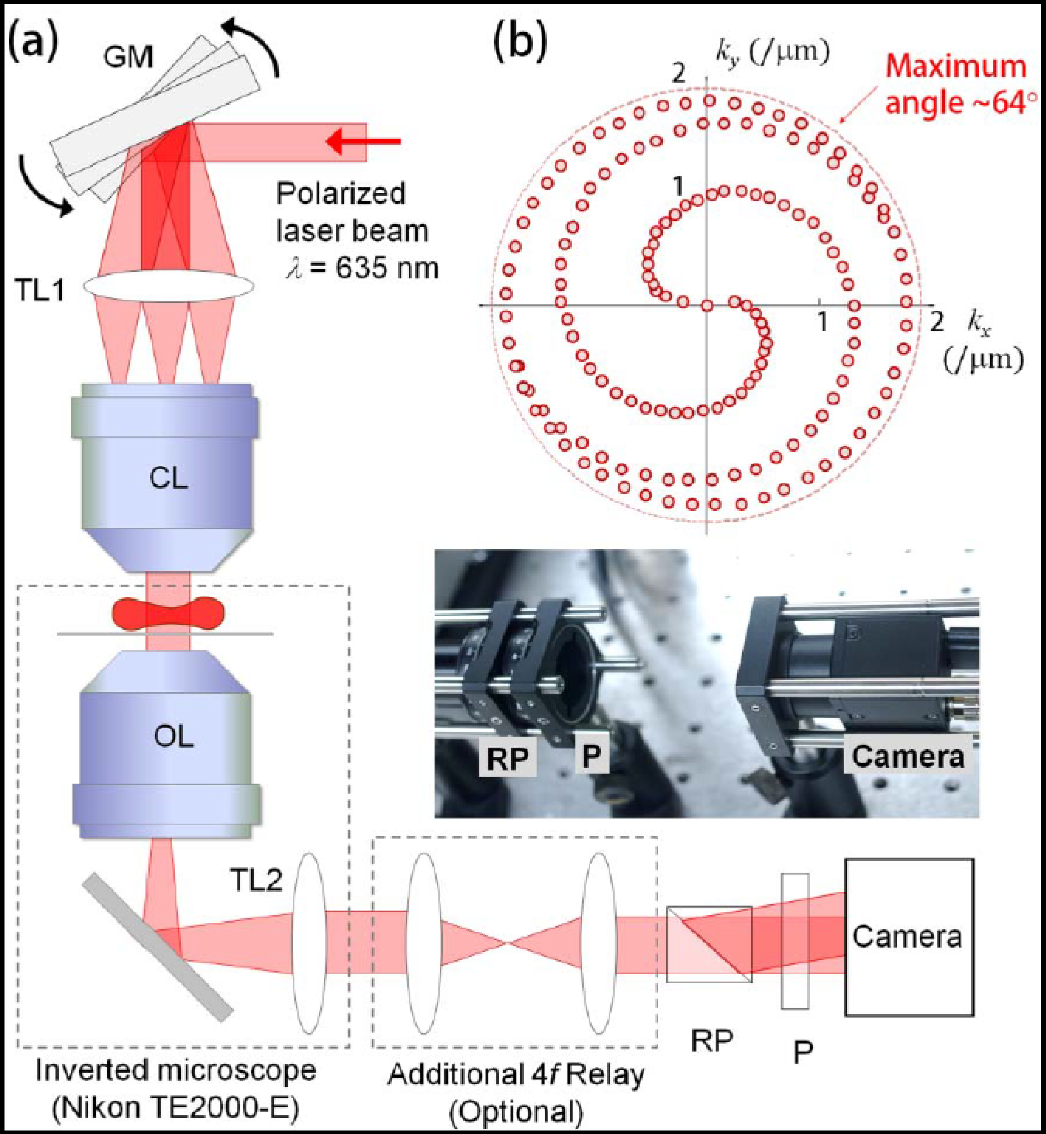

Beam scanning

Diffraction tomography result

DHM phase measurement

Original 3D Fourier spectrum

iterative non-negative constraint

Final 3D Fourier spectrum

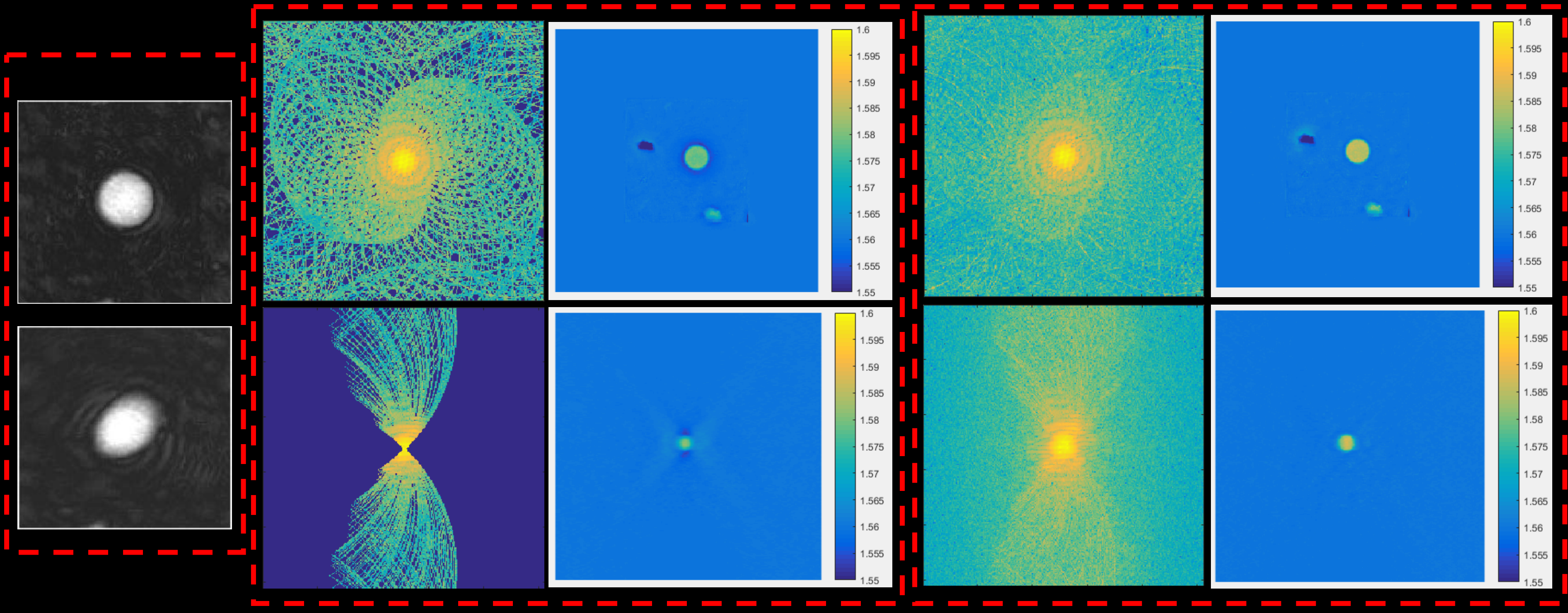

Results

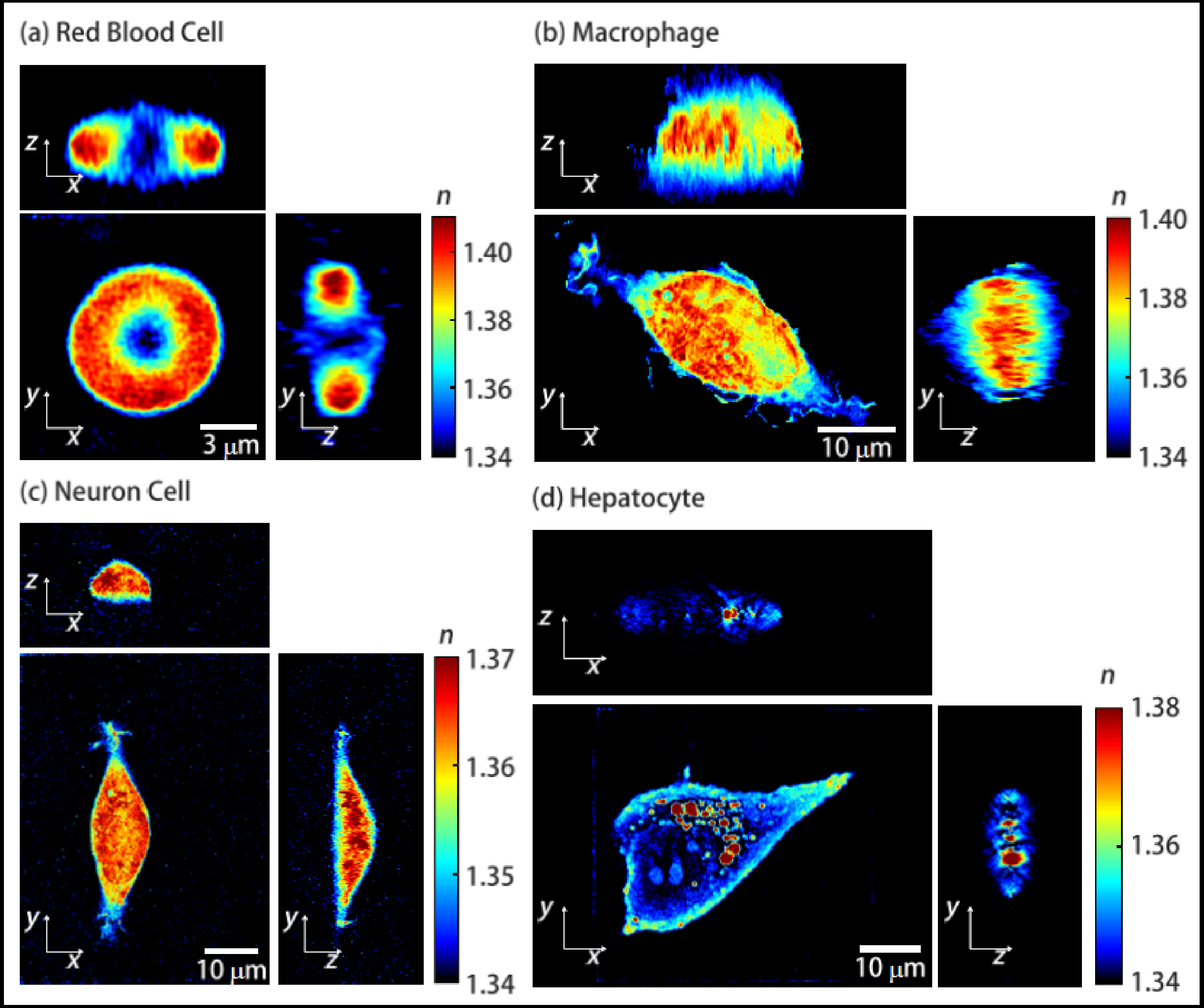
(a) Red Blood Cell
3 μm
n
1.40
1.38
1.36
1.34
(b) Macrophage
10 μm
n
1.40
1.38
1.36
1.34
(c) Neuron Cell
10 μm
n
1.37
1.36
1.35
1.34
(d) Hepatocyte
10 μm
n
1.38
1.36
1.34

Commercial product of ODT

Tomocube

PRODUCT | APPLICATIONS | PUBLICATIONS
NEWS & EVENTS | SUPPORT | COMPANY

Revolutionary holotomographic (3D holographic) microscopy opens new era for label-free live cell imaging

Cellular analysis plays a crucial role in a wide variety of research and diagnostic activities in the life science. However, the information available to researchers and clinicians is limited by current microscopy techniques. An innovative new tool – Holotomographic microscopy – can overcome many of these limitations and open new vistas for researchers and clinicians to understand, diagnose and treat human diseases.

Holotomographic Microscopy – New era of microscopy Tomocube's holotomography series utilize optical diffraction tomography (ODT), which enables users to quantitatively and noninvasively investigate biological cells and thin tissues. ODT reconstructs the 3D refractive index (RI) distributions of live cells and by doing so, provides structural and chemical information about the cell including dry mass, morphology, and dynamics of the cellular membrane.

Commercial product of ODT

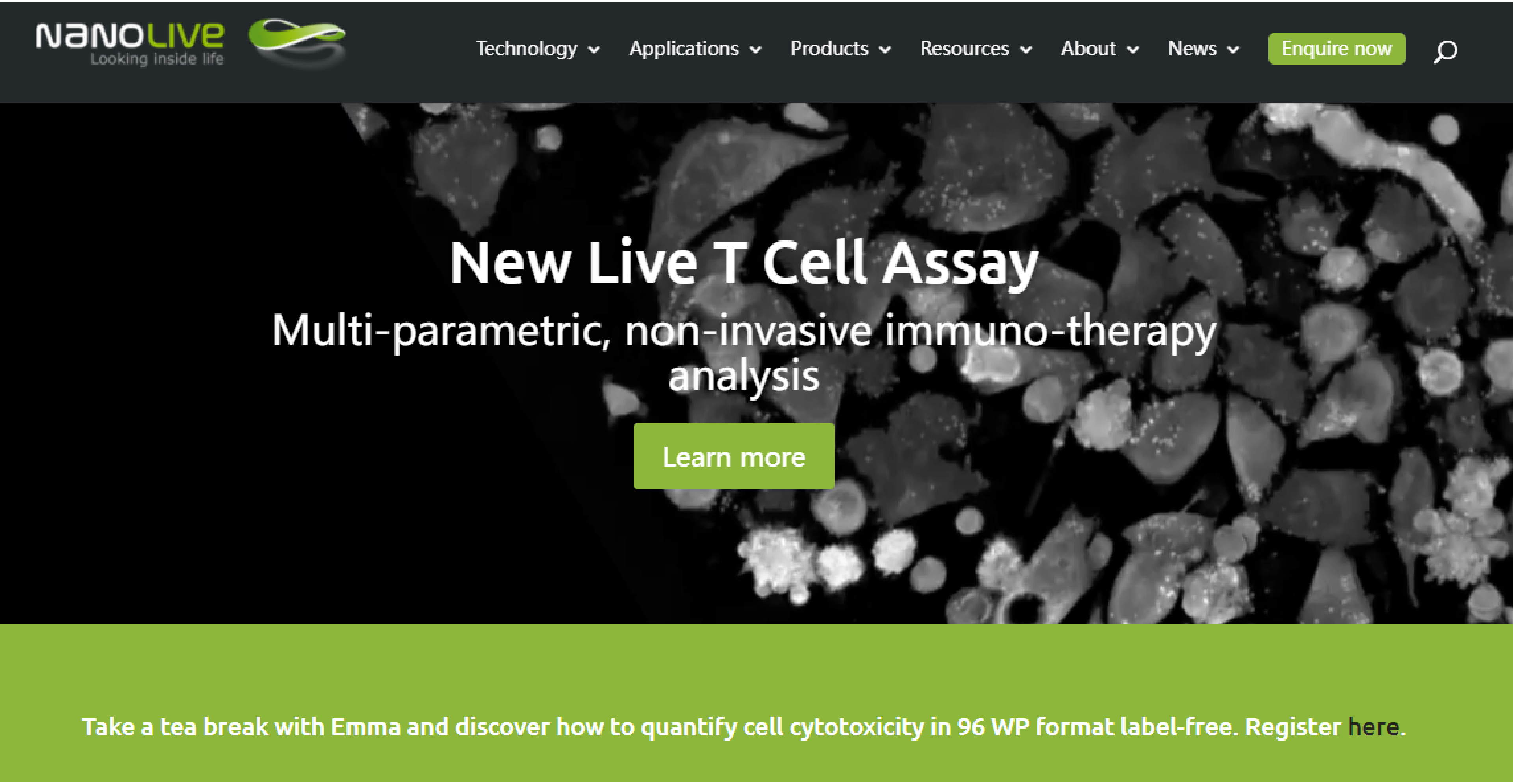

Applications

A selected overview of Nanolive’ s top applications

Live T Cell Assay

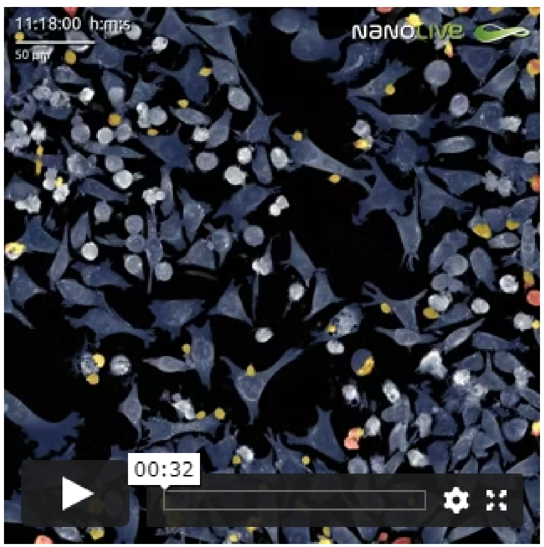

Mitochondria & Cell Metabolism

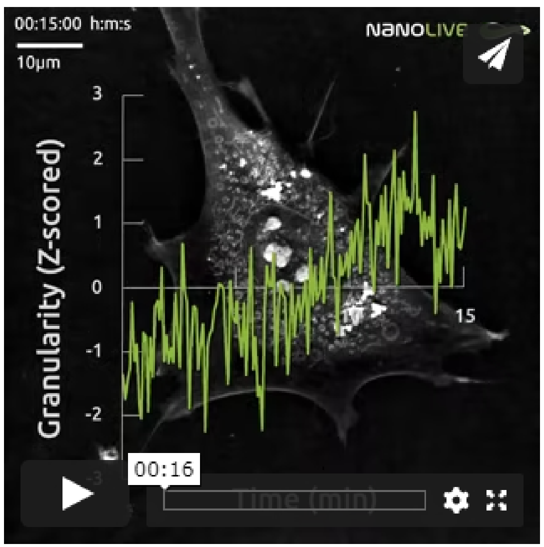

Cytotoxicity

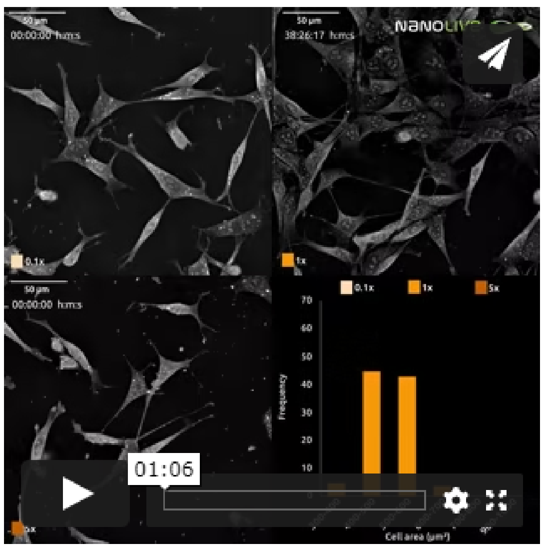

https://www.nanolive.ch/

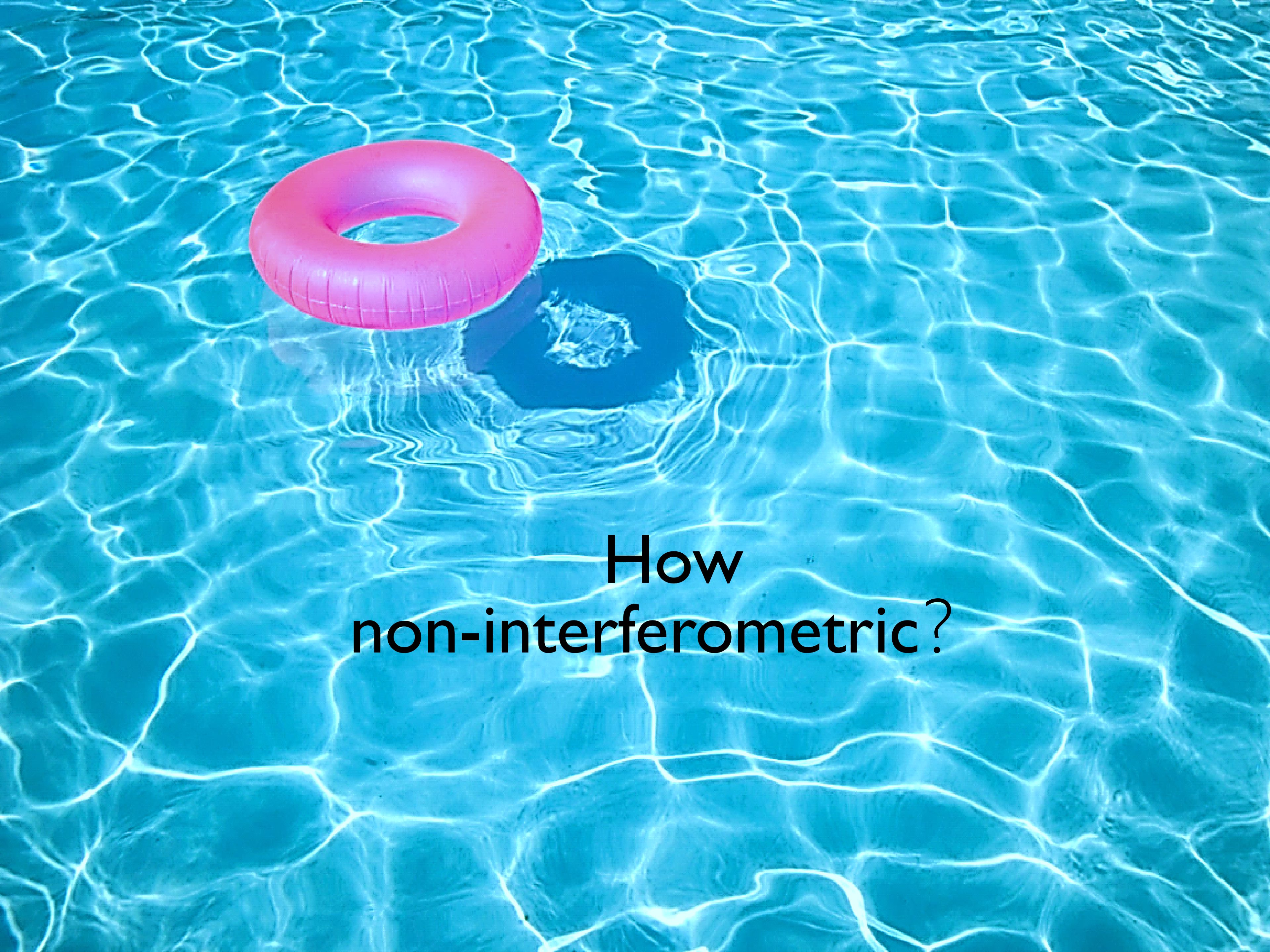
How
non-interferometric?

Transport-of-intensity diffraction tomography (TIDT)

Fourier diffraction theorem

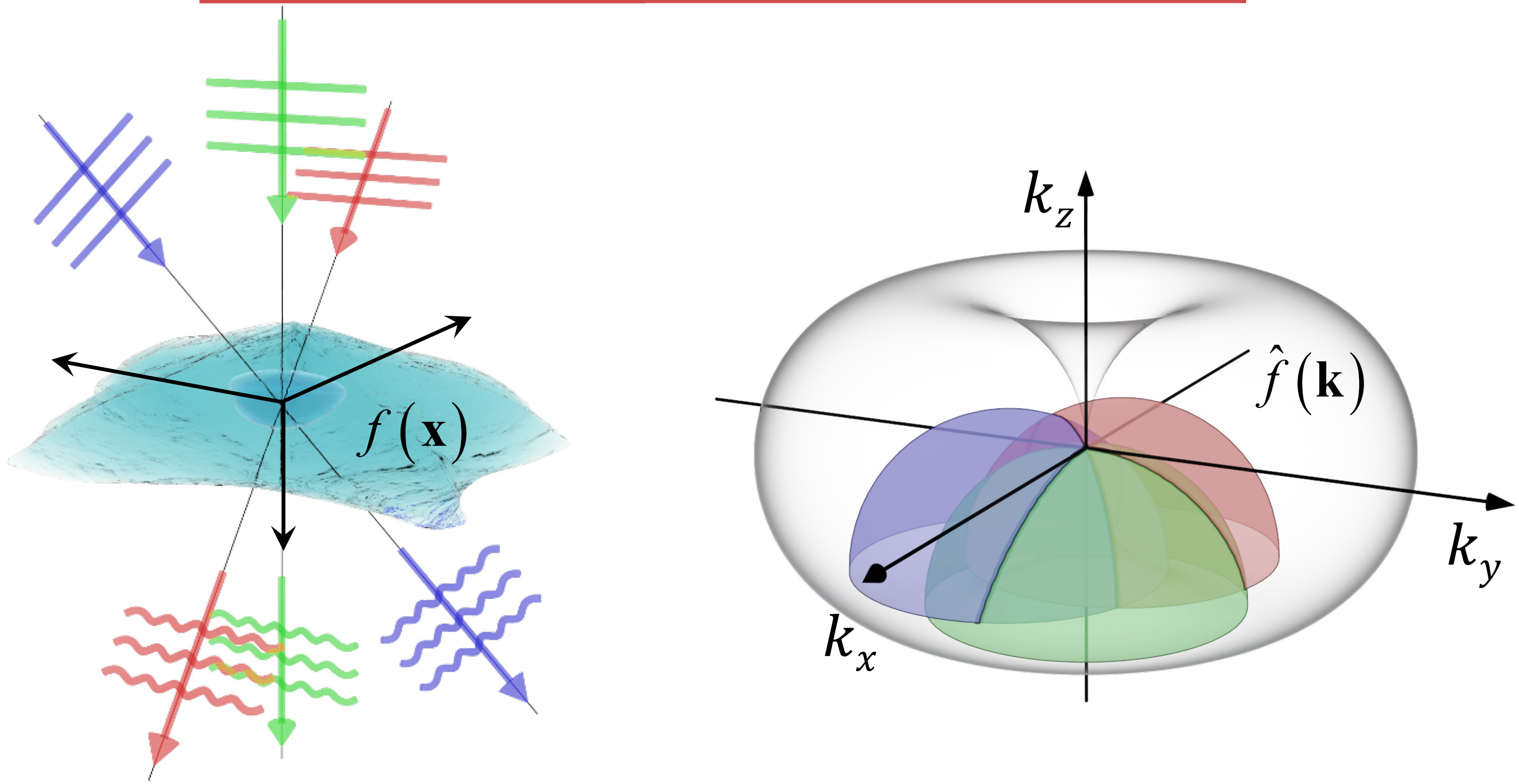

3D real space

3D Fourier space

Free-space: semi-sphere in 3D Fourier space

E Wolf. Opt. Commun. 1, 153–156 (1969).

Transport-of-intensity diffraction tomography (TIDT)

Fourier diffraction theorem for a limit-aperture system

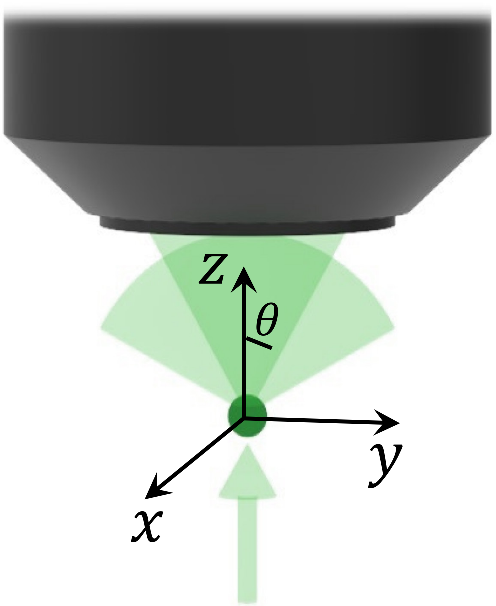

3D real space

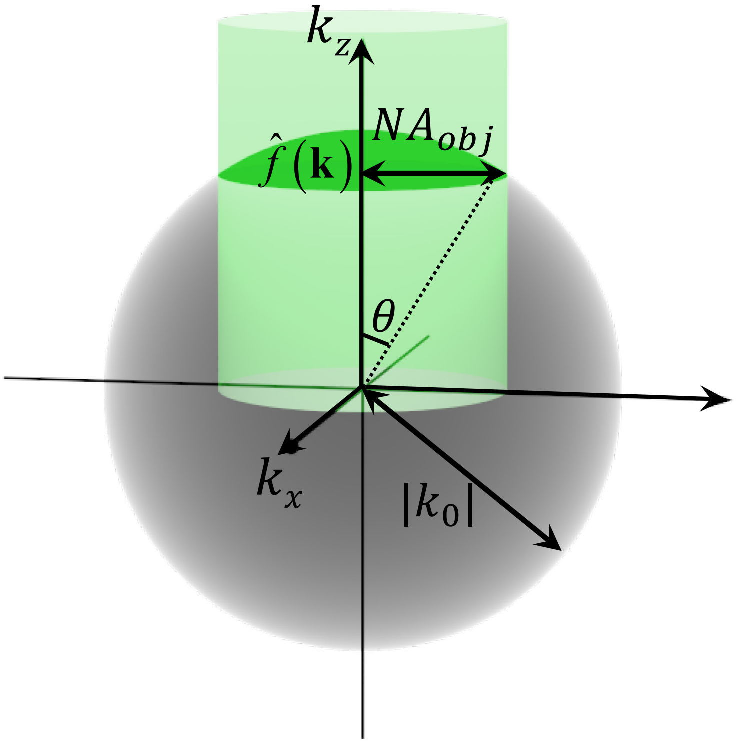

3D Fourier space

Microscopic imaging: partial spherical cap bounded by the lens aperture

E Wolf. *Opt. Commun.* 1, 153–156 (1969).

3D phase imaging ?

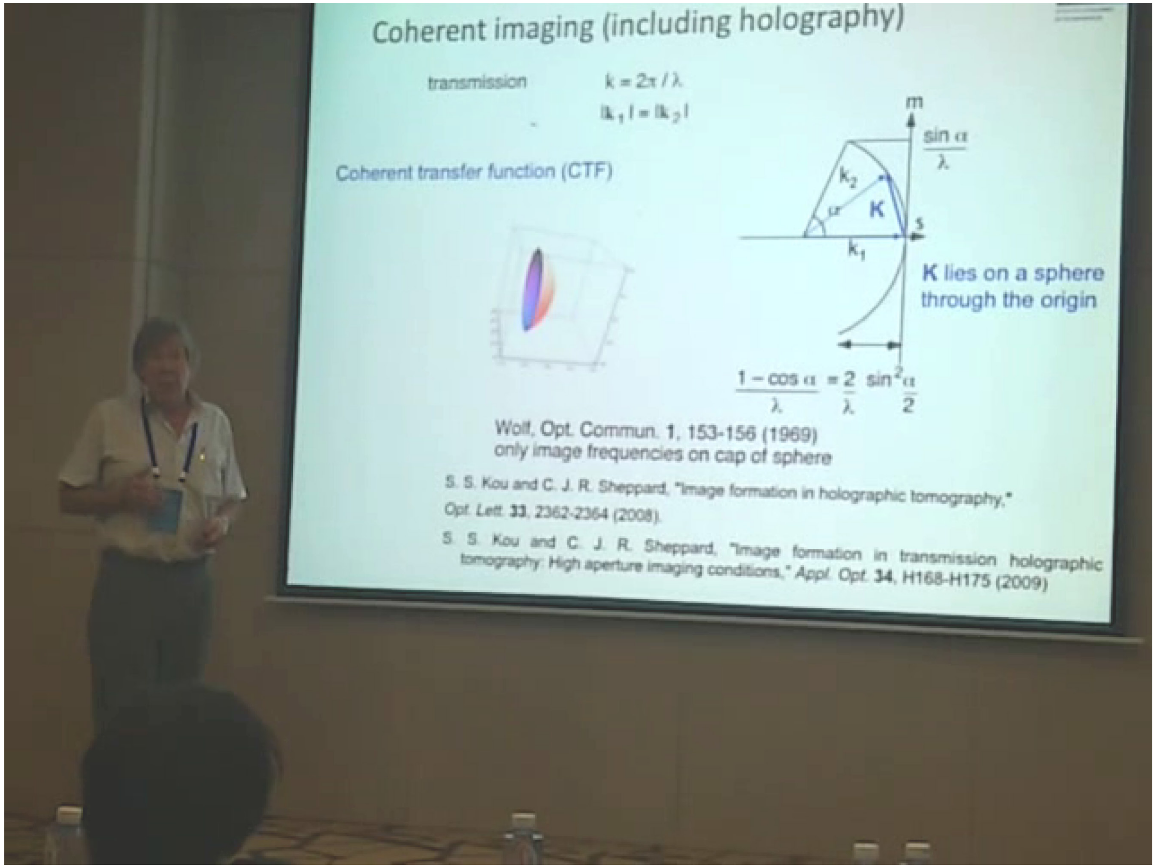

Lensless TIE microscopy

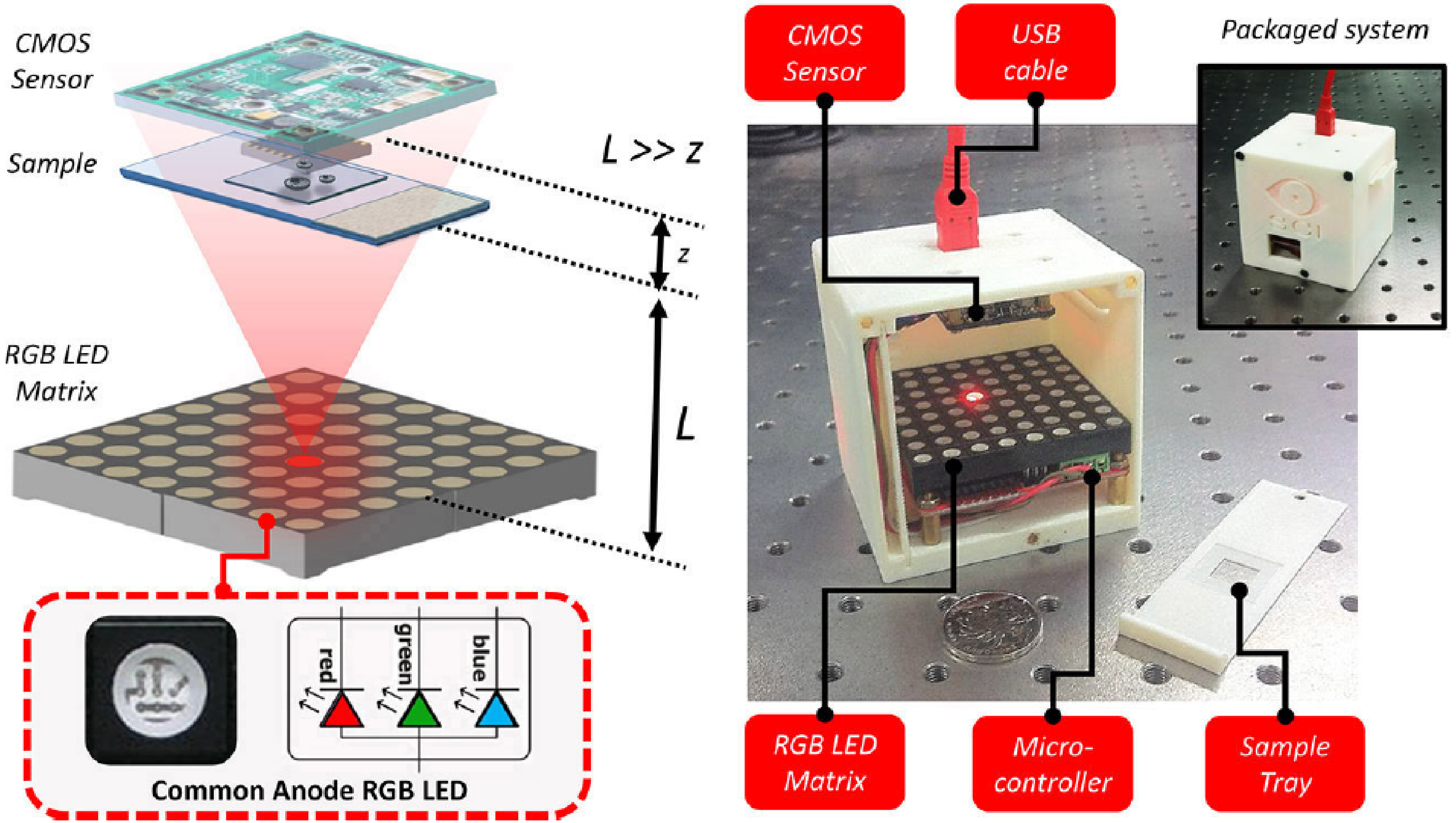

Lensless TIE microscope

Lensless TIE microscopy

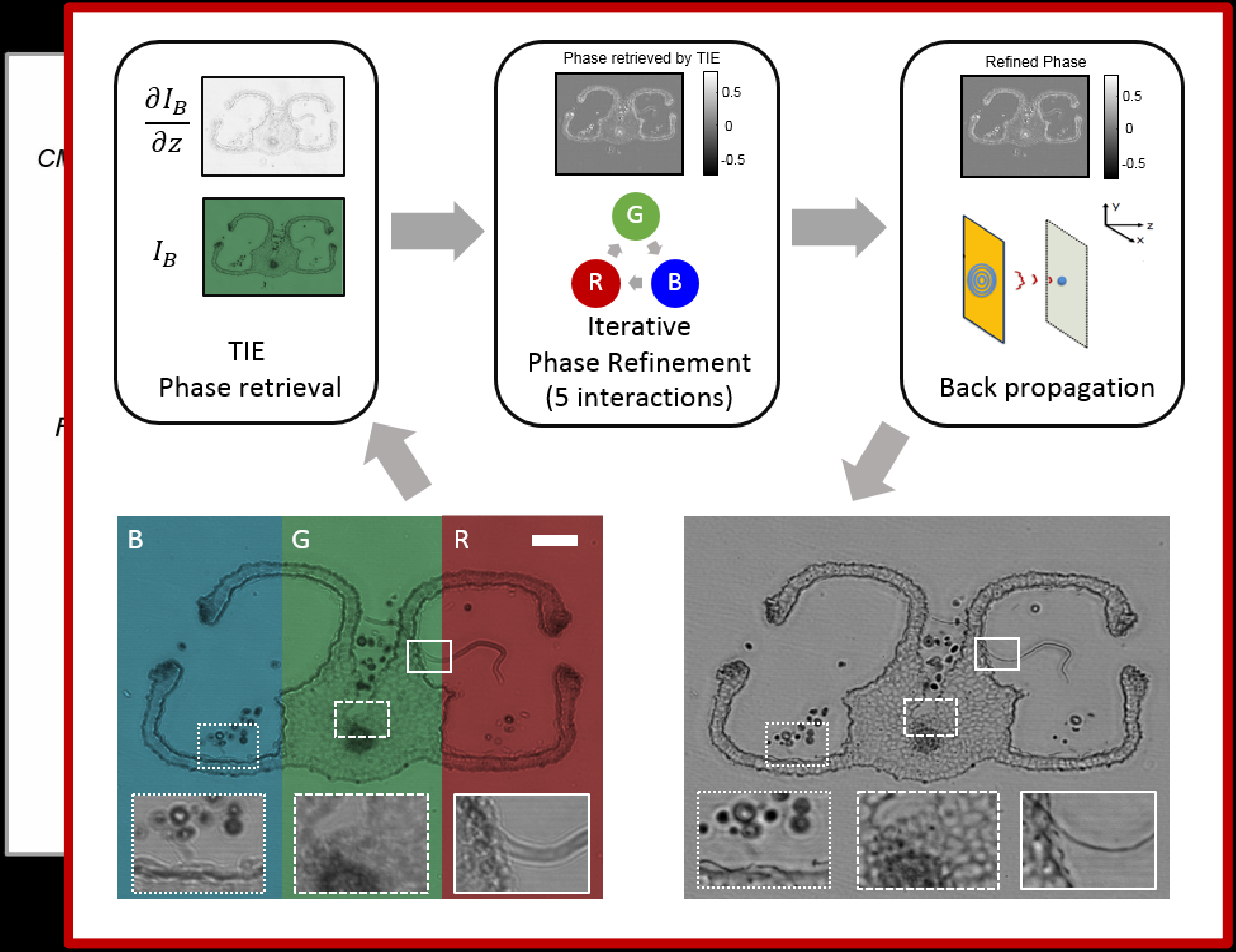

C. Zuo, J. Sun, J. Zhang, Y. Hu, and Q. Chen, Optics Express 23, 14314-14328 (2015).

Lensless TIE microscopy

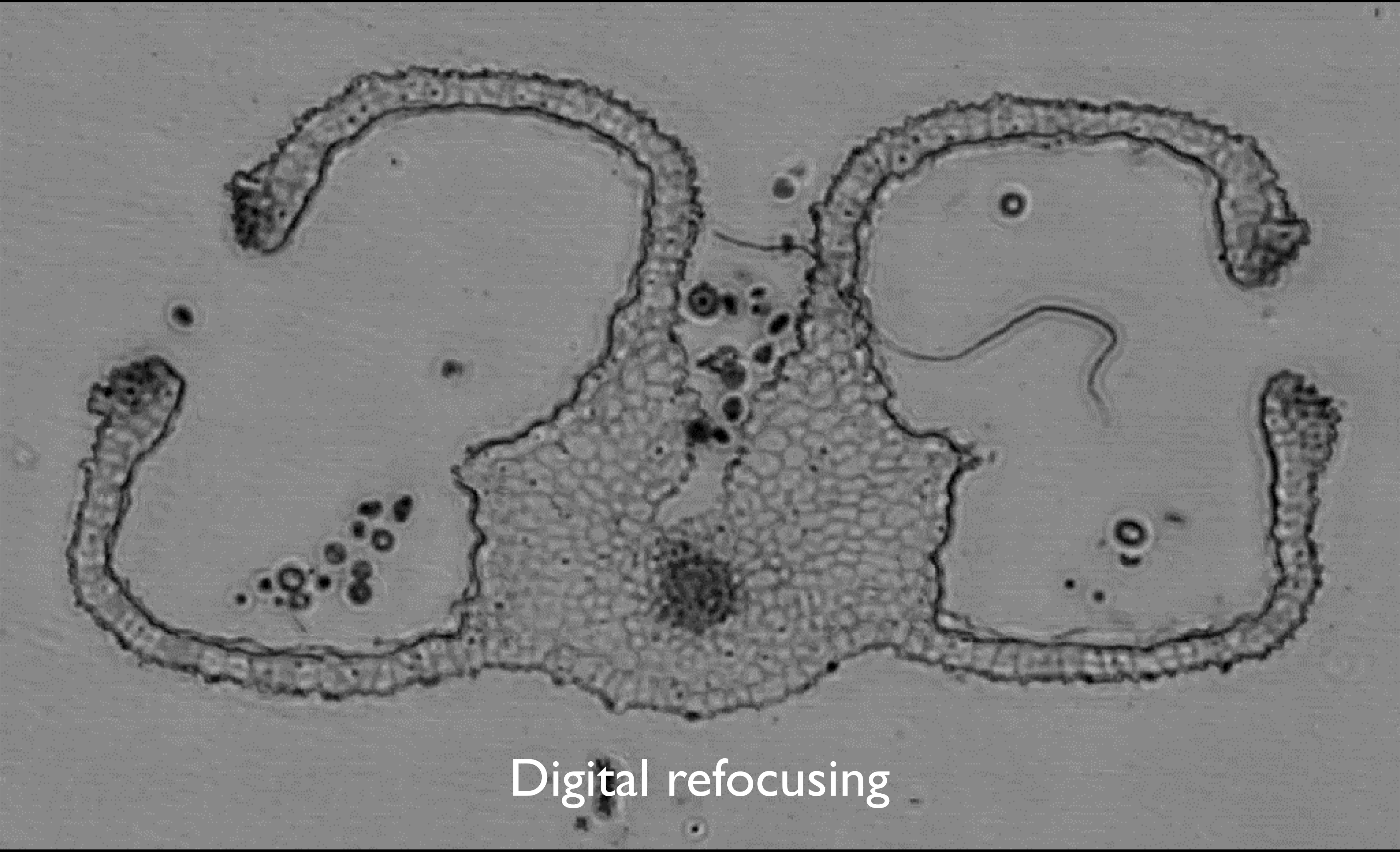

C. Zuo, J. Sun, J. Zhang, Y. Hu, and Q. Chen, Optics Express 23, 14314-14328 (2015).

Lensless TIE tomography

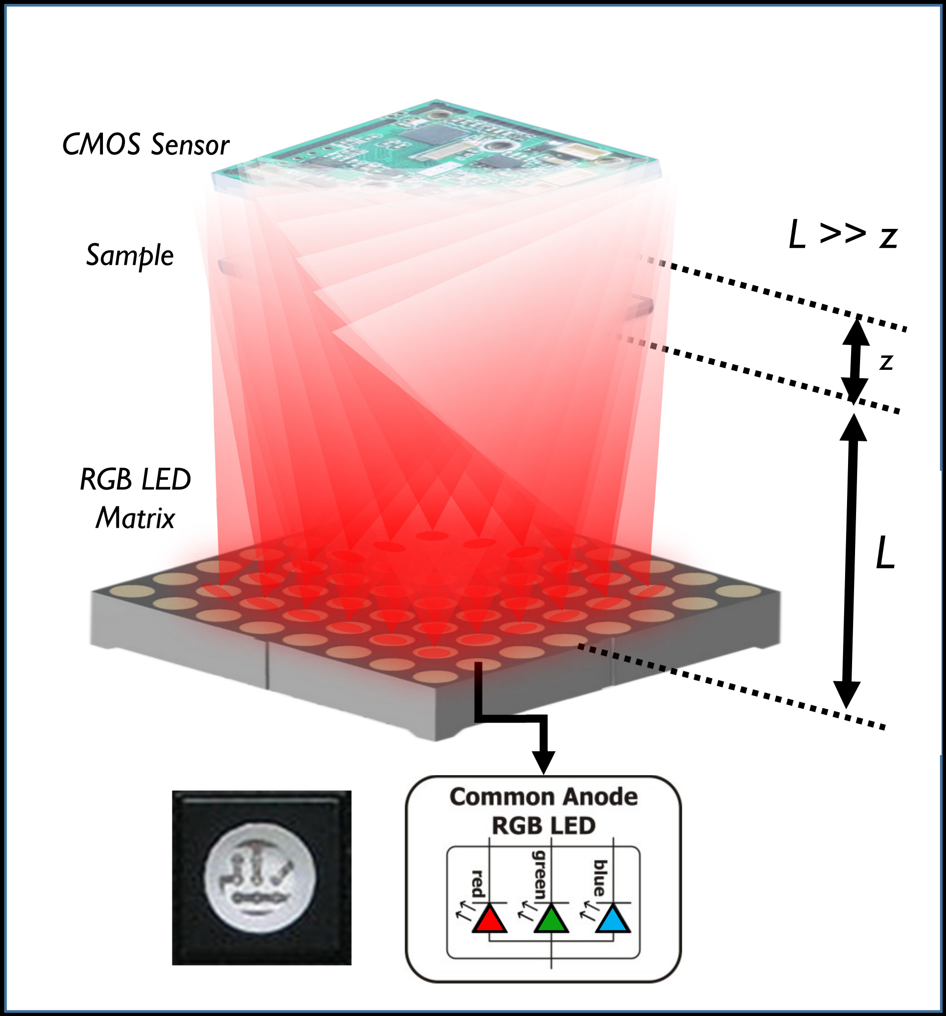

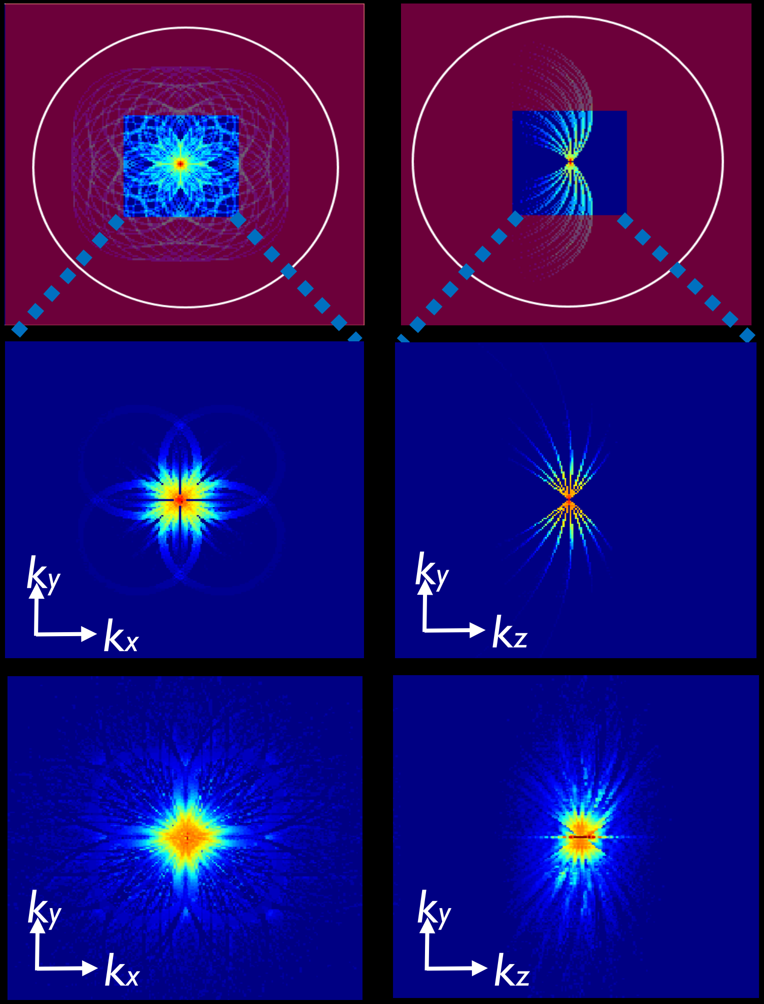

Change Illumination angle (≈±45°)

Fill the 3D Fourier Space of the object

C. Zuo, J. Sun, J. Zhang, Y. Hu, and Q. Chen, Optics Express 23, 14314-14328 (2015).

Lensless TIE tomography

The uterus of Parascaris equorum

Phase tomography

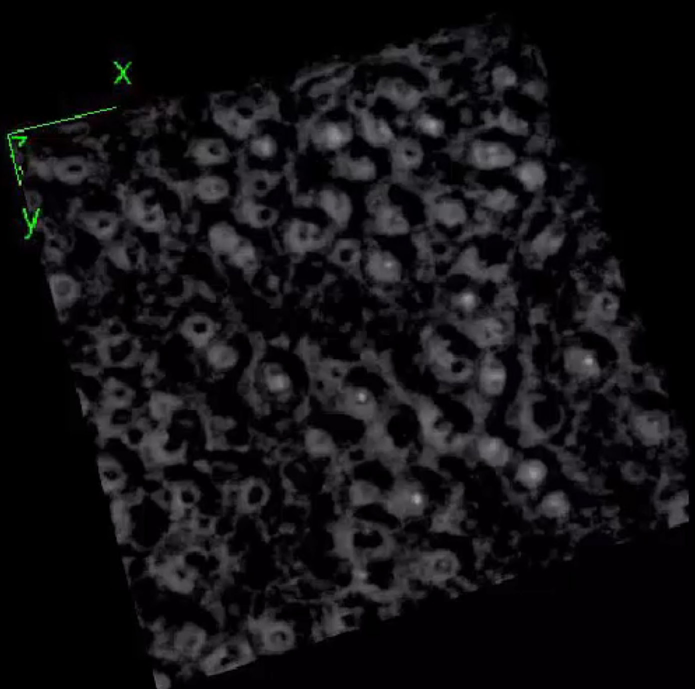

Absorption tomography

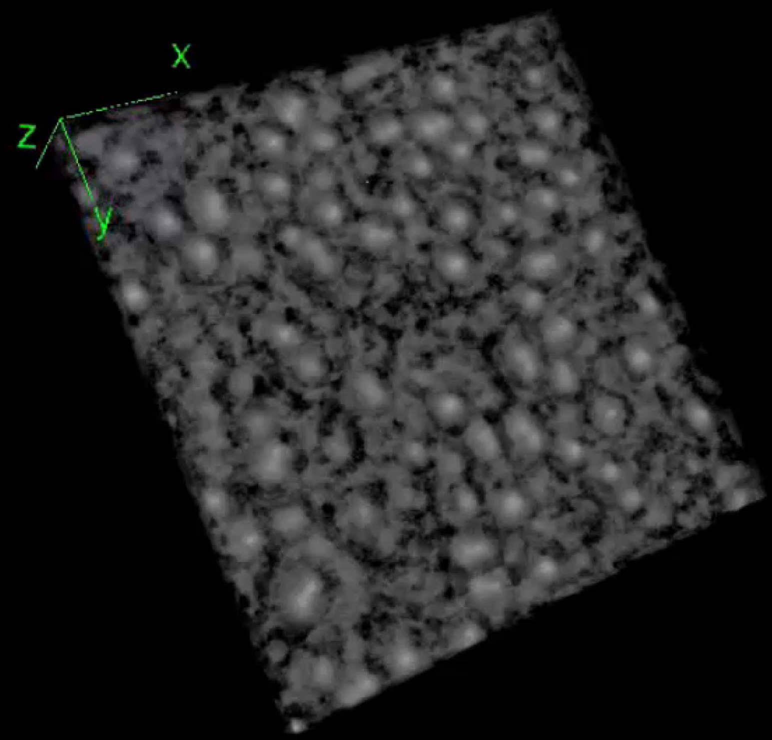

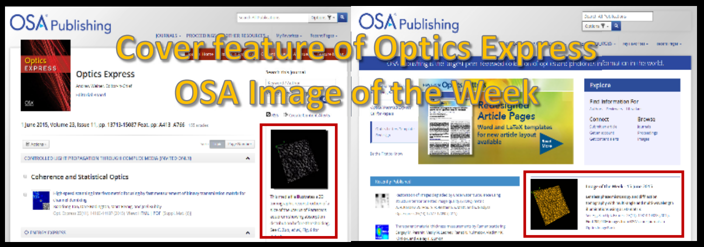

C. Zuo, J. Sun, J. Zhang, Y. Hu, and Q. Chen, Optics Express 23, 14314-14328 (2015).

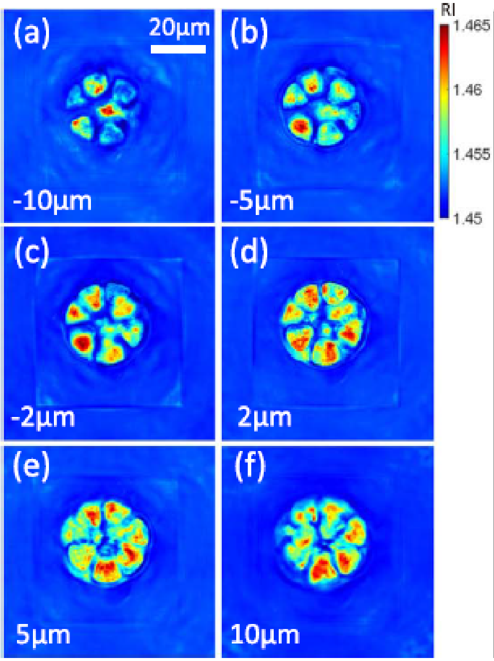

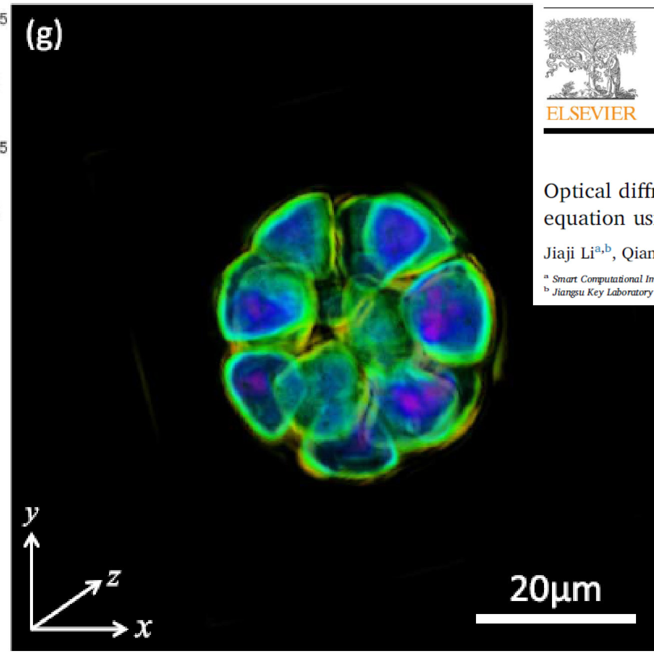

Optics and Lasers in Engineering 95 (2017) 26–34

Contents lists available at ScienceDirect

Optics and Lasers in Engineering

journal homepage: www.elsevier.com/locate/optlaseng

Optical diffraction tomography microscopy with transport of intensity equation using a light-emitting diode array

Jiaji Li[a,b], Qian Chen[b], Jialin Zhang[a,b], Zhao Zhang[a,b], Yan Zhang[a,b], Chao Zuo[a,b,*]

[a] Smart Computational Imaging (SCI) Laboratory, Nanjing University of Science and Technology, Nanjing, Jiangsu 210094, China
[b] Jiangsu Key Laboratory of Spectral Imaging & Intelligent Sense, Nanjing University of Science and Technology, Nanjing, Jiangsu 210094, China

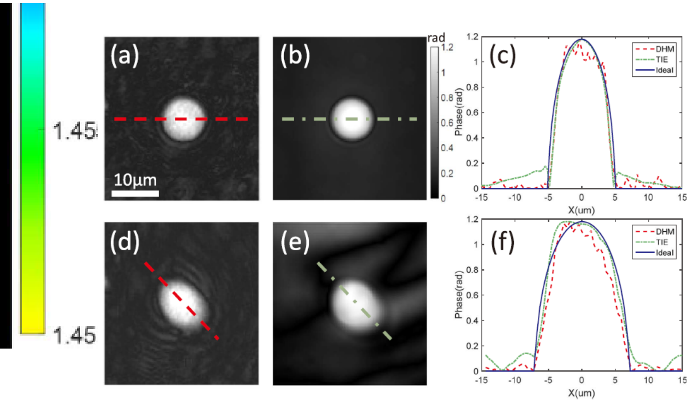

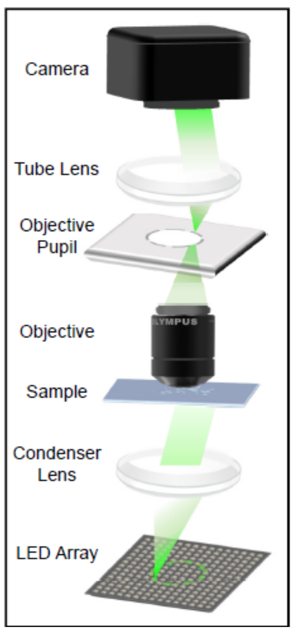

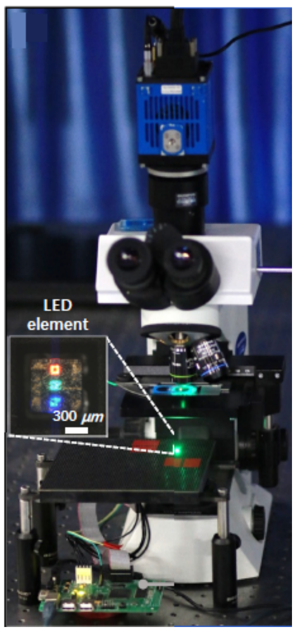

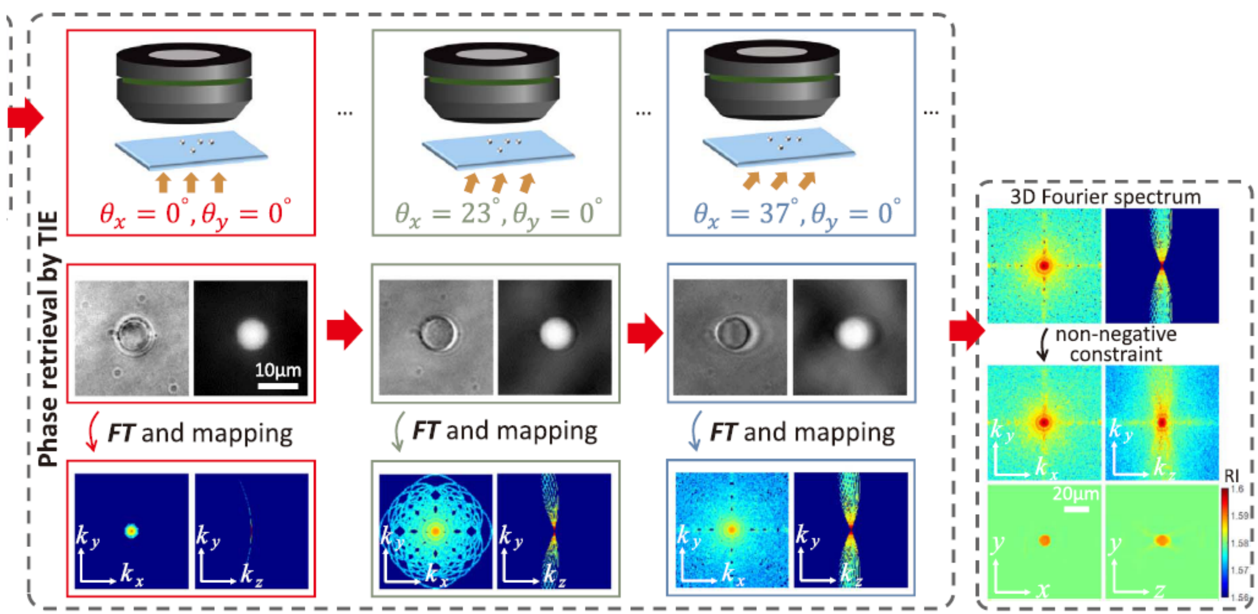

Transport of intensity equation

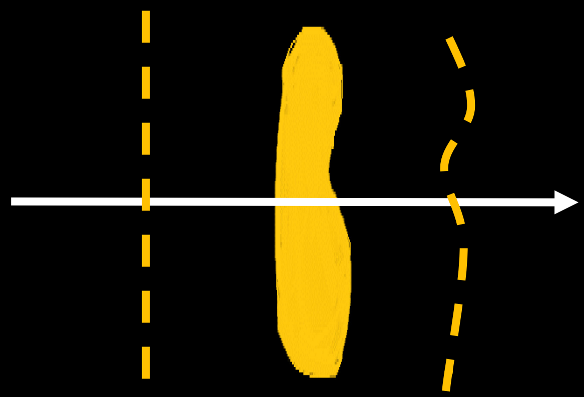

$$-k\frac{\partial I}{\partial z} = \nabla \cdot (I\nabla \emptyset)$$

$$-k\ \left(\frac{I_{-\Delta z} - I_{+\Delta z}}{2\Delta z}\right)\ = \nabla I \cdot \nabla \emptyset + I\nabla^2 \emptyset$$

沿着光轴采集两幅图像，
光强的轴向微分

当相位为常数时，等式右边为0，此时观察不到光强传输现象。当物体为纯相位物体(或者弱吸收物体)，其光波场的光强I为常数时，等式右边则变为$I\nabla^2\emptyset$

$$-k\frac{\partial I}{\partial z} = I\nabla^2 \emptyset$$

TIE Phase retrieval(noise-free)

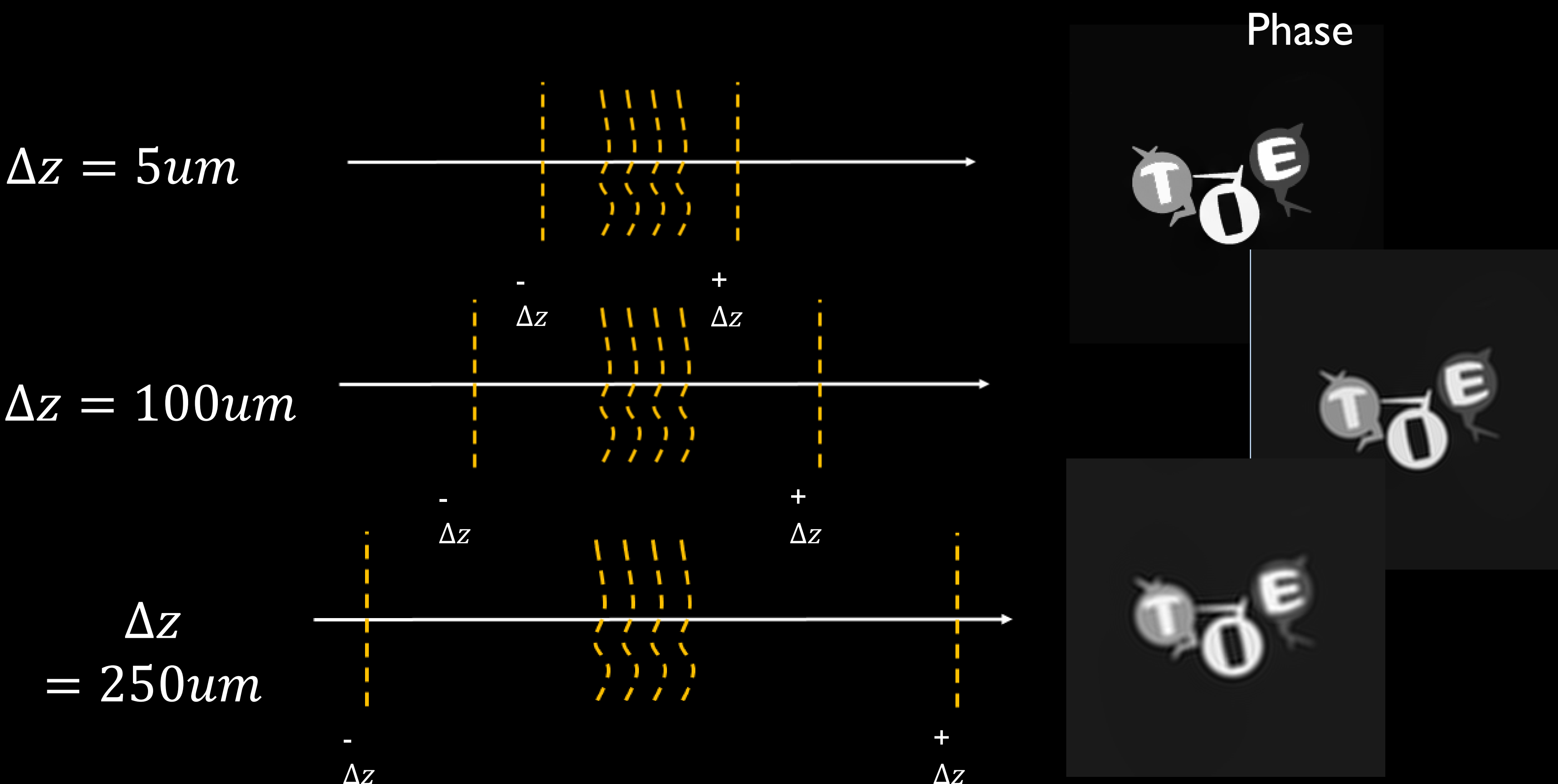

TIE Phase retrieval(Gauss noise 0.002)

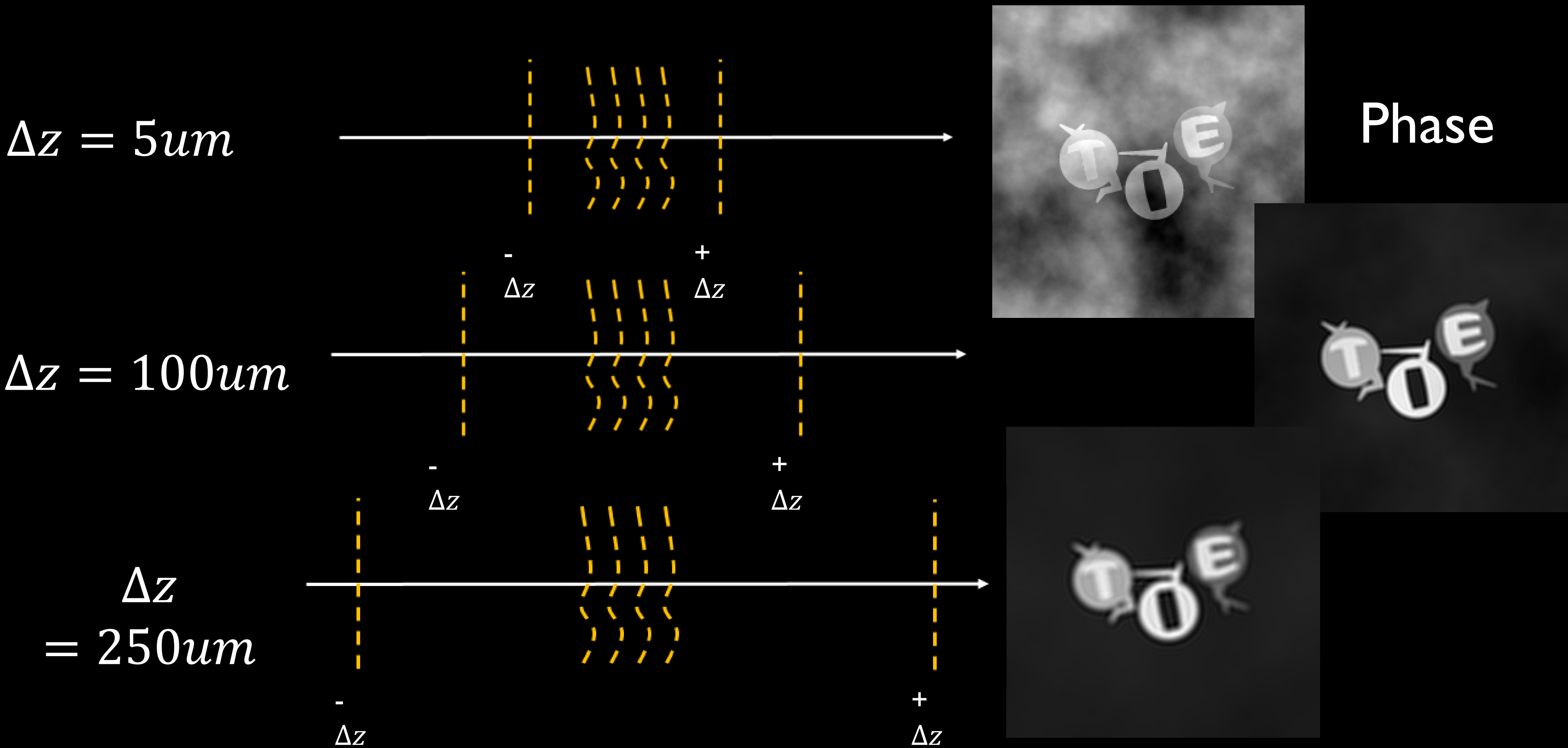

About Setup

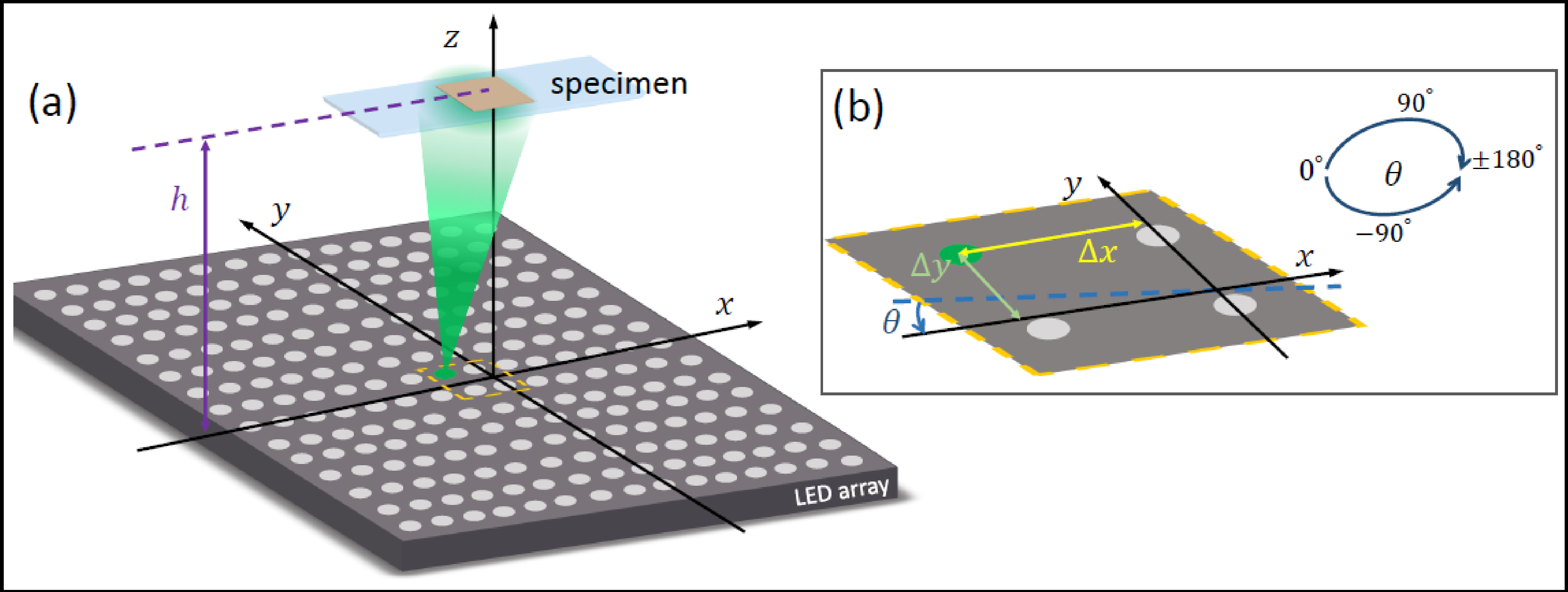

Schematic diagram of imaging system

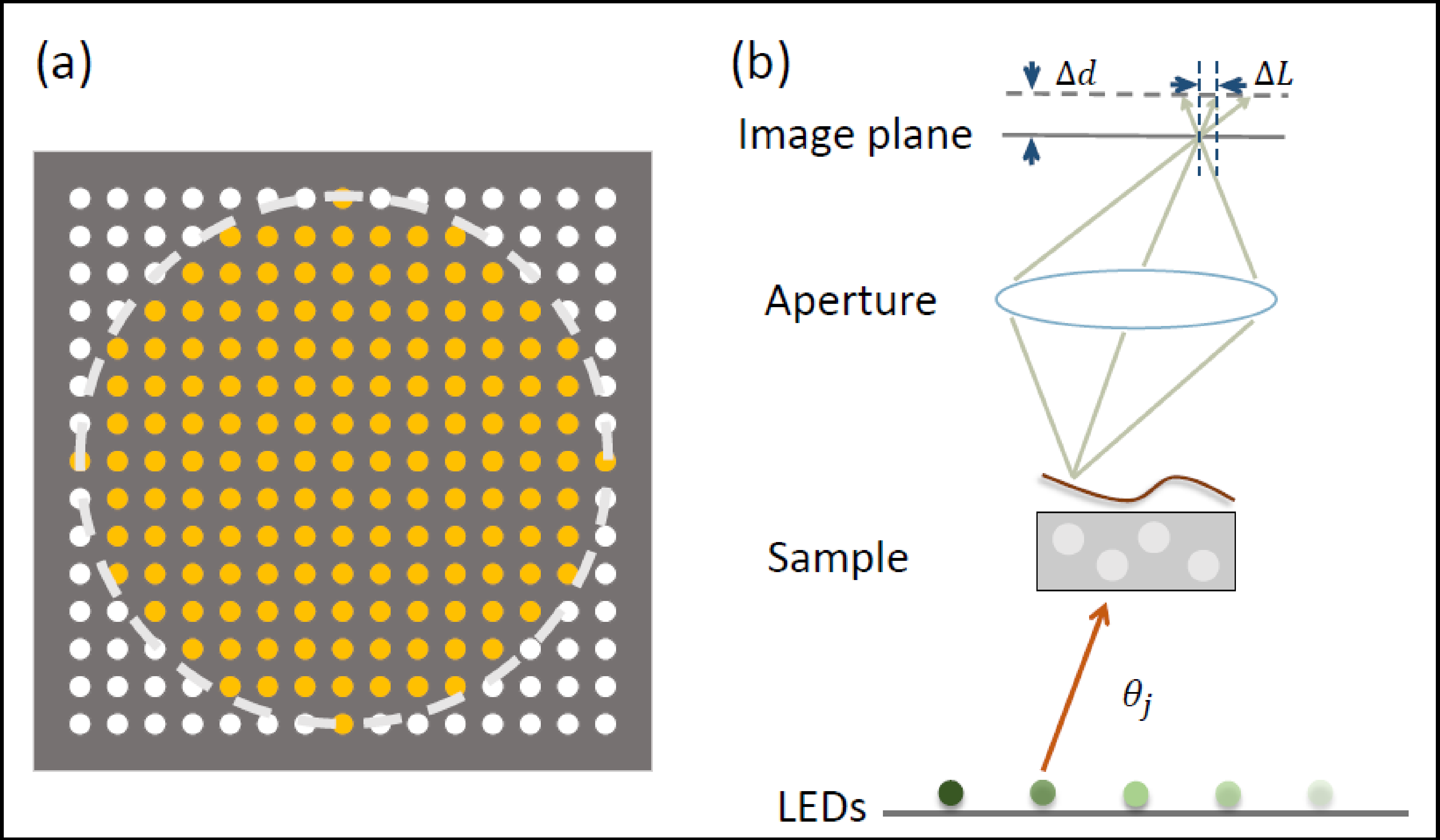

The procedure of diffraction tomography imaging

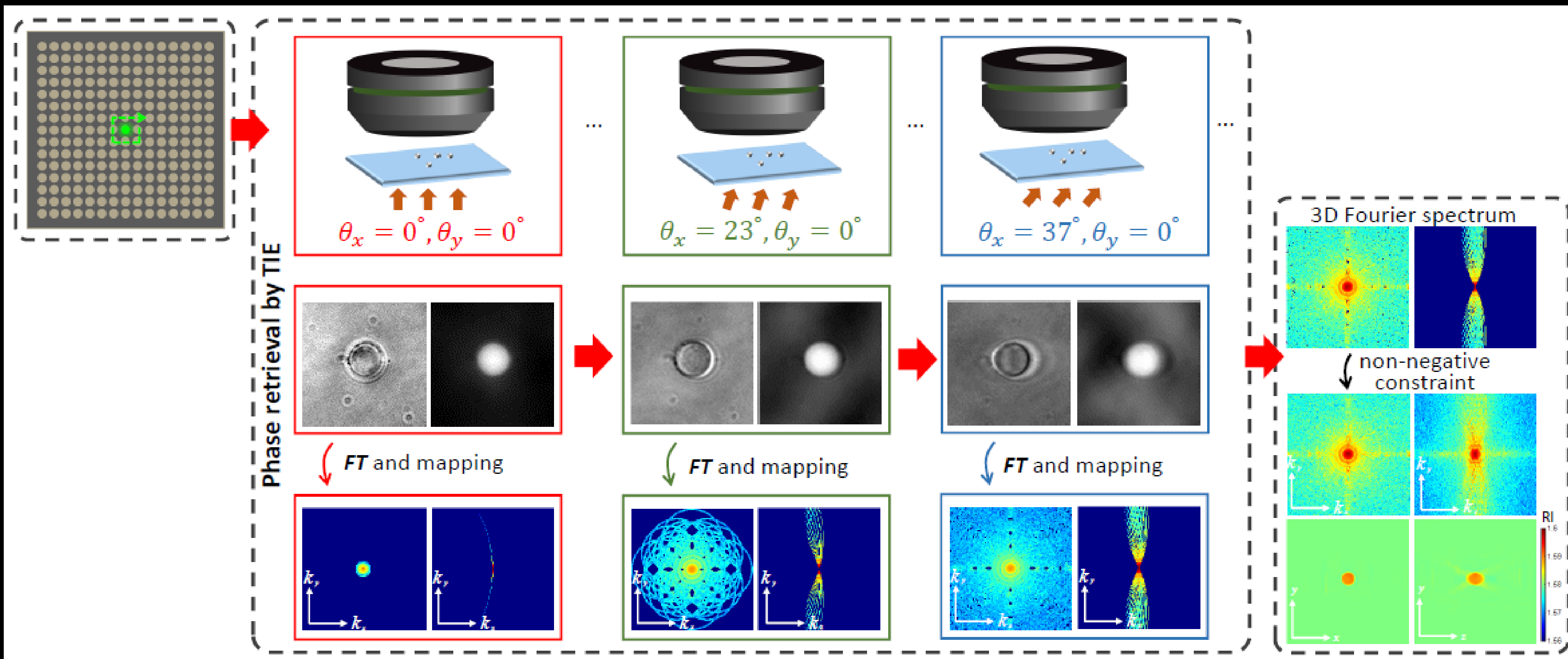

Positional misalignment correction for LED array

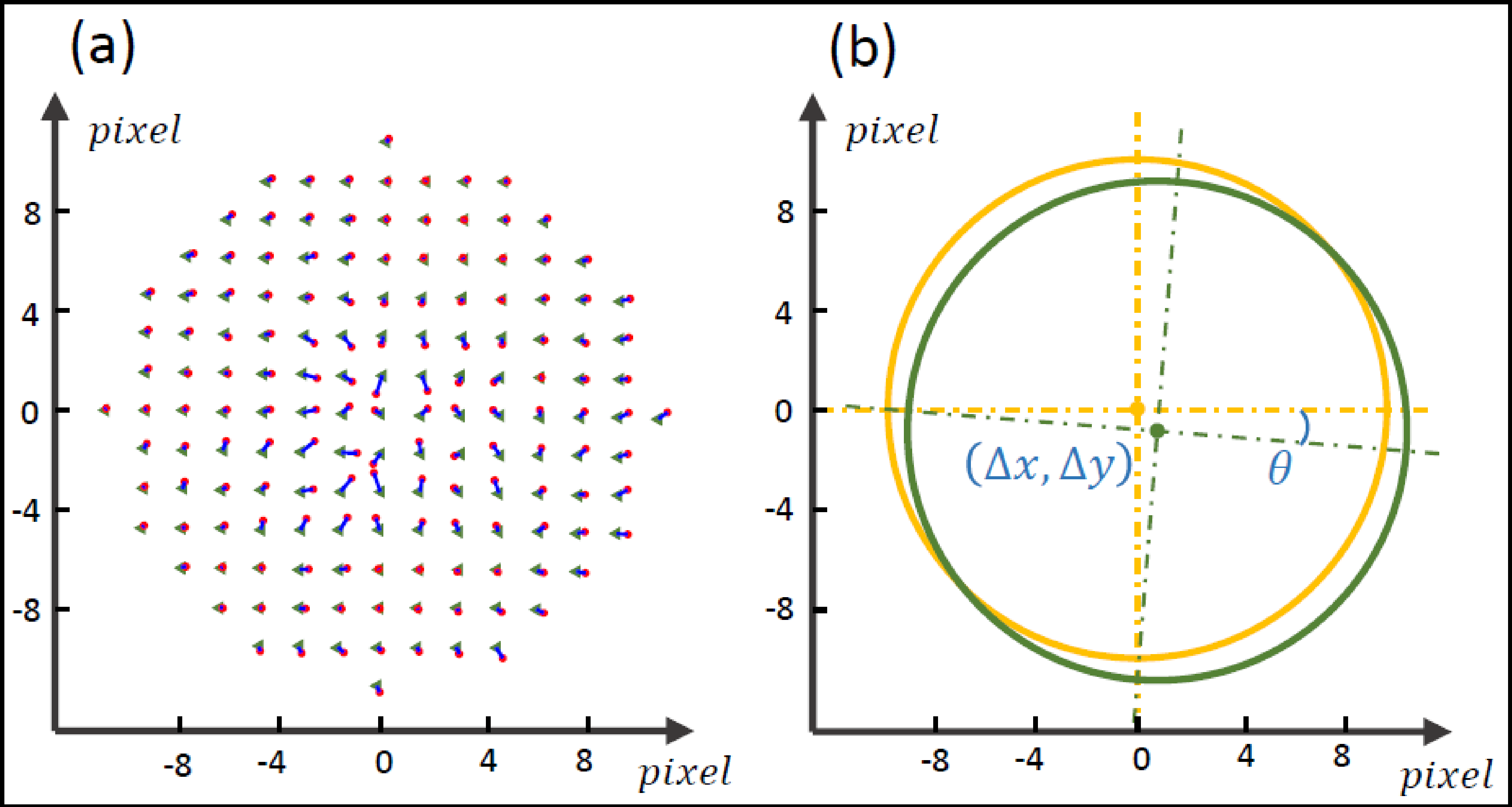

Comparison results of phase measurement between DHM and TIE

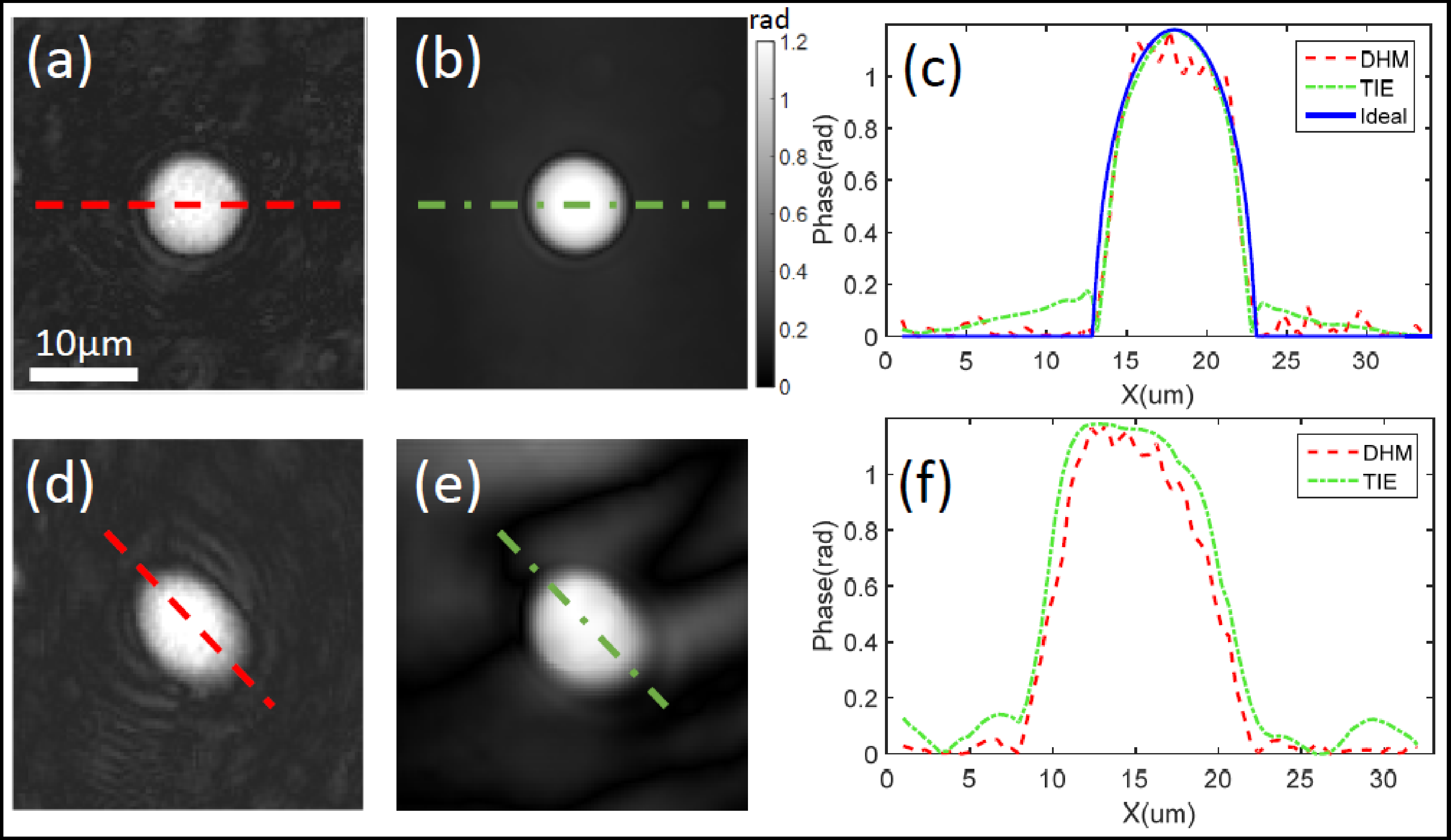

The comparison images of final 3D structure and Fourier spectrum

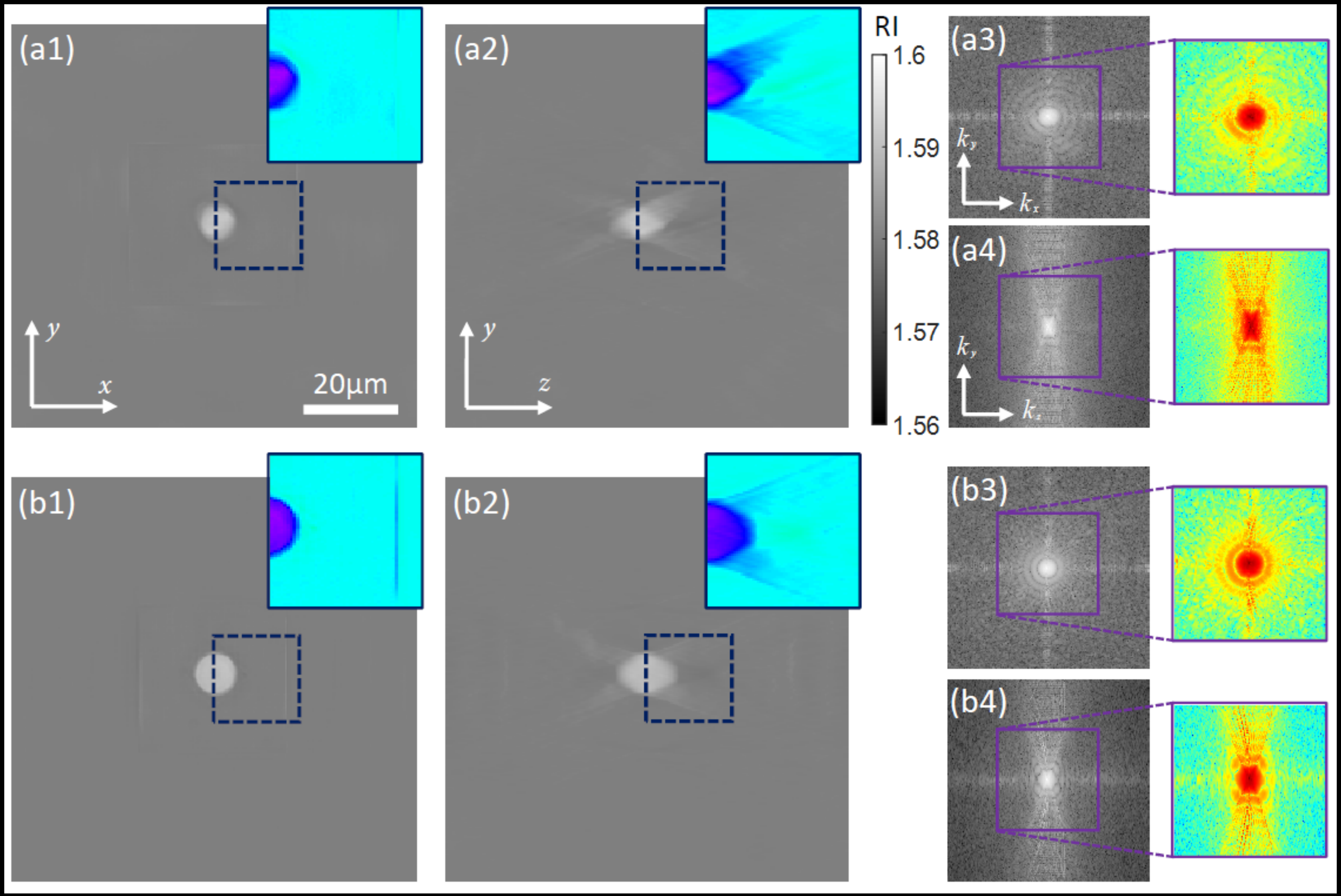

Tomographic reconstruction of polystyrene bead

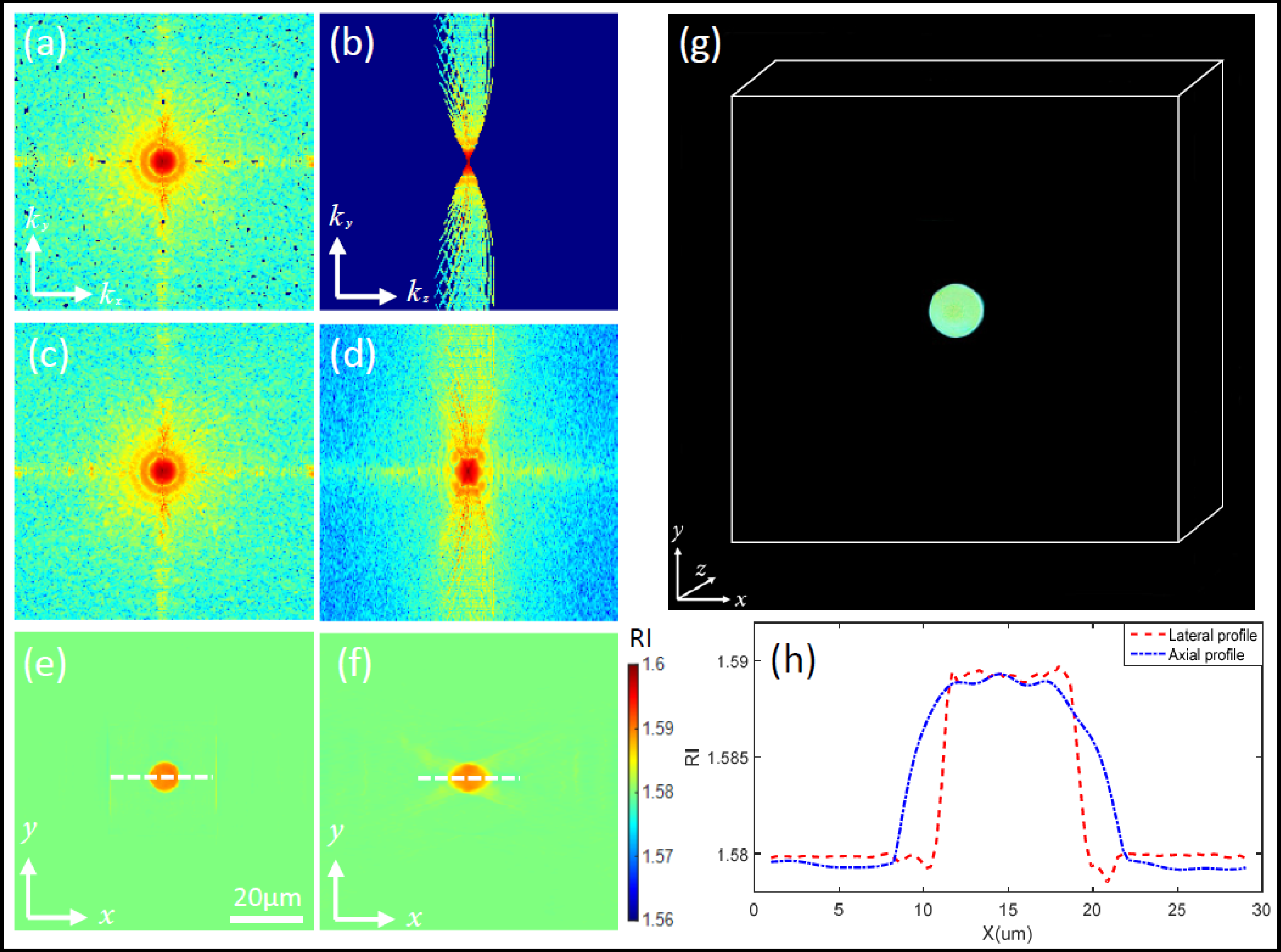

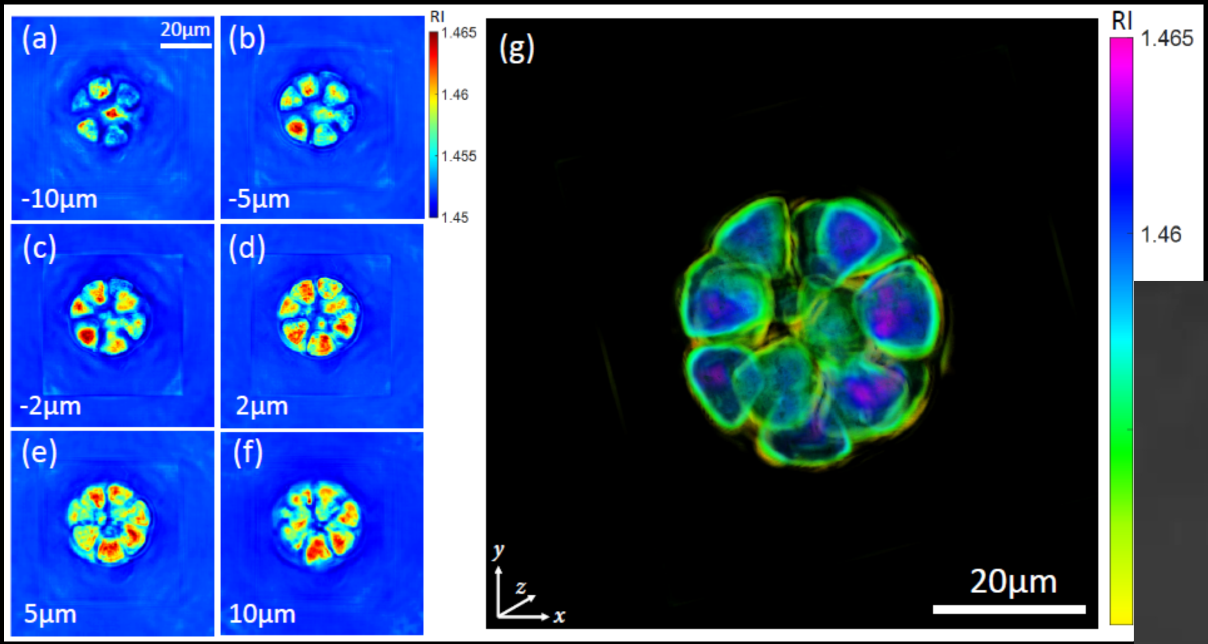

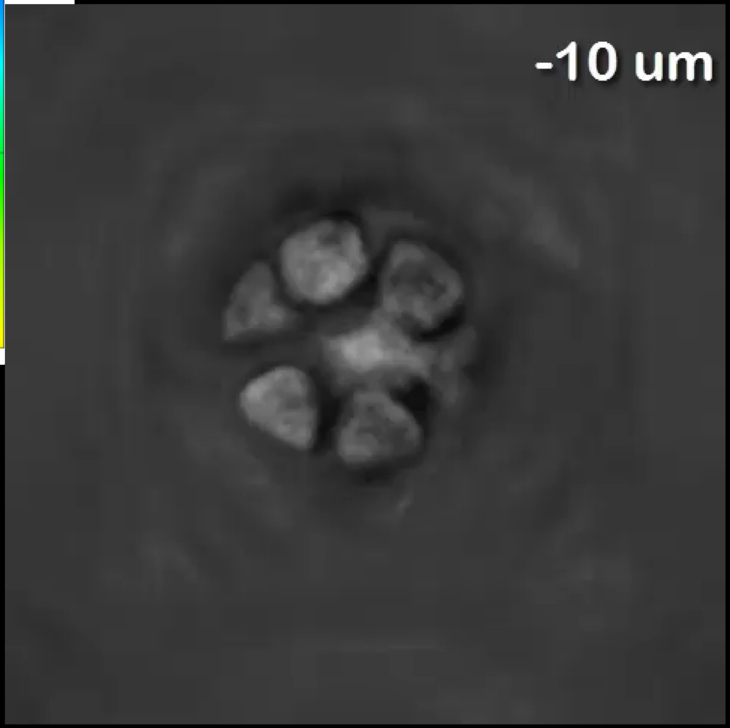

Imaging results of the fixed sample of Pandorina morum

3D refractive index tomograms rendering of lung cancer cell and HeLa cell

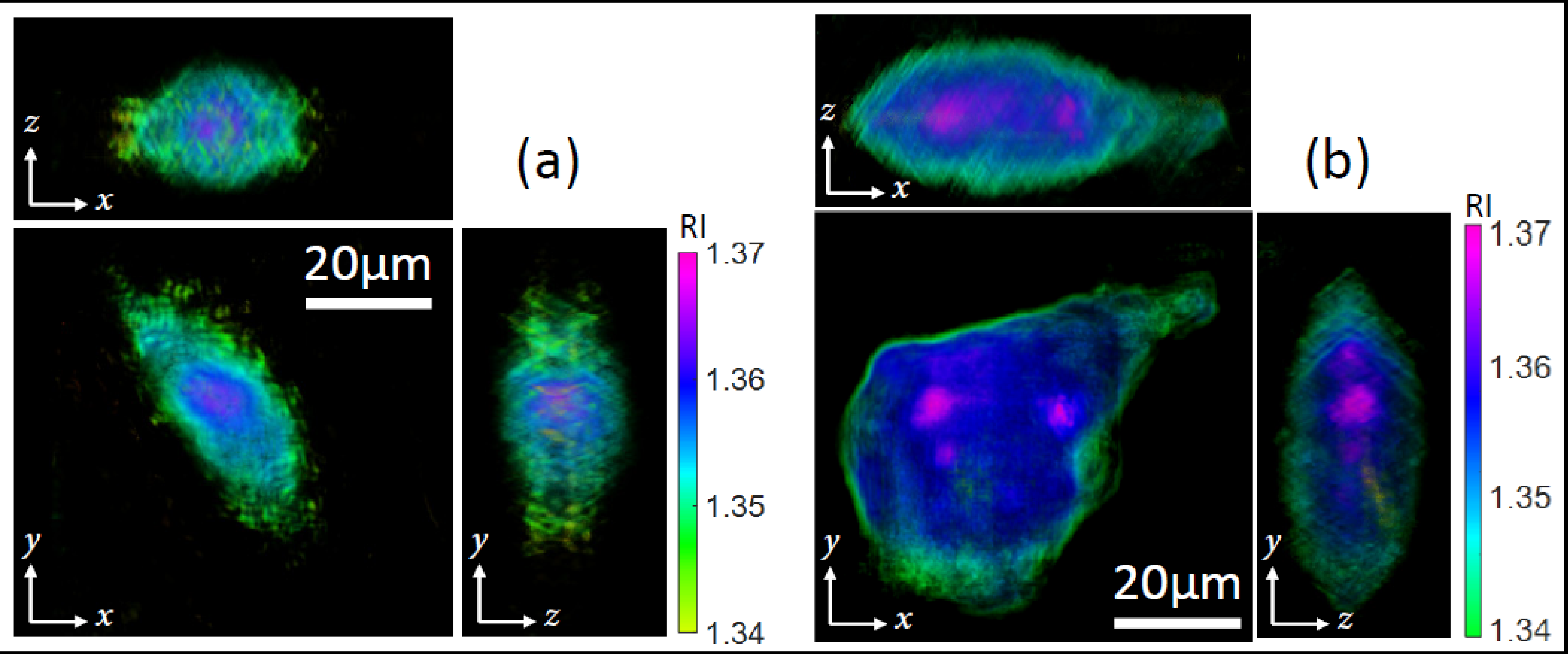

Iterative method for Diffraction tomography

Fourier ptychographic diffraction tomography (FPDT)

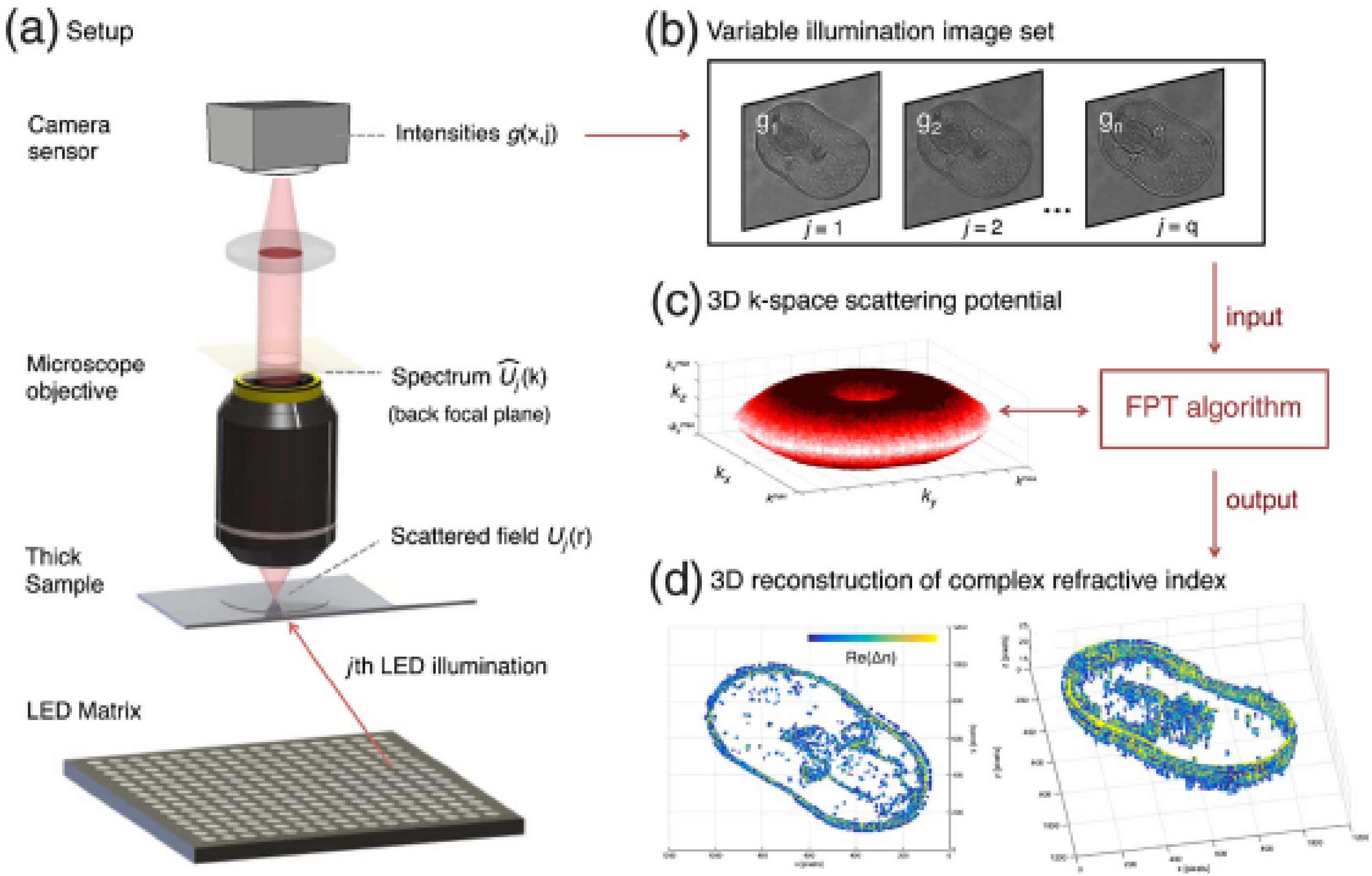

Horstmeyer, Roarke, et al. *Optica* 3.8 (2016): 827-835.

Fourier ptychographic diffraction tomography (FPDT)

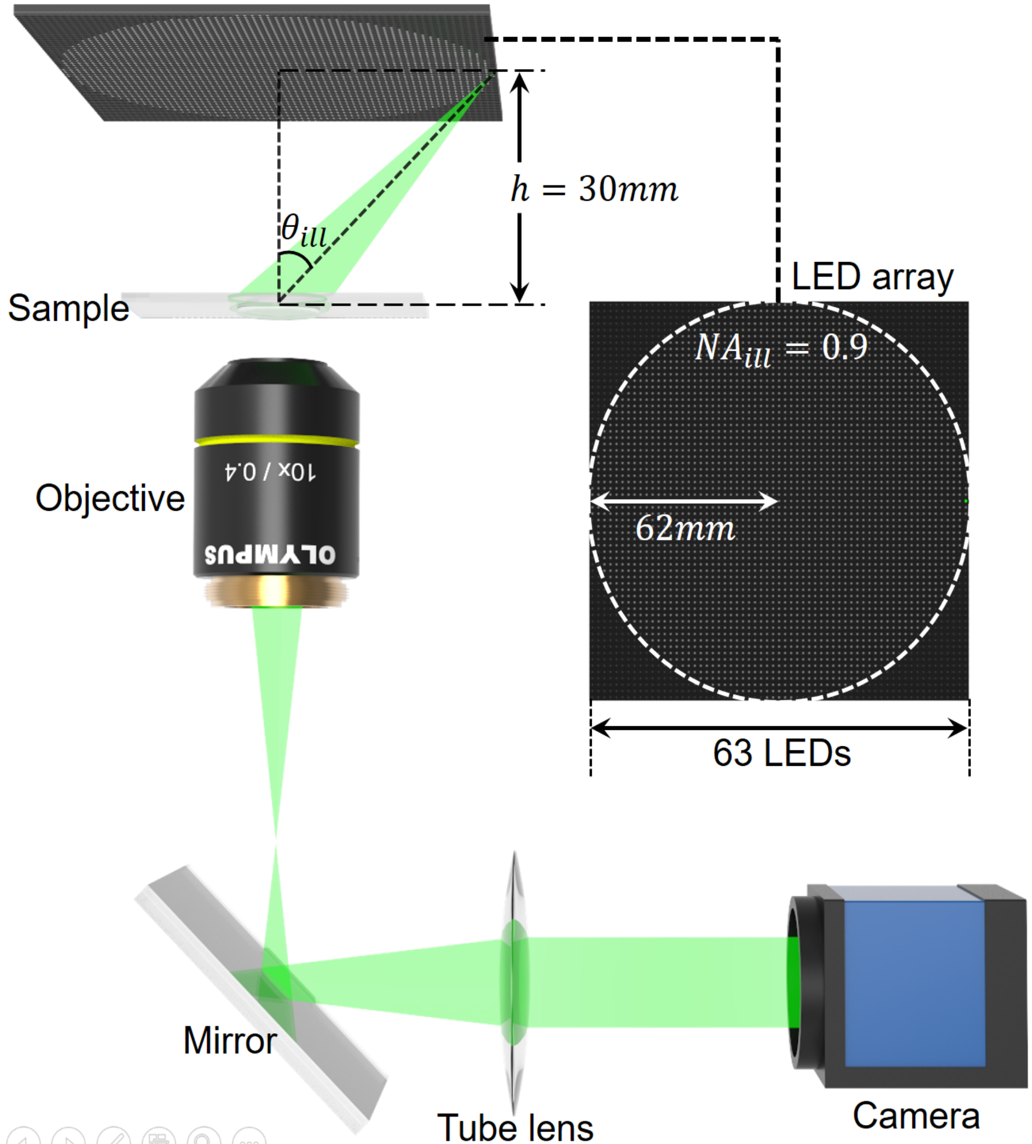

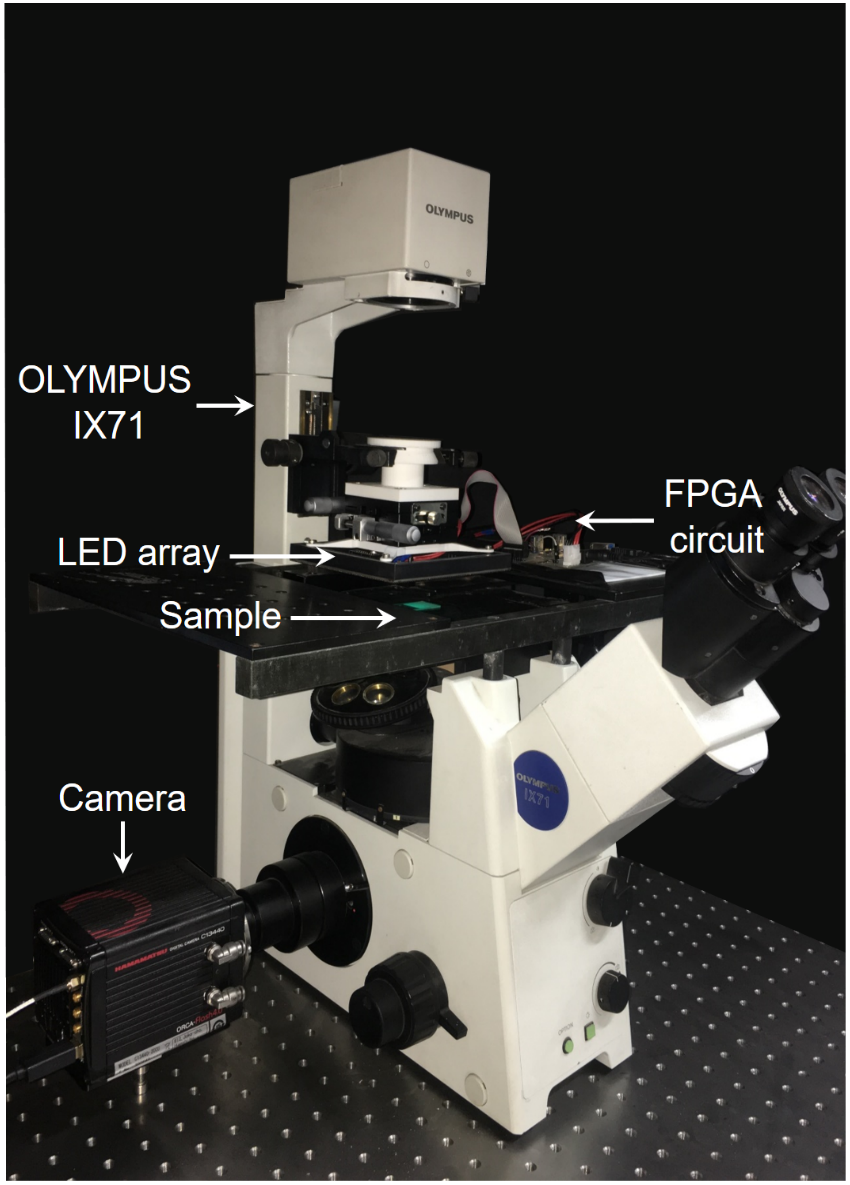

FPDT image formation

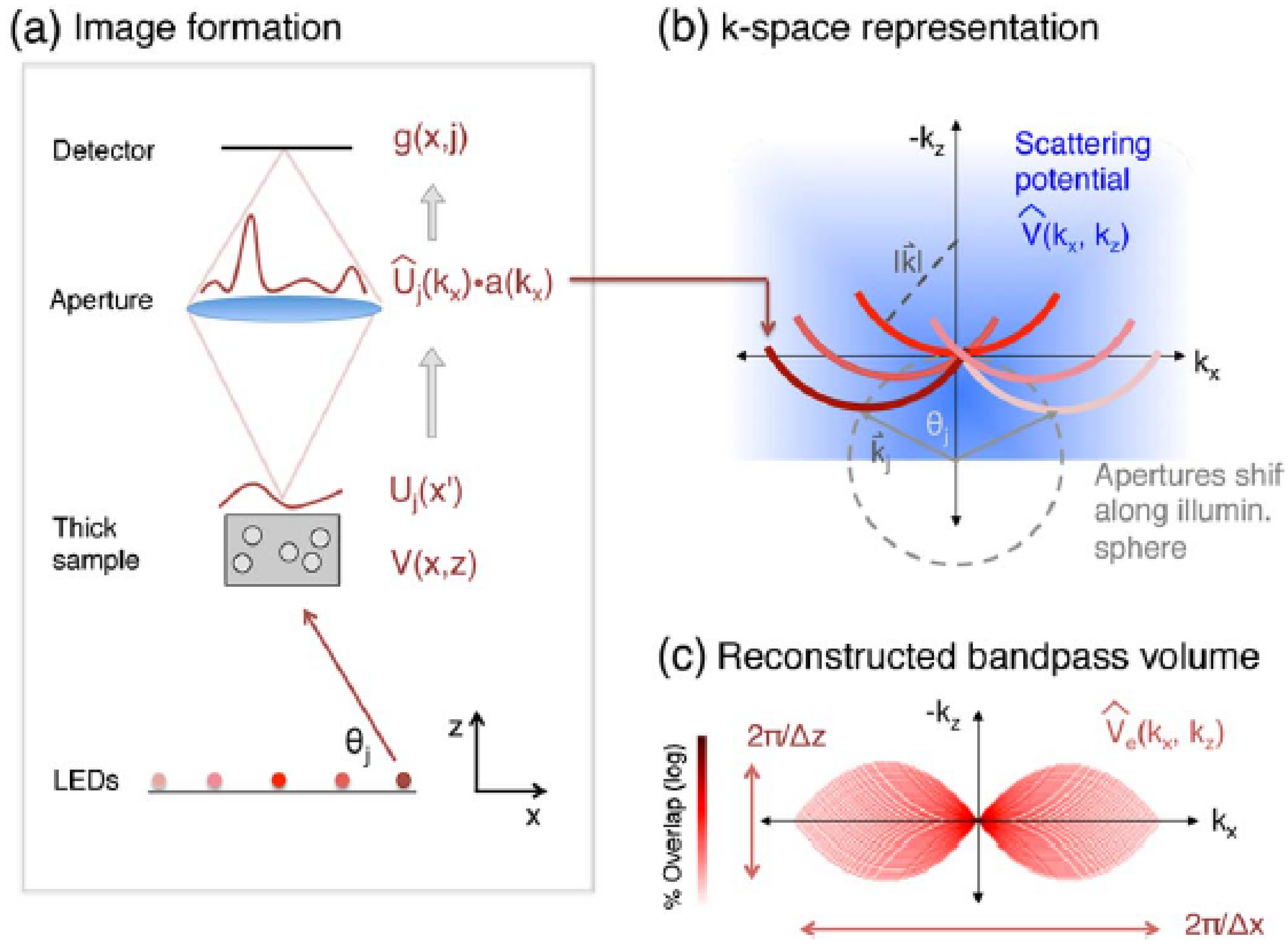

Fourier ptychographic diffraction tomography (FPDT)

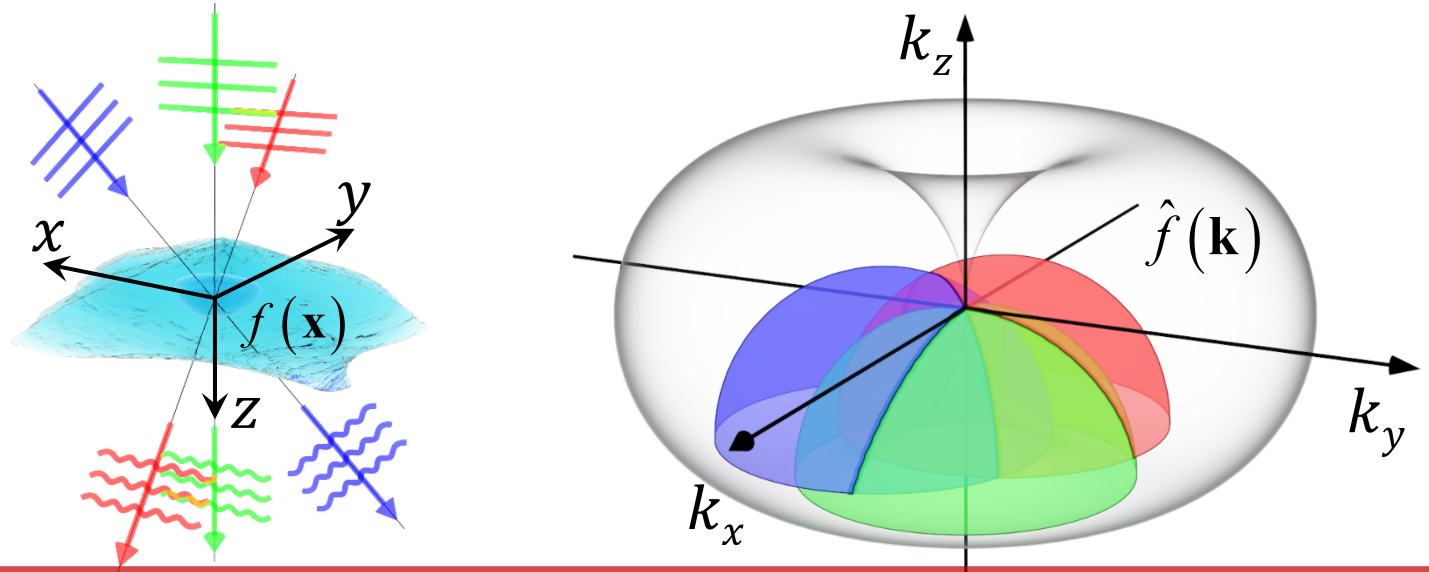

Free-space: semi-sphere in 3D Fourier space

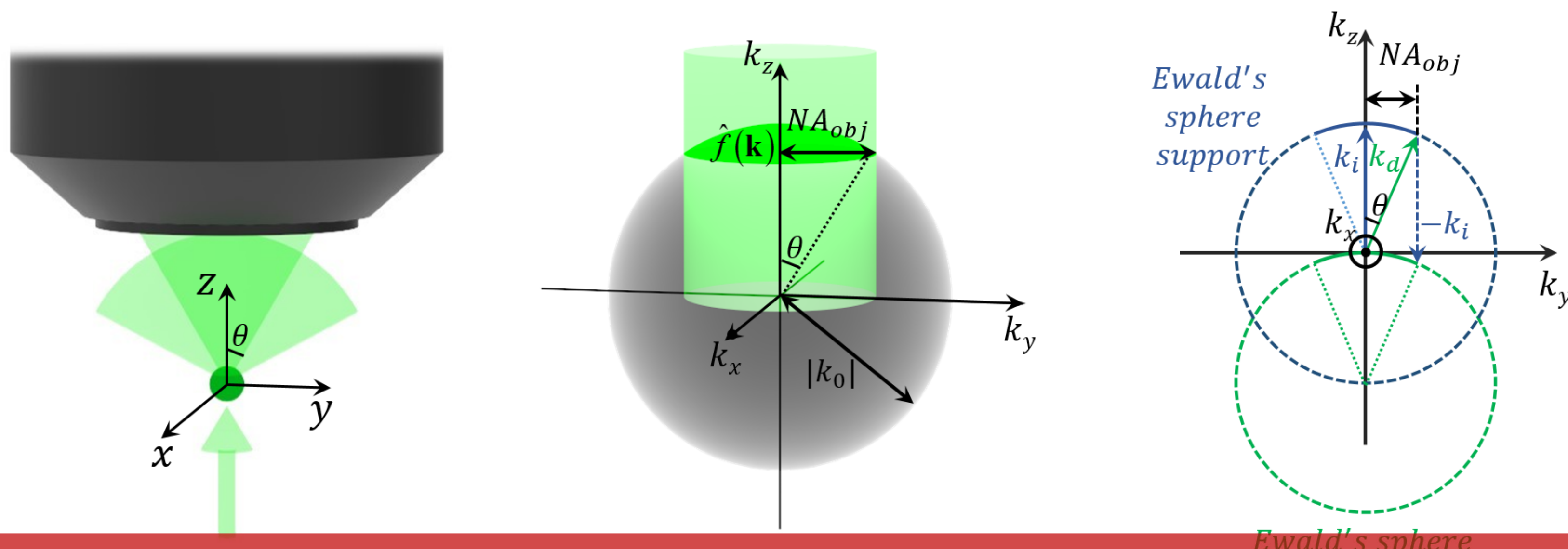

Microscopic imaging: partial spherical cap bounded by the lens aperture

Fourier ptychographic diffraction tomography (FPDT)

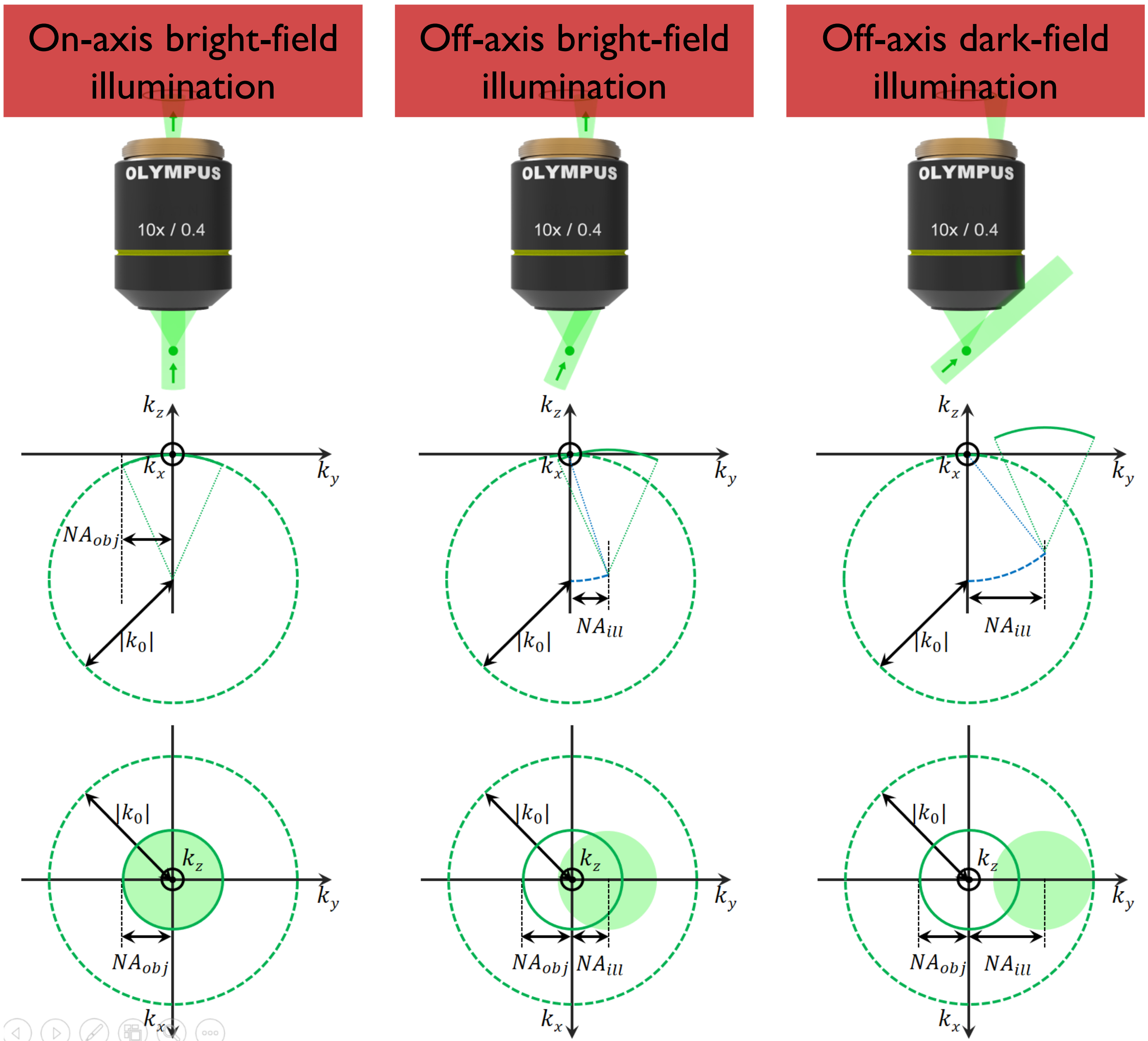

On-axis bright-field illumination

Synthetic aperture using bright-field images

Synthetic aperture using both bright- and dark-field (0.9NA) images

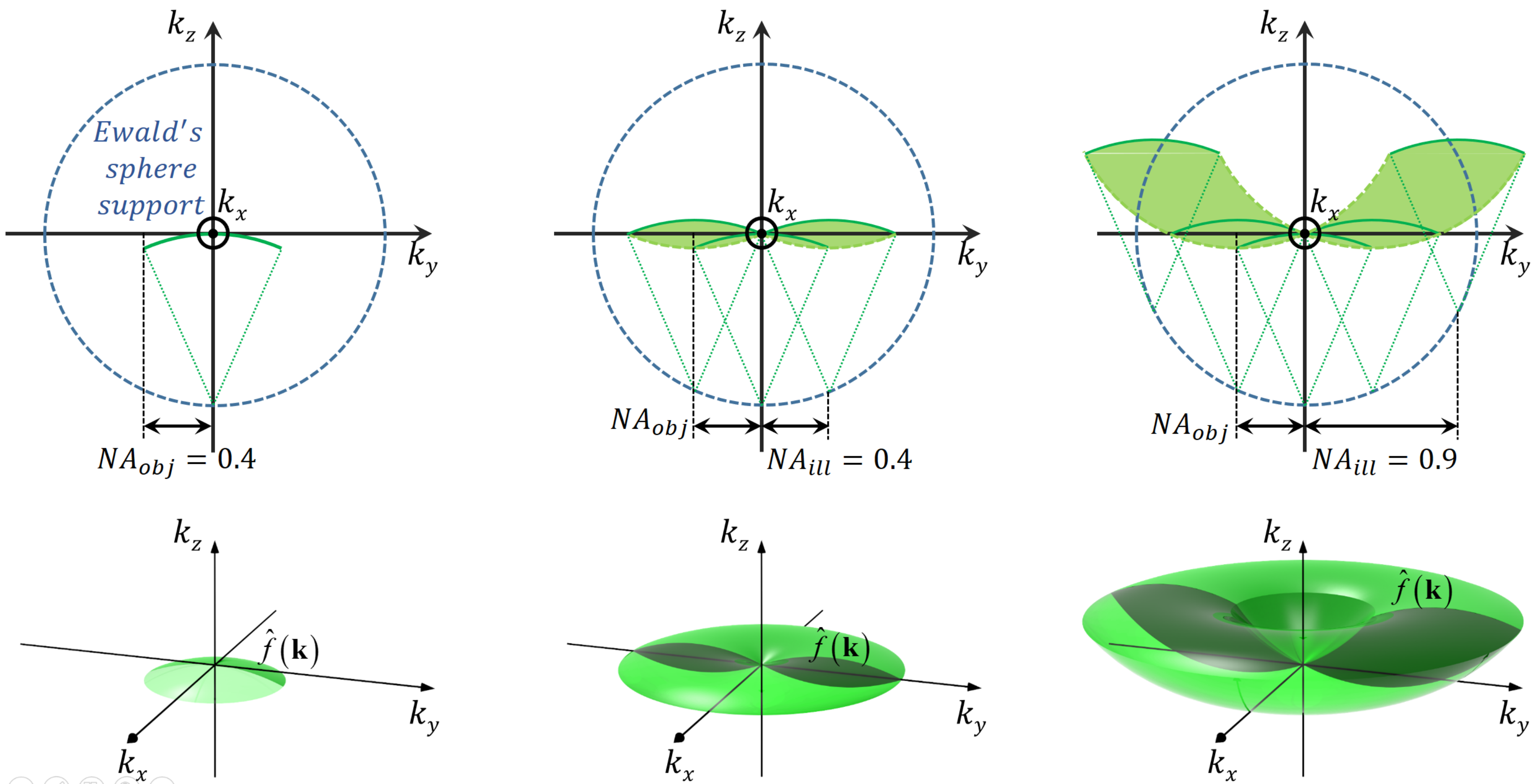

$$NA_{obj} = 0.4 \;\; \lambda = 507\text{nm}$$

Fourier ptychographic diffraction tomography (FPDT)

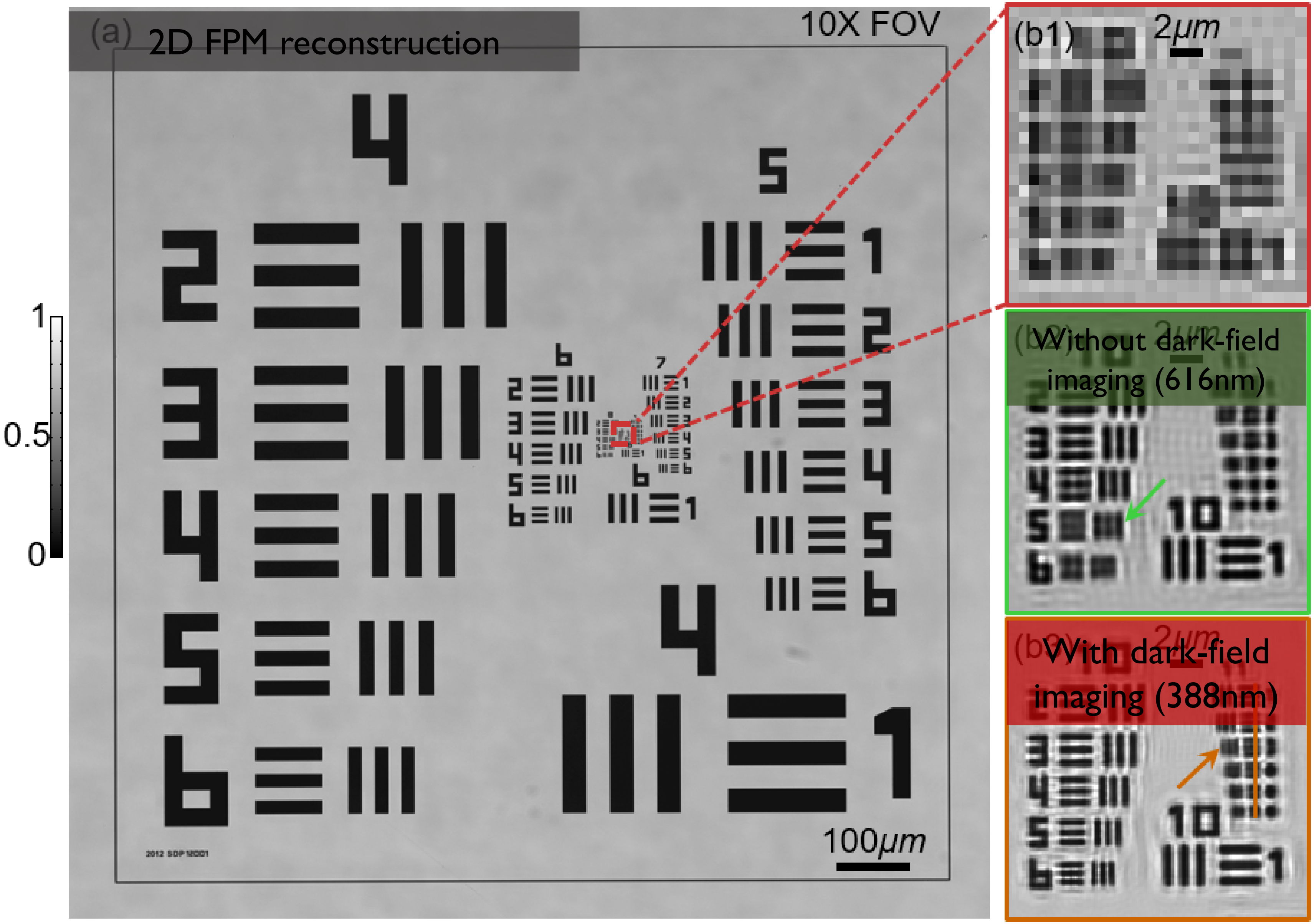

Fourier ptychographic diffraction tomography (FPDT)

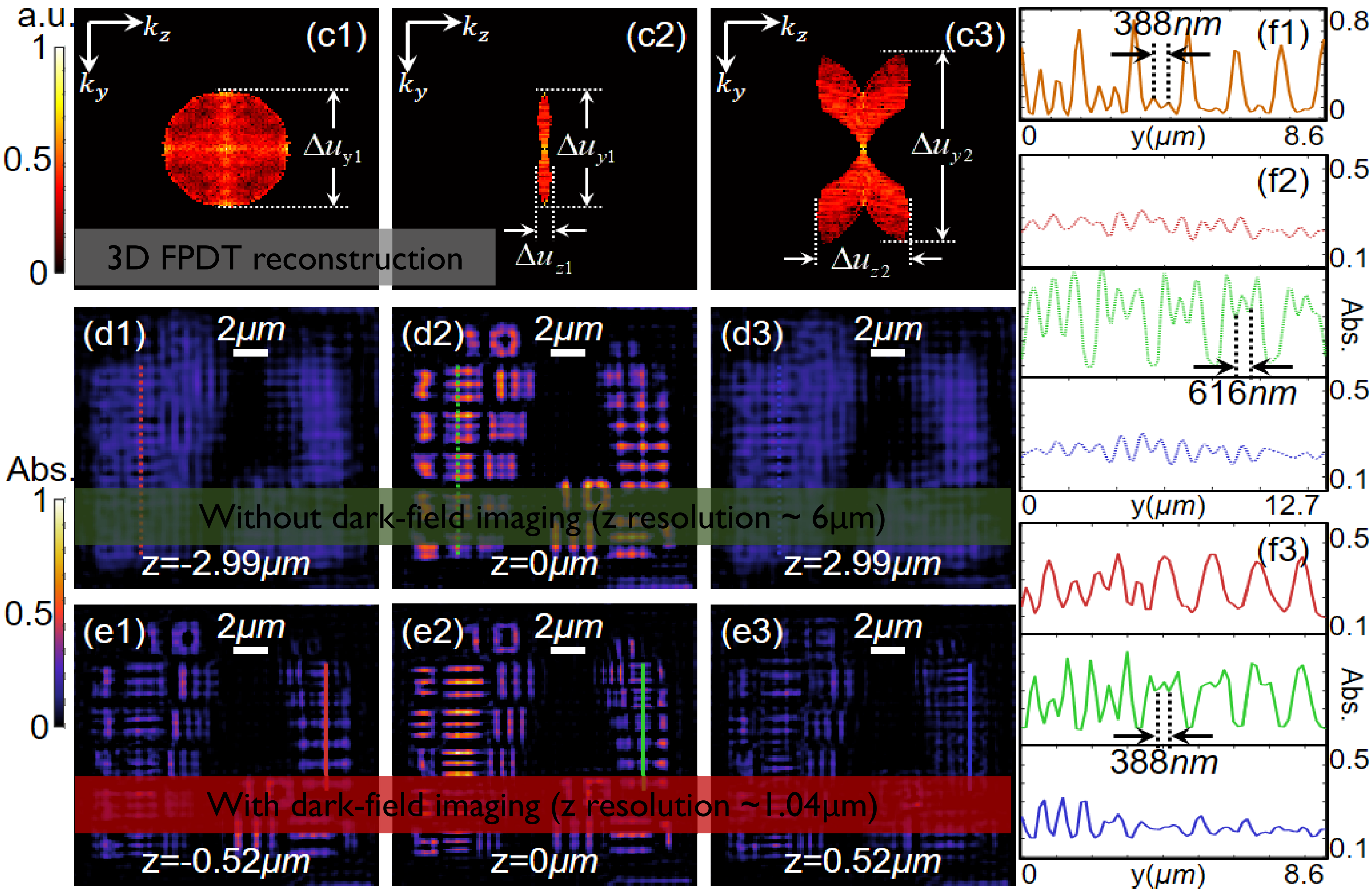

Fourier ptychographic diffraction tomography (FPDT)

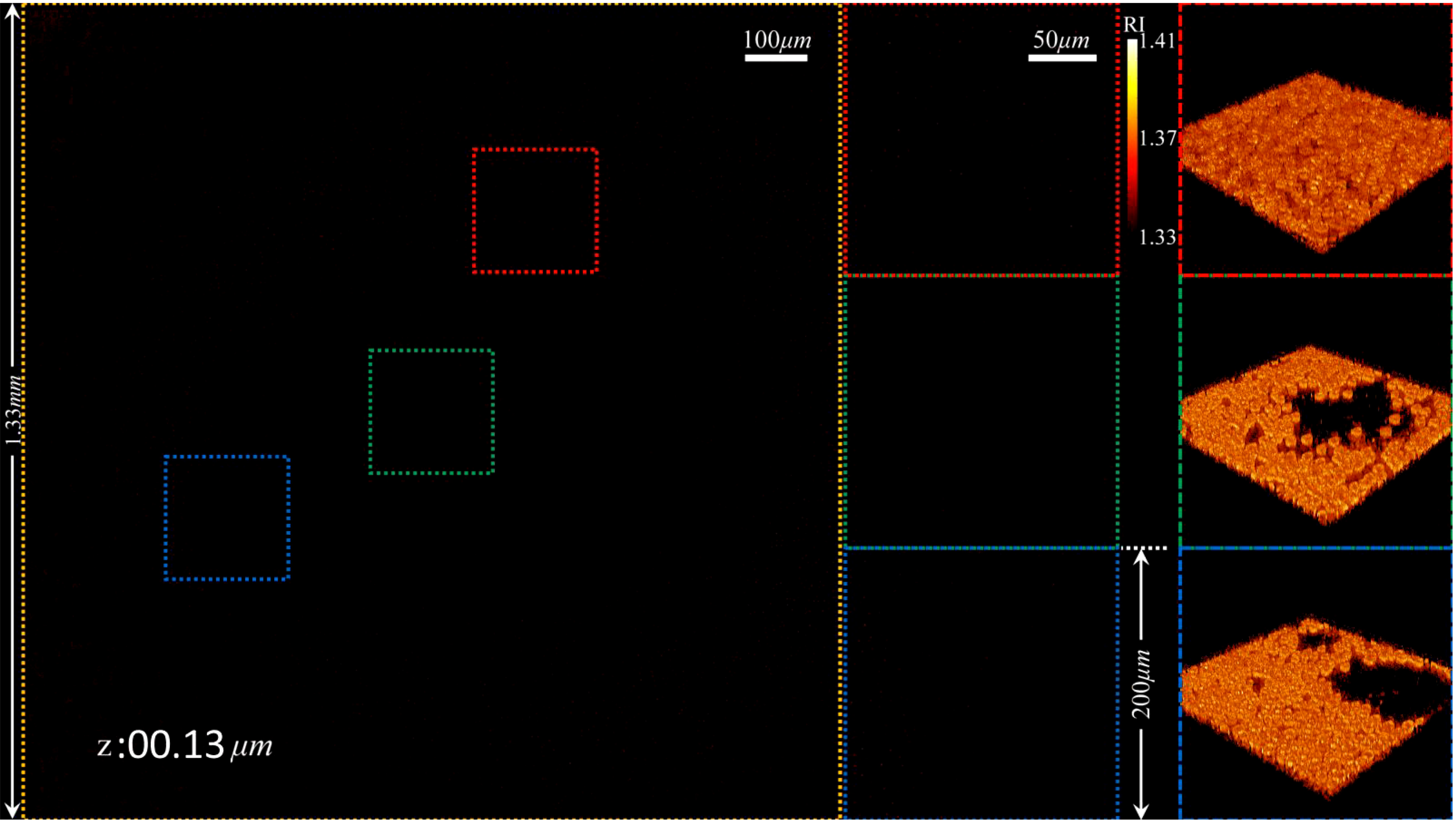

Full-FOV 3D quantitative RI reconstruction of unstained blood smear **(~ 20,000 RBC)**

Fourier ptychographic diffraction tomography (FPDT)

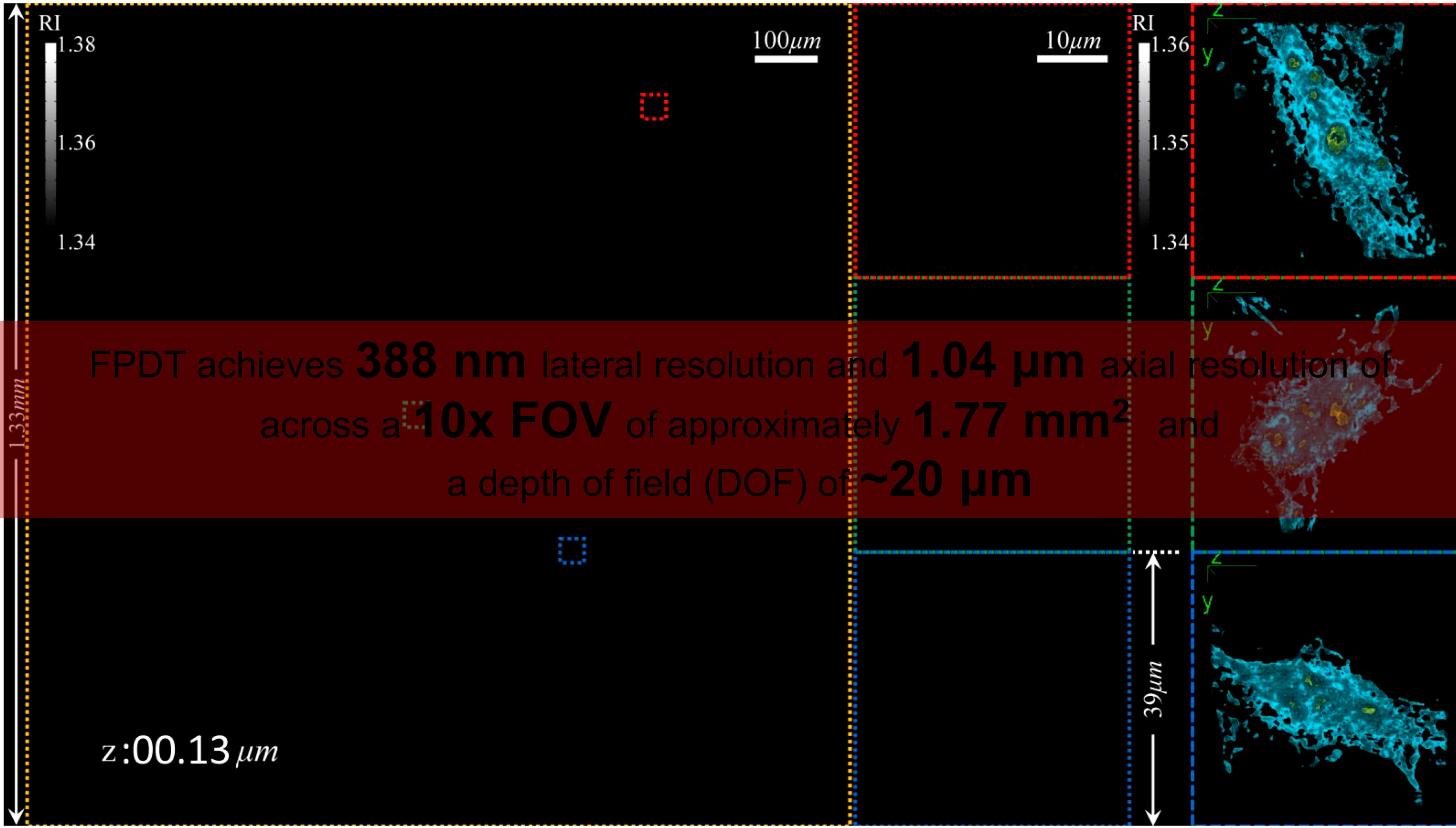

FPDT achieves **388 nm** lateral resolution and **1.04 μm** axial resolution of across a **10x FOV** of approximately **1.77 mm^2** and a depth of field (DOF) of **~20 μm**

Full-FOV 3D quantitative RI reconstruction of unstained HeLa cells

Coherent / partially coherent ODT

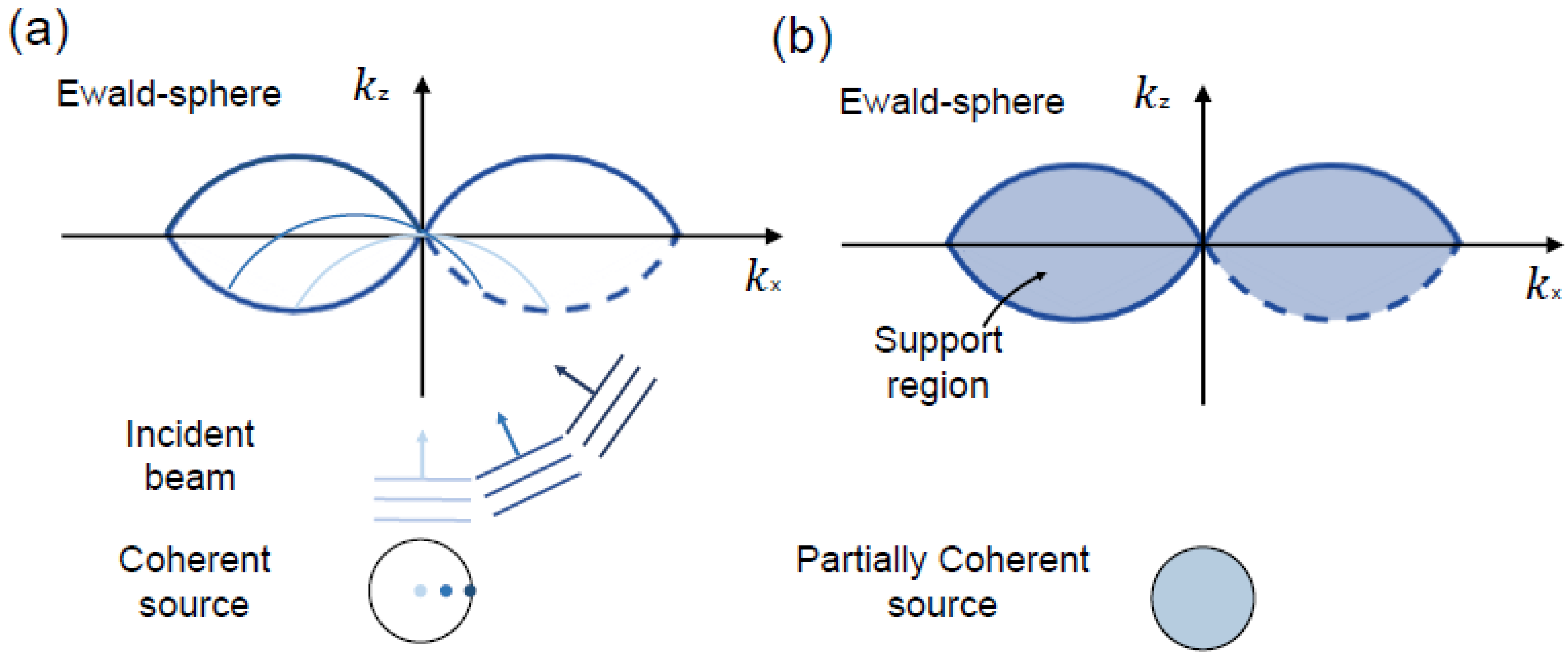

Theory

- 3D Fluorescence deconvolution microscopy
- 3D Optical diffraction tomography microscopy
- 3D Deconvolution phase microscopy

P. Sarder and A. Nehorai, "Deconvolution methods for 3-D fluorescence microscopy images," IEEE Signal Processing Magazine **23, 32-45 (2006).**

E. Wolf, "Three-dimensional structure determination of semi-transparent objects from holographic data," Optics Communications **1, 153-156 (1969).**

N. Streibl, "Three-dimensional imaging by a microscope," JOSA A **2, 121-127 (1985).**

3-D Fluorescence Microscopy

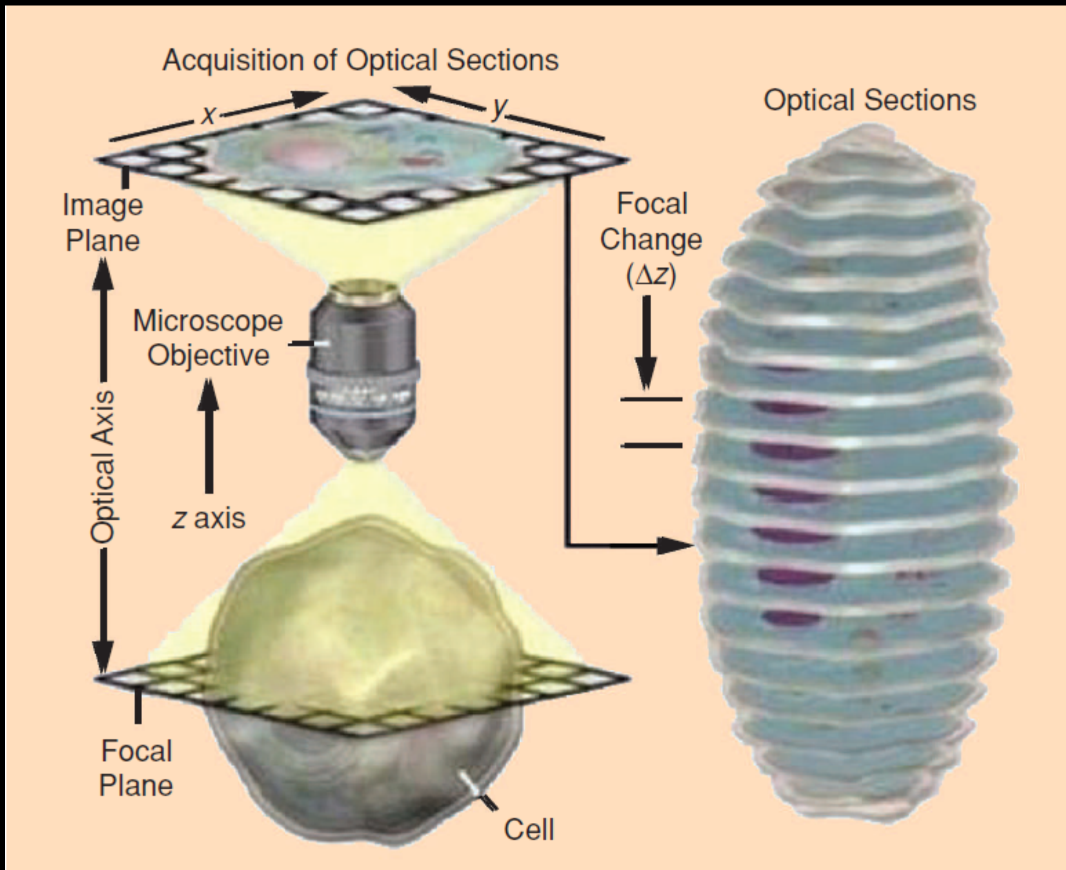

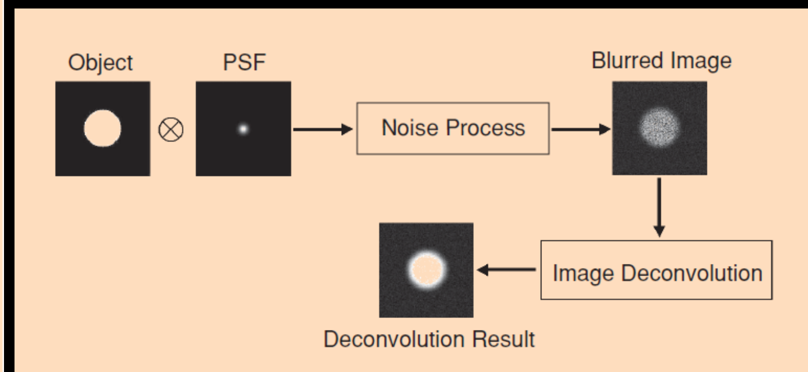

P. Sarder and A. Nehorai, "Deconvolution methods for 3-D fluorescence microscopy images," IEEE Signal Processing Magazine **23, 32-45 (2006).**

3D Optical diffraction tomography microscopy

Volume 1, number 4 OPTICS COMMUNICATIONS September/October 1969

THREE-DIMENSIONAL STRUCTURE DETERMINATION OF SEMI-TRANSPARENT OBJECTS FROM HOLOGRAPHIC DATA *

Emil WOLF
Department of Physics and Astronomy, University of Rochester, Rochester, N.Y. 14627, USA

Received 11 August 1969

E. Wolf, "Three-dimensional structure determination of semi-transparent objects from holographic data," Optics Communications **1, 153-156 (1969).**

Emil Wolf

Emil Wolf

Czech-American physicist

Emil Wolf was a Czech-born American physicist who made advancements in physical optics, including diffraction, coherence properties of optical fields, spectroscopy of partially coherent radiation, and the theory of direct scattering and inverse scattering.
Wikipedia

Born: July 30, 1922, Prague, Czechia

Died: June 2, 2018, Rochester, NY

Doctoral students: Girish Agarwal; M. Suhail Zubairy

Research interests: Optics, Coherence

Emil Wolf, pioneer of optical physics, dies at 95

June 4, 2018

Emil Wolf was one of the most recognized optical scientists of his generation and served on the Rochester faculty for more than 50 years. (University of Rochester photo / Richard Baker)

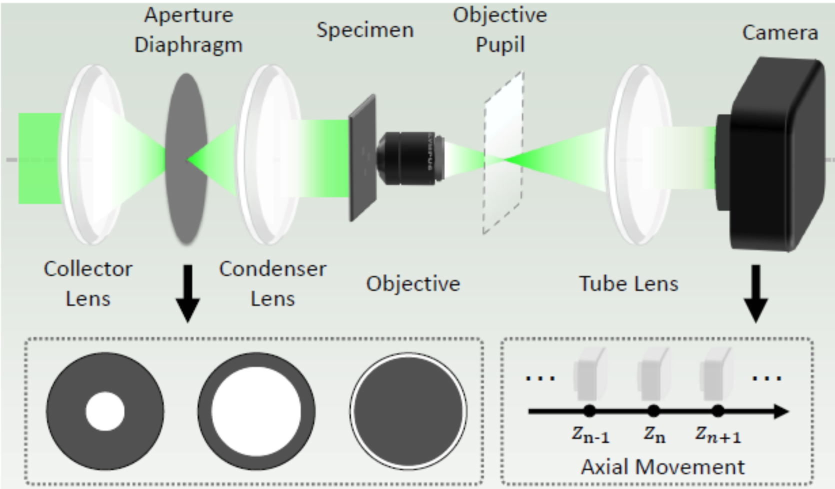

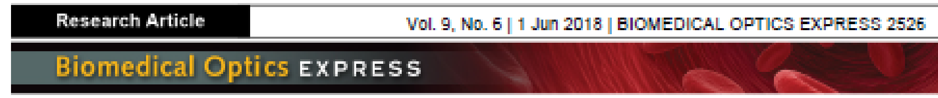
Research Article Vol. 9, No. 6 | 1 Jun 2018 | BIOMEDICAL OPTICS EXPRESS 2526
Biomedical Optics EXPRESS

Three-dimensional tomographic microscopy technique with multi-frequency combination with partially coherent illuminations

JIAJI LI,[1,2,3] QIAN CHEN,[1,2,4] JIASONG SUN,[1,2,3] JIALIN ZHANG,[1,2,3] JUNYI DING,[1,2,3] AND CHAO ZUO[1,2,3,*]

[1]School of Electronic and Optical Engineering, Nanjing University of Science and Technology, No. 200 Xiaolingwei Street, Nanjing, Jiangsu Province 210094, China
[2]Jiangsu Key Laboratory of Spectral Imaging & Intelligent Sense, Nanjing University of Science and Technology, Nanjing, Jiangsu Province 210094, China
[3]Smart Computational Imaging Laboratory (SCILab), Nanjing University of Science and Technology, Nanjing, Jiangsu Province 210094, China
[4]chenqian@njust.edu.cn
*surpasszuo@163.com

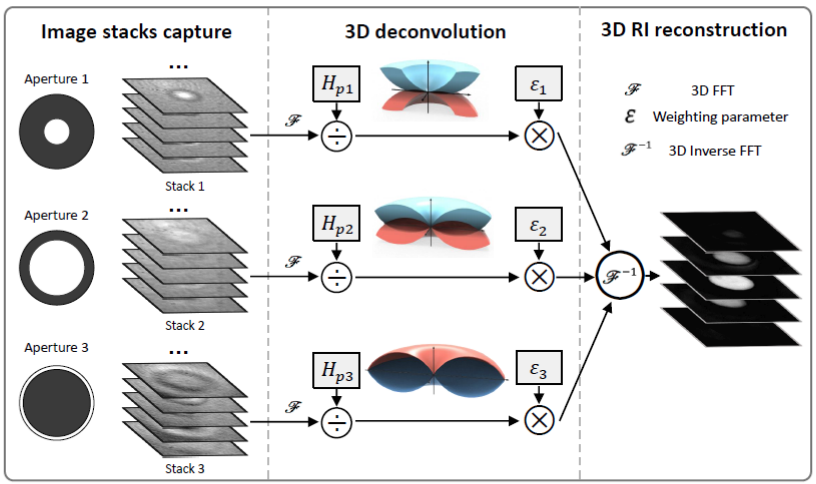

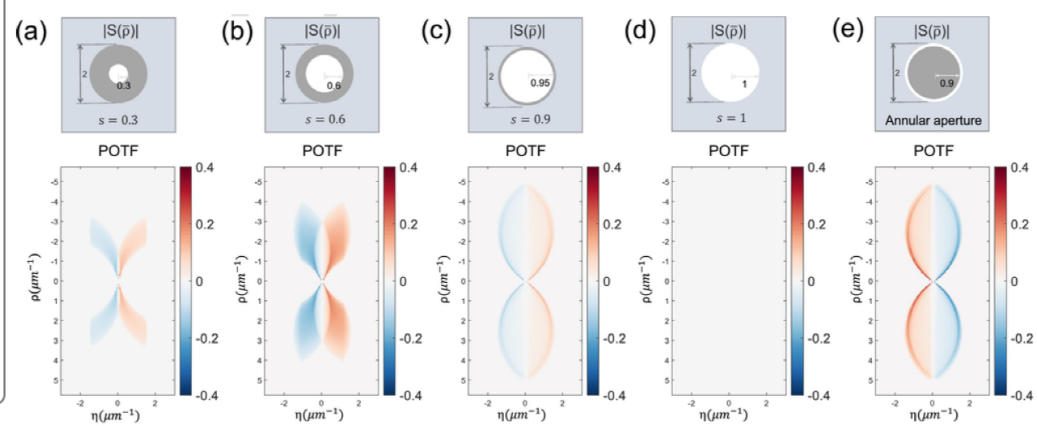

3D intensity spectrum

$$\widetilde{I}(\zeta) = B\delta(\zeta) + \widetilde{\Phi}(\zeta) T_P(\zeta) + \widetilde{A}(\zeta) T_A(\zeta)$$

3D phase / amplitude transfer function

Transport-of-intensity diffraction tomography (TIDT)

J Li, et. al. Biomed. Opt. Express 9, 2526-2542 (2018)

3D Deconvolution phase microscopy

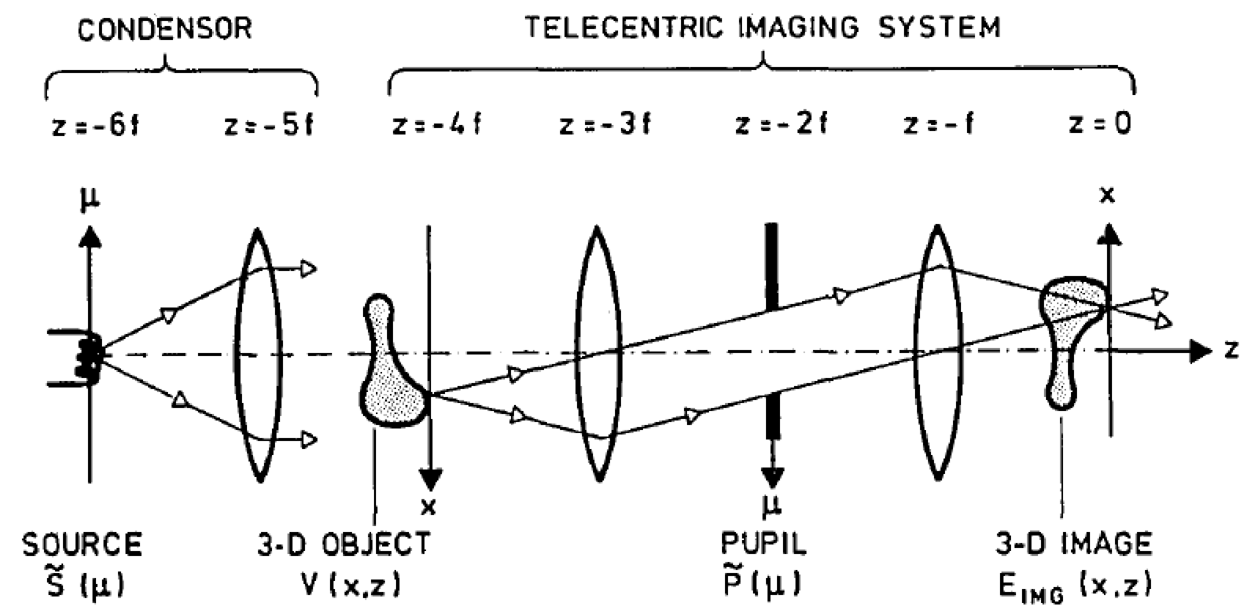

Fig. 1. 3-D imaging of a partially coherently transilluminated object by a telecentric system.

N. Streibl, "Three-dimensional imaging by a microscope," JOSA A **2, 121-127 (1985).**

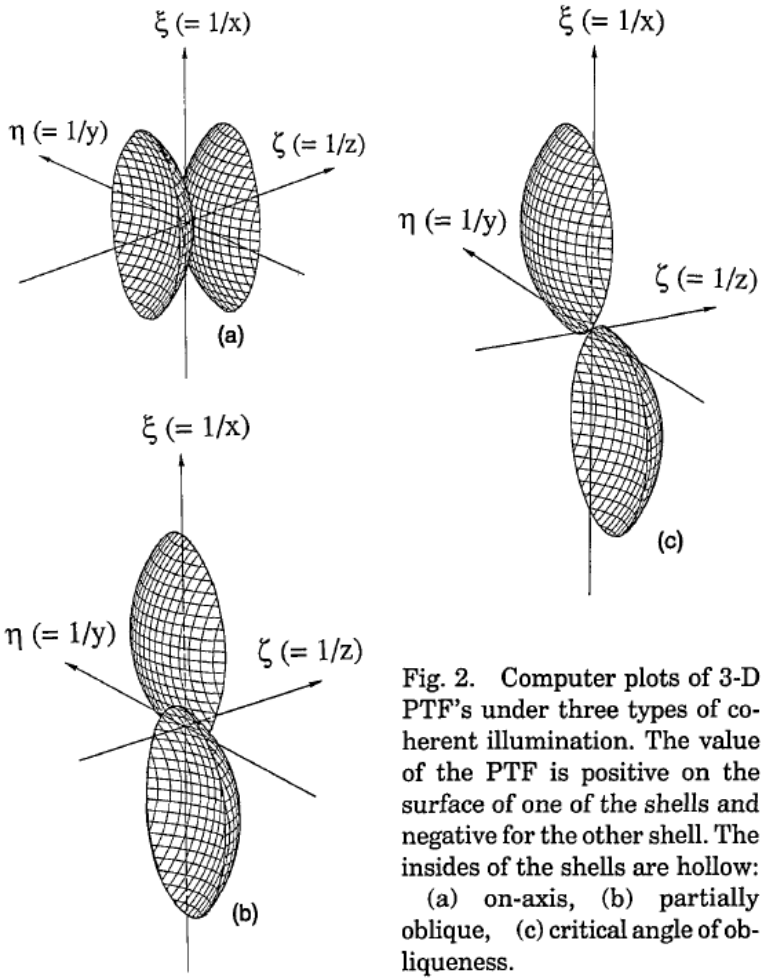

Fig. 2. Computer plots of 3-D PTF's under three types of coherent illumination. The value of the PTF is positive on the surface of one of the shells and negative for the other shell. The insides of the shells are hollow: (a) on-axis, (b) partially oblique, (c) critical angle of obliqueness.

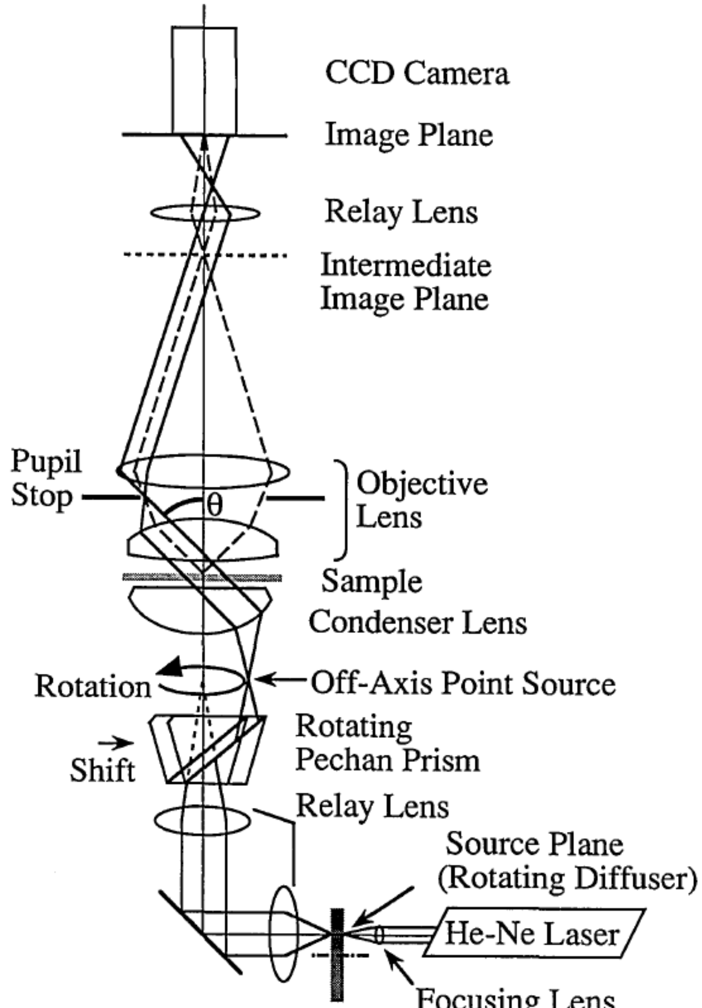

3D OTF for coherent illumination source

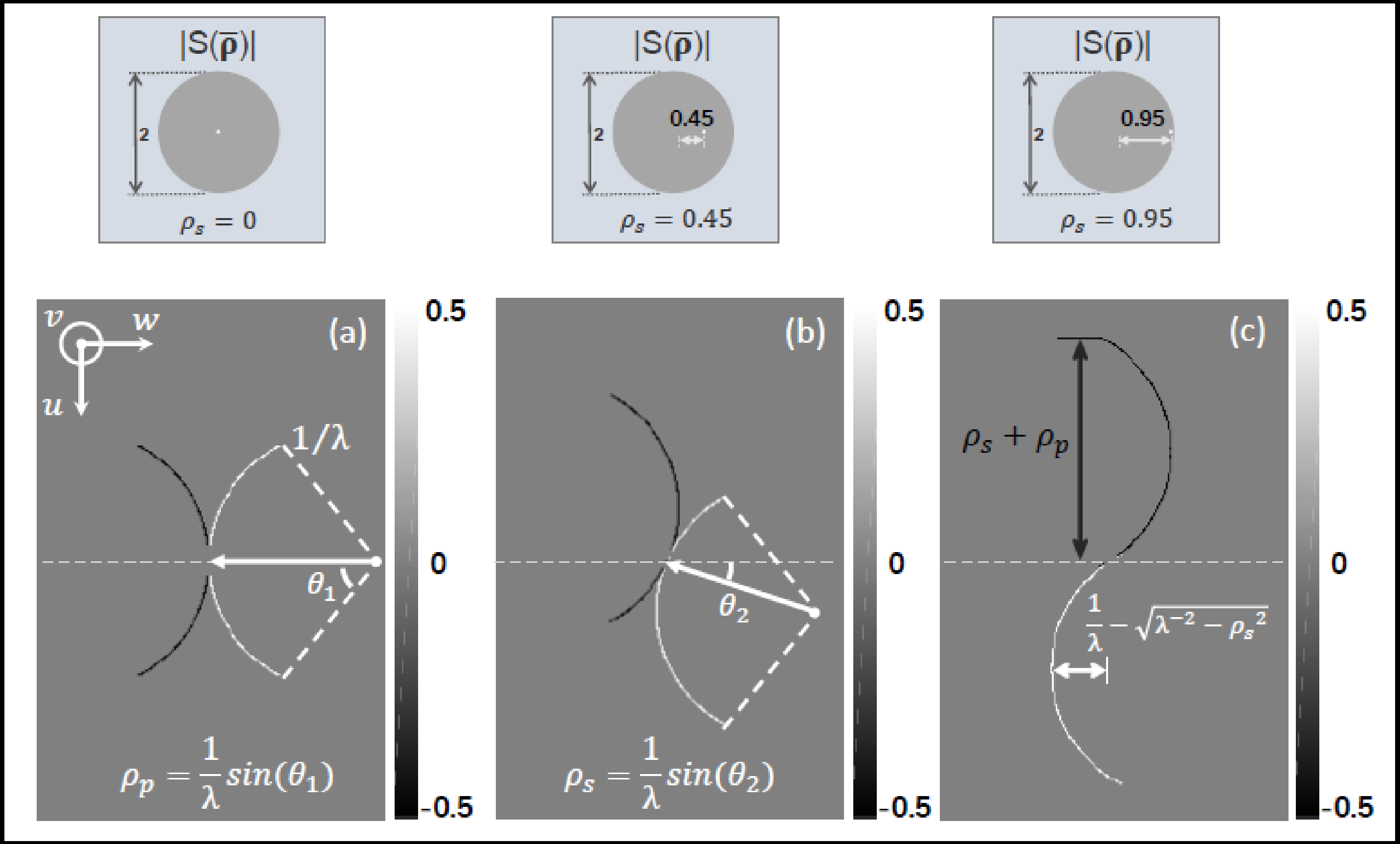

Rendering result of 3D OTF

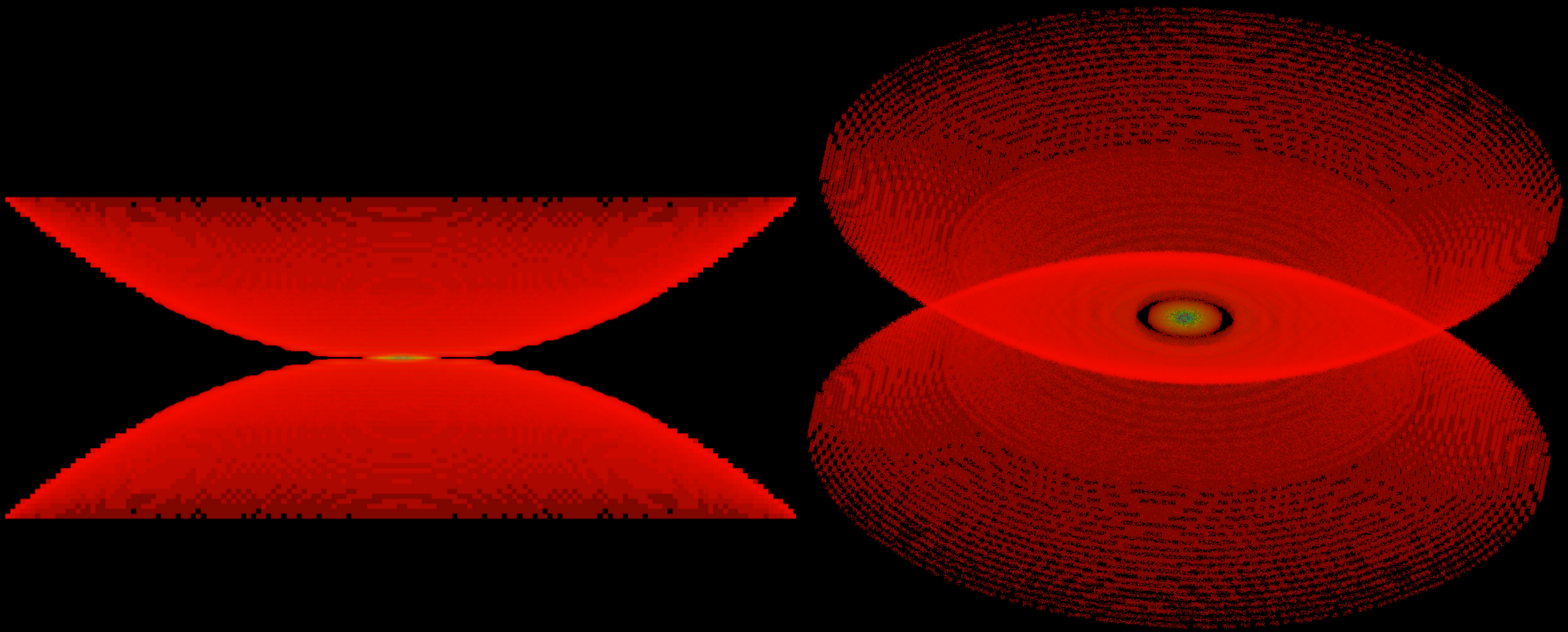

3D K-space of Scattering potential

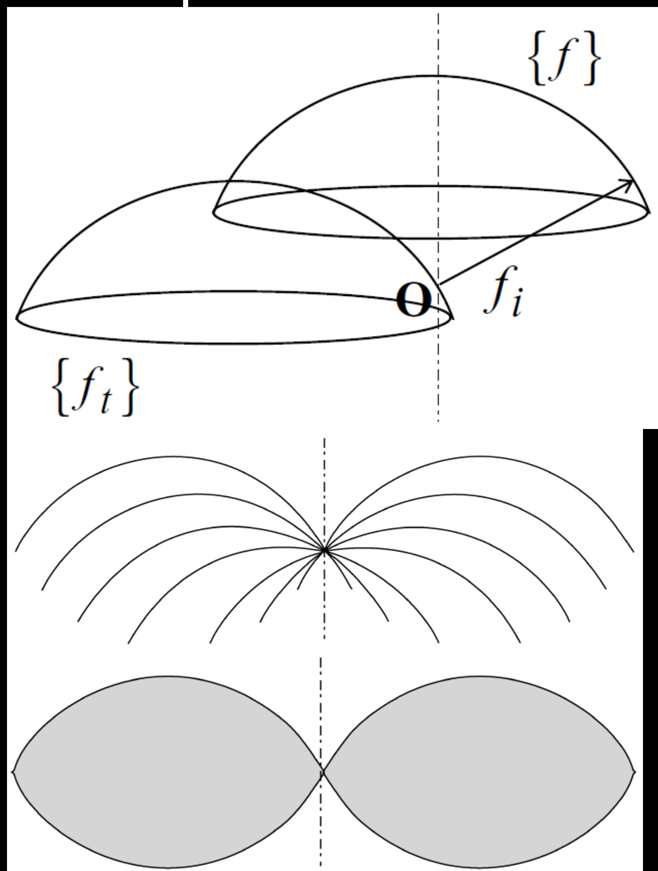

3D OTF for transmission microscope

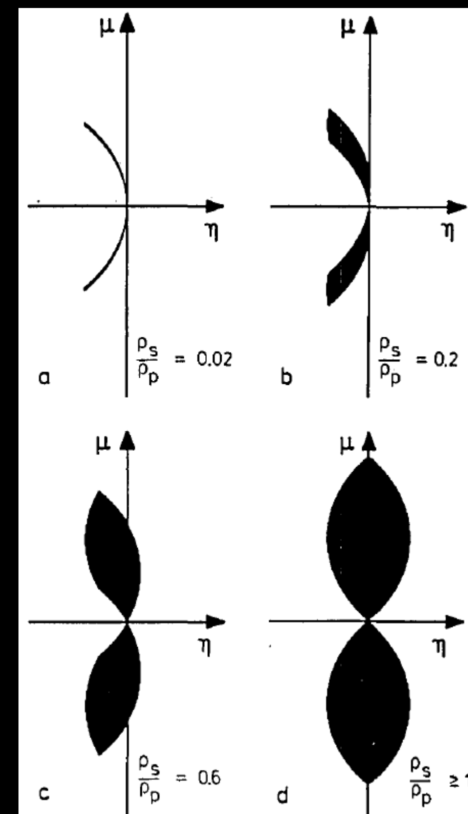

N. Streibl, "Three-dimensional imaging by a microscope," JOSA A **2, 121-127 (1985).**

Partially coherent 3D imaging

$$
\begin{aligned}
WOTF\left(\mathbf{u}\right) \equiv TCC\left(\mathbf{u},\mathbf{0}\right) \\
= \iint S\left(\mathbf{u}'\right) H\left(\mathbf{u}' + \mathbf{u}\right) H^{*}\left(\mathbf{u}'\right) d\mathbf{u}'
\end{aligned}
$$

$$
\begin{aligned}
H\left(\rho, l\right) &= \int P\left(\rho\right) e^{jkz\sqrt{1-\lambda^2\rho^2}} e^{-j2\pi z l} dz \\
&= P\left(\rho\right) \delta\left(l - \sqrt{\left(\frac{1}{\lambda}\right)^2 - \rho^2}\right)
\end{aligned}
$$

Mapping of 3D Ewald sphere

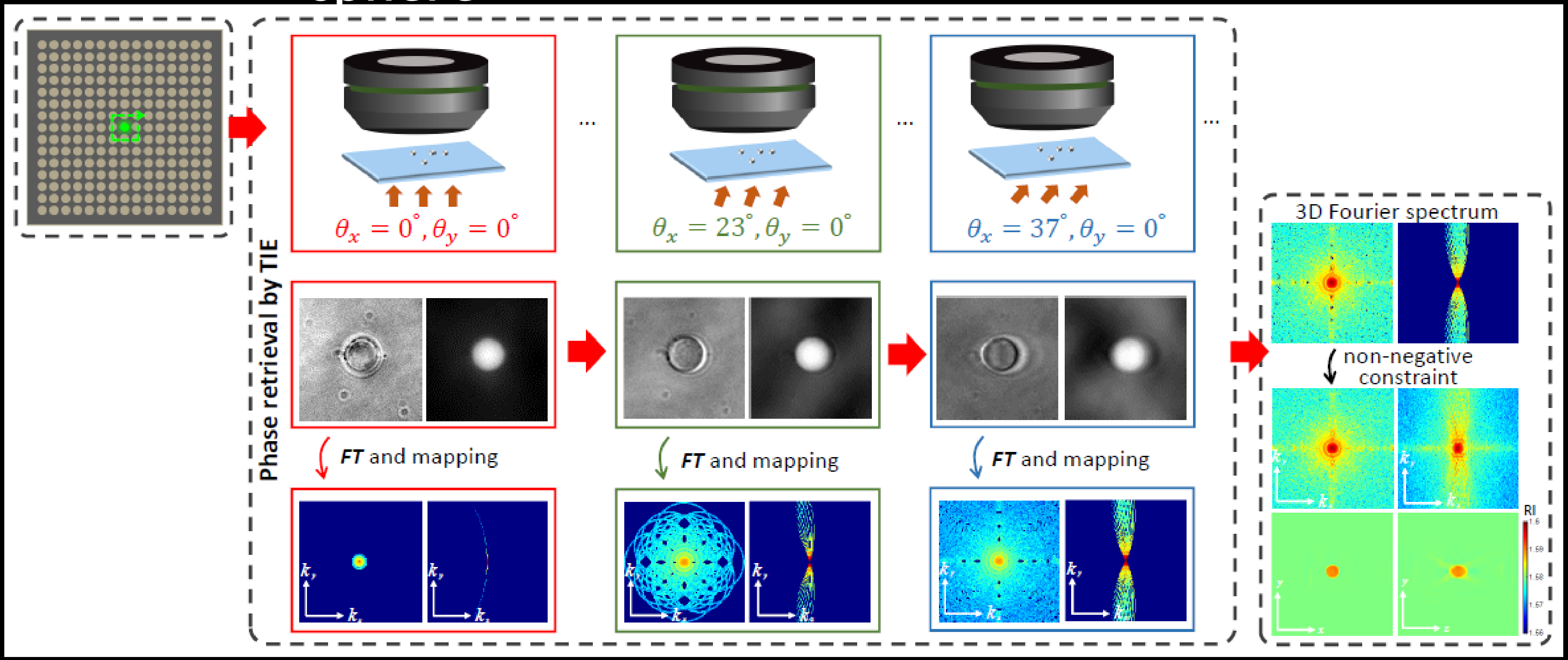

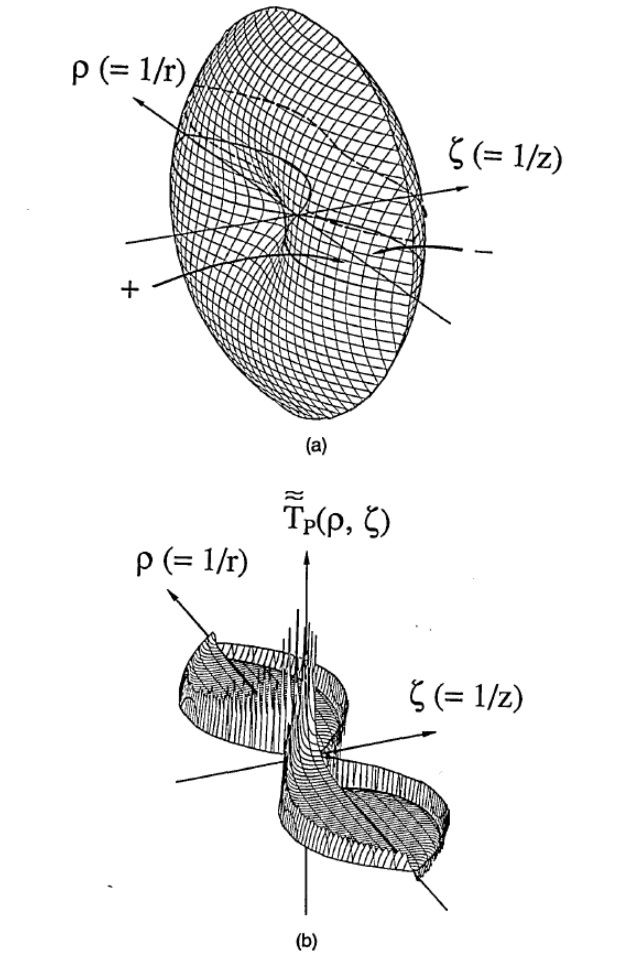

Fig. 3. (a) Computer plot of 3-D PTF under annular illumination; (b) perspective plot of the PTF value of $\rho(= 1/r)$ and $\zeta(= 1/z)$.

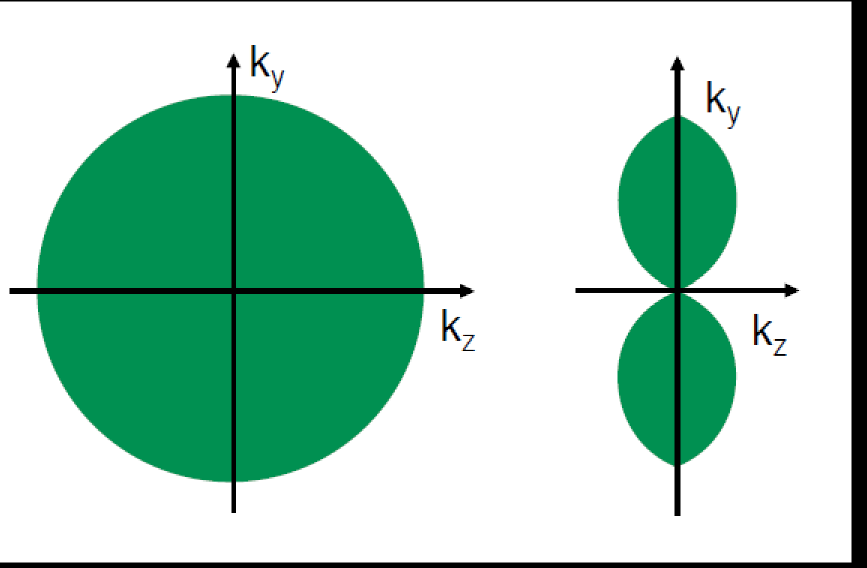

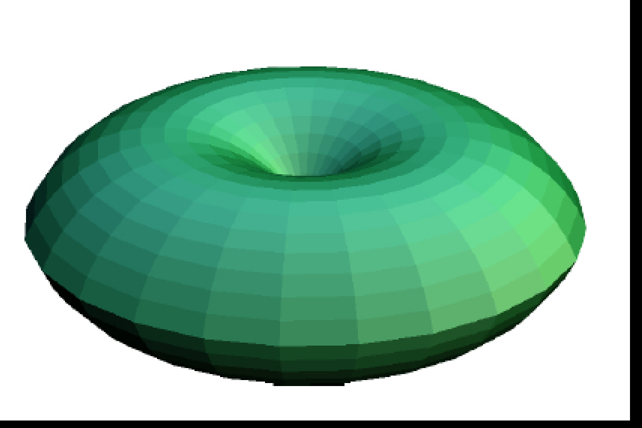

3D OTF for optical microscope

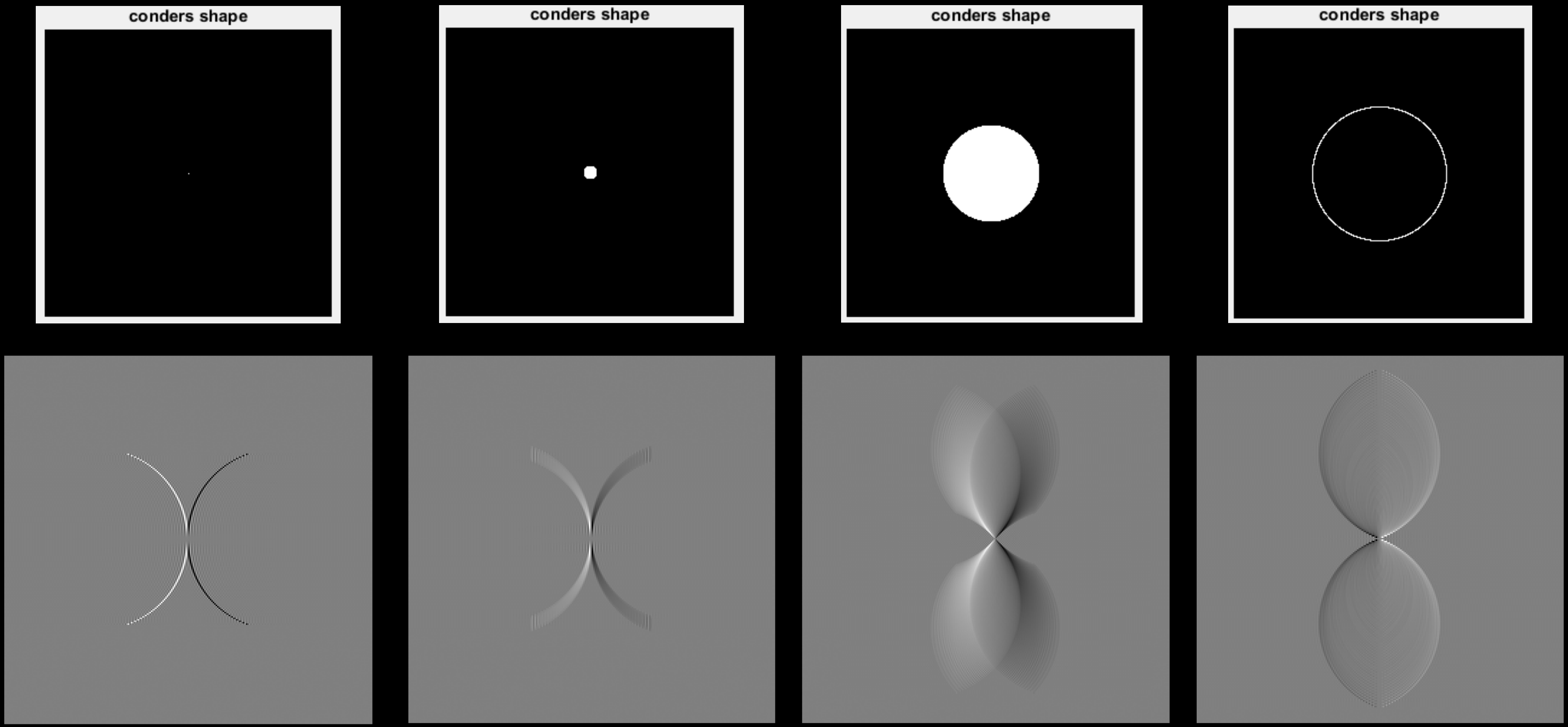

N. Streibl, "Three-dimensional imaging by a microscope," JOSA A **2, 121-127 (1985).**

Partially coherent 3D imaging

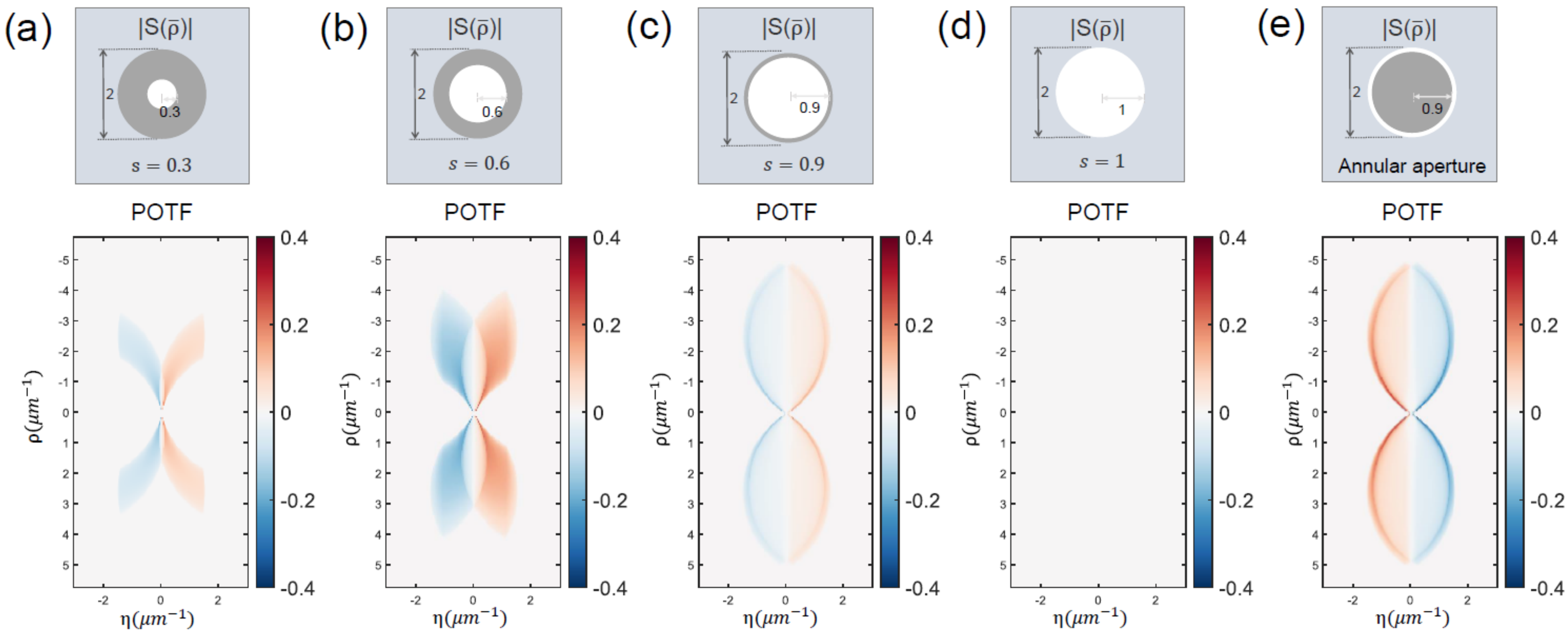

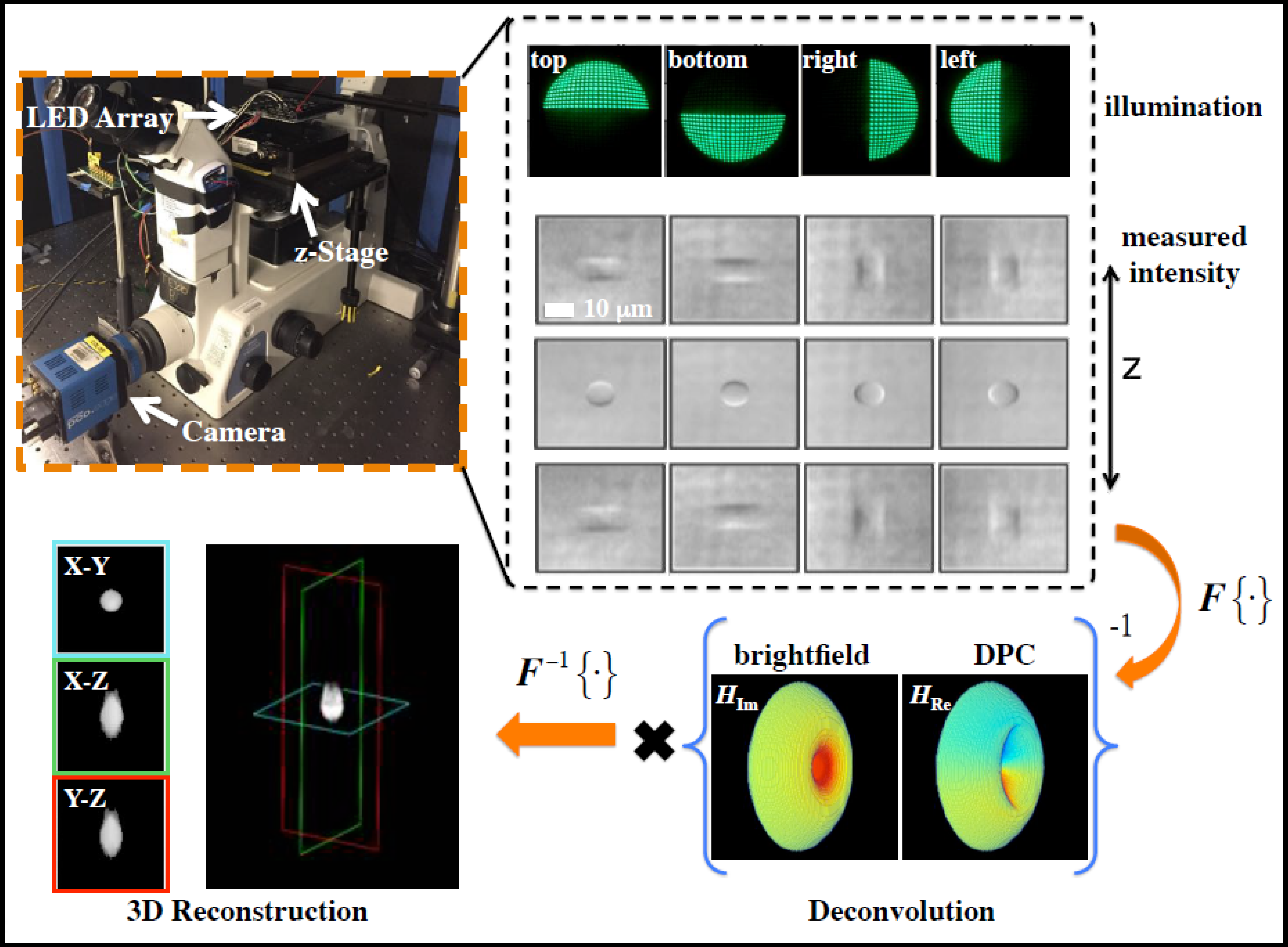

LED Array
z-Stage
Camera
top
bottom
right
left
illumination
measured
intensity
10 μm
z
$F\{\cdot\}$
-1
brightfield
DPC
H_{Im}
H_{Re}
$F^{-1}\{\cdot\}$
X-Y
X-Z
Y-Z
3D Reconstruction
Deconvolution

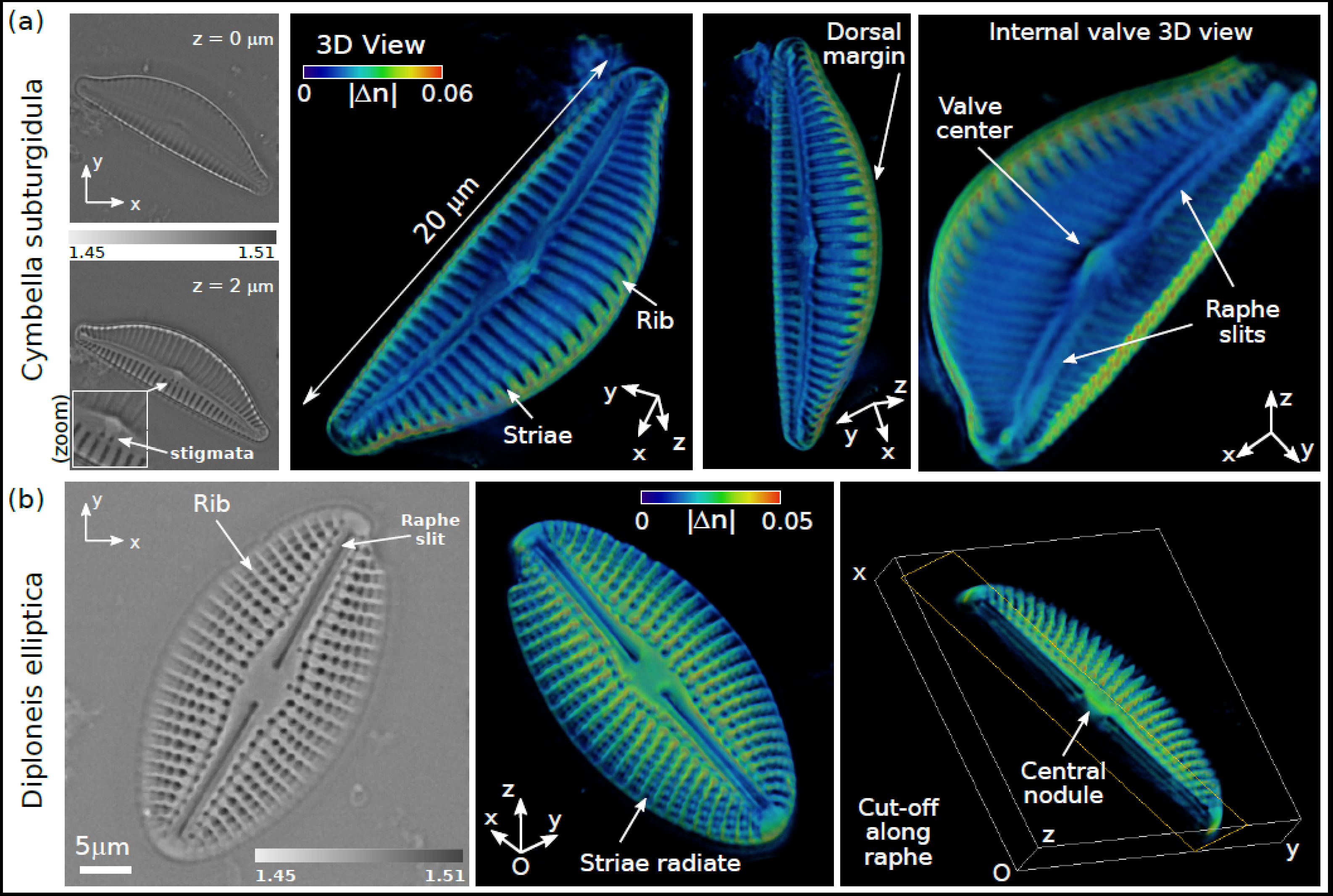

(a)
Cymbella subturgidula
z = 0 μm
y
x
1.45
1.51
z = 2 μm
(zoom)
stigmata
3D View
0
|Δn|
0.06
20 μm
Rib
Striae
y
x
z
Dorsal margin
z
y
x
Internal valve 3D view
Valve center
Raphe slits
z
x
y
(b)
Diploneis elliptica
y
x
Rib
Raphe slit
5μm
1.45
1.51
0
|Δn|
0.05
z
x
y
O
Striae radiate
x
Central nodule
Cut-off along raphe
z
y
O

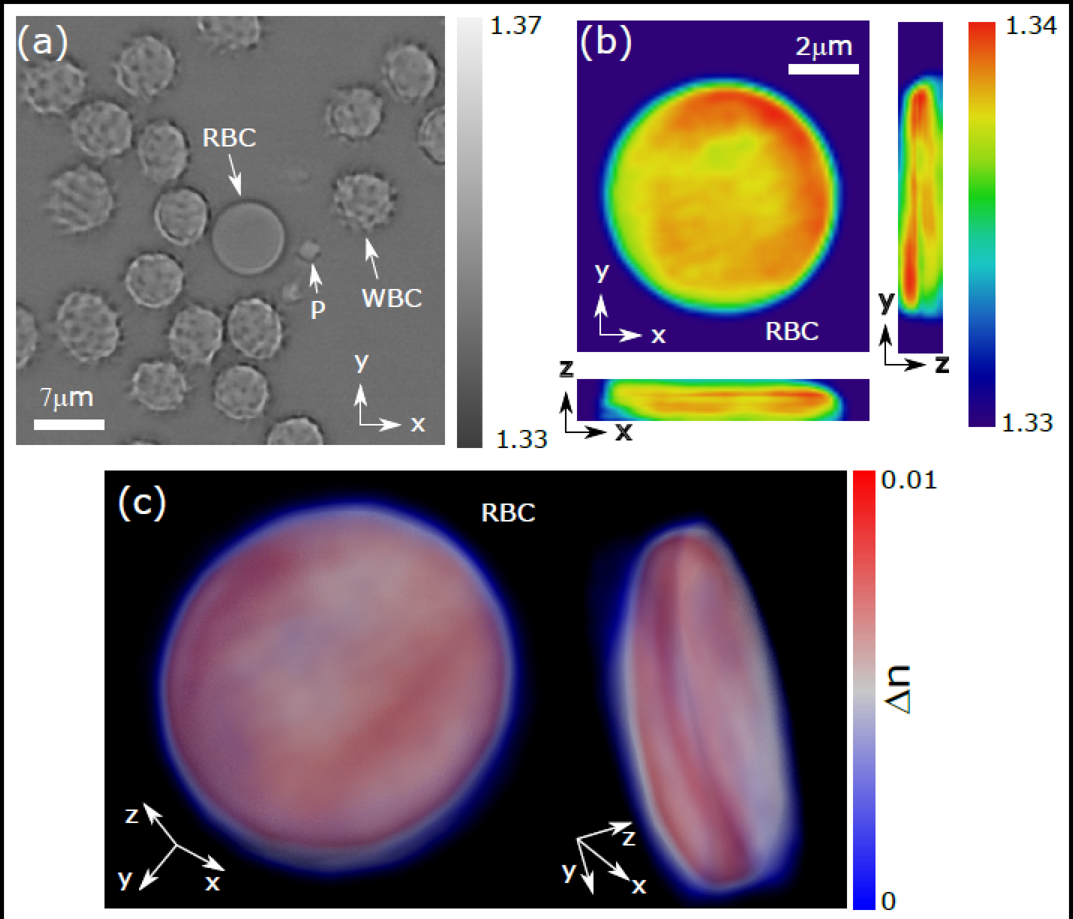

(a)
RBC
P
WBC
7μm
y
x
1.37
1.33
(b)
2μm
y
x
RBC
z
y
z
x
1.34
1.33
(c)
RBC
z
y
x
z
y
x
0.01
Δn
0

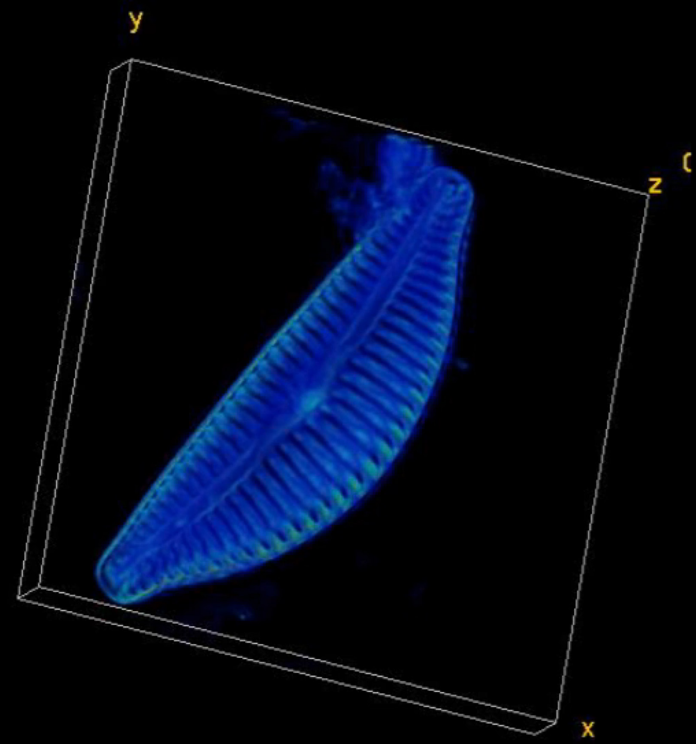

Full rotation of the RI

Optical transport of bacteria: Real-time reconfigurable trajectory

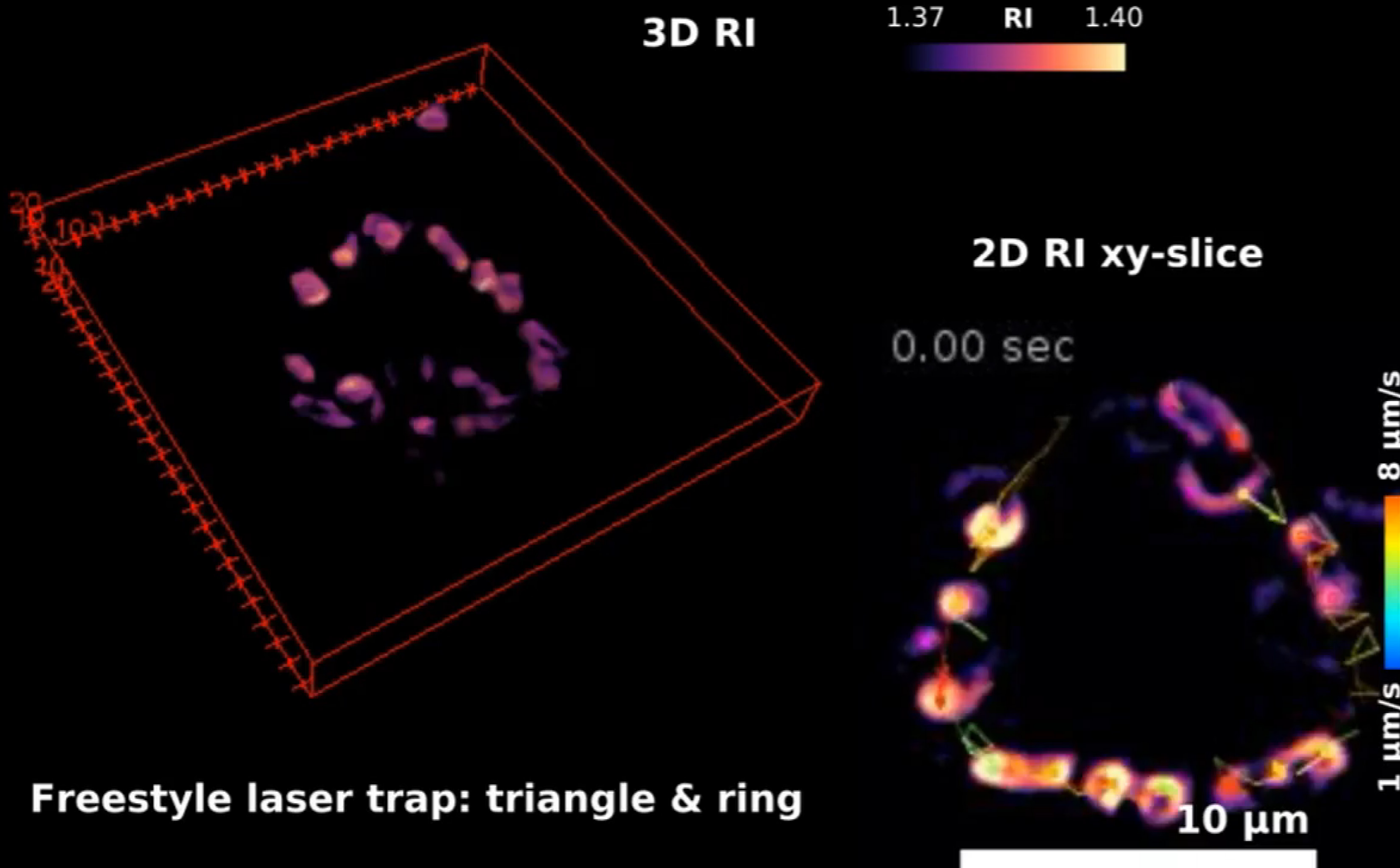

Annular-illumination ODT

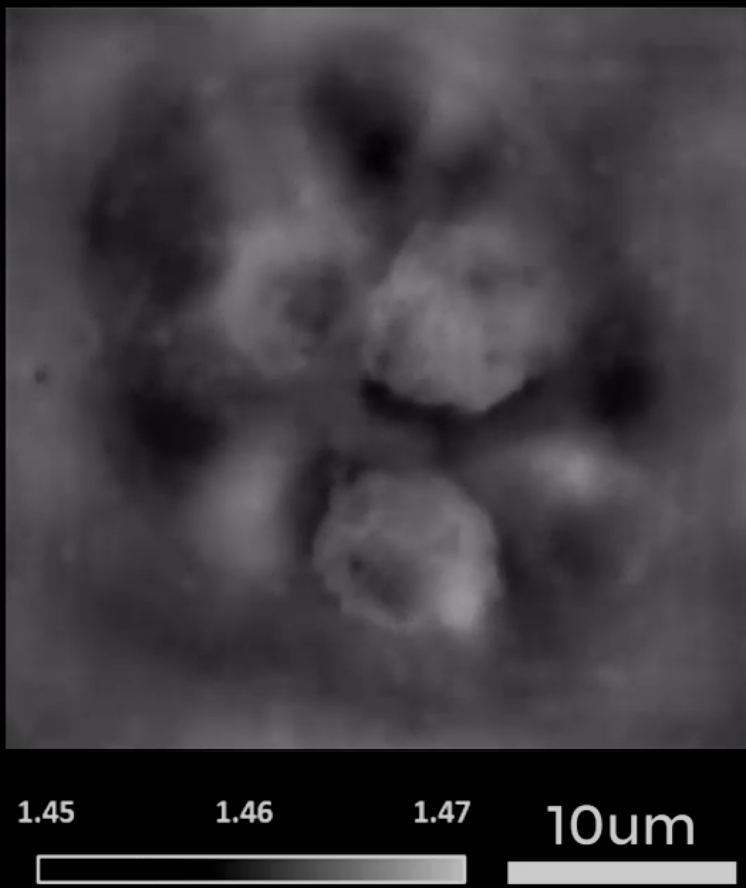

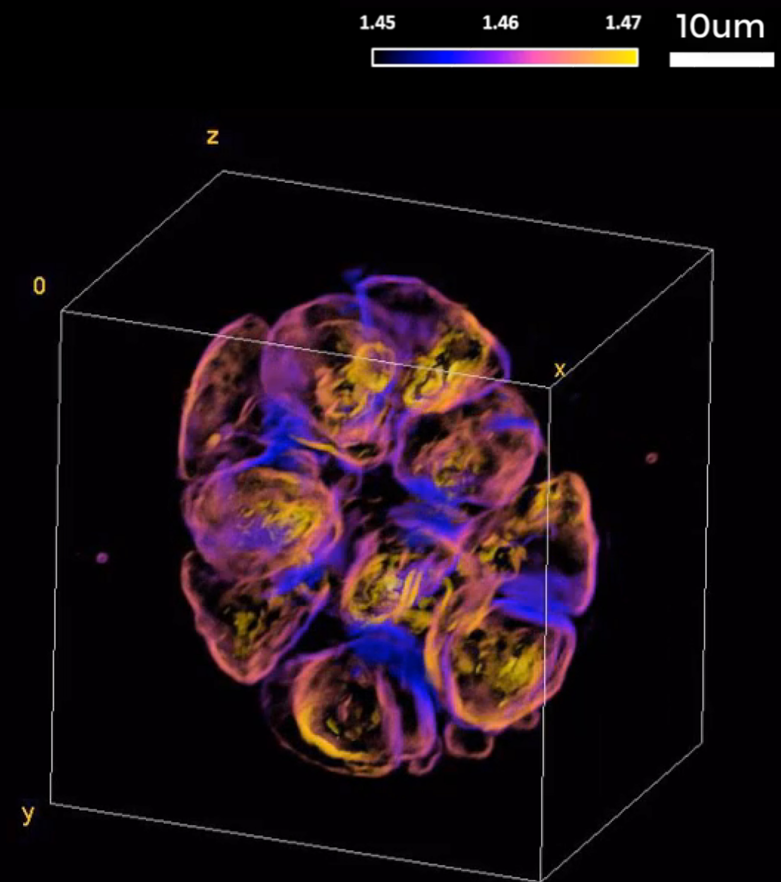

3D rendering of Pandorina

1.4 NAill + 1.4 NAobj 100X MO; Lateral resolution 200nm; axial resolution 650 nm.

J Li, et. al. Biomed. Opt. Express 9, 2526-2542 (2018)

Annular-illumination ODT

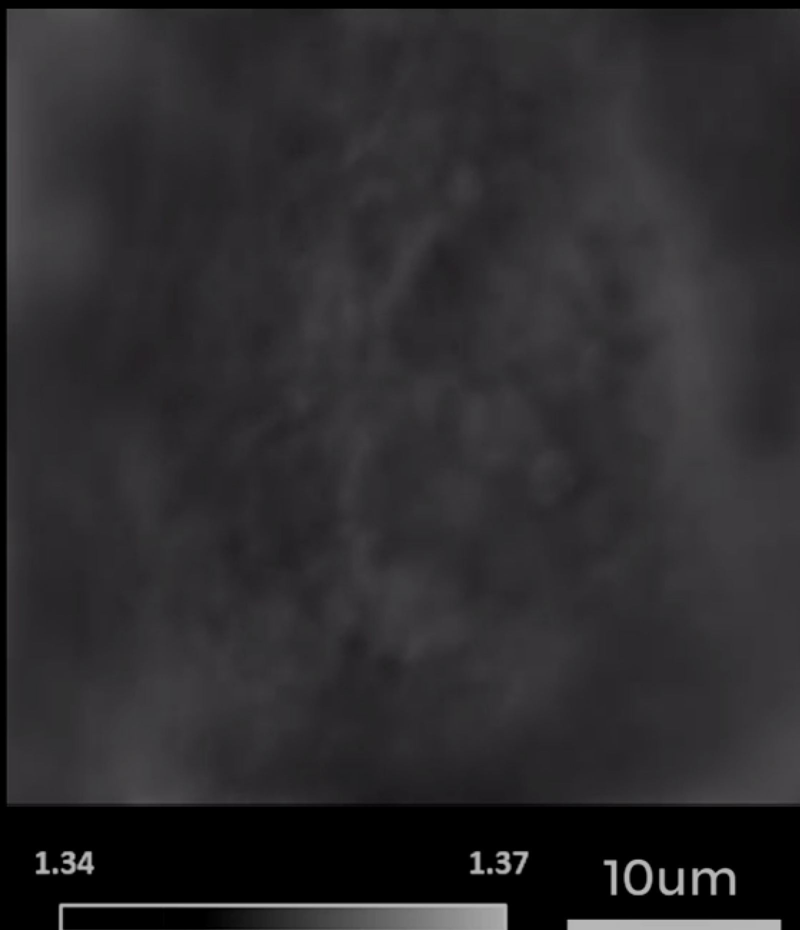

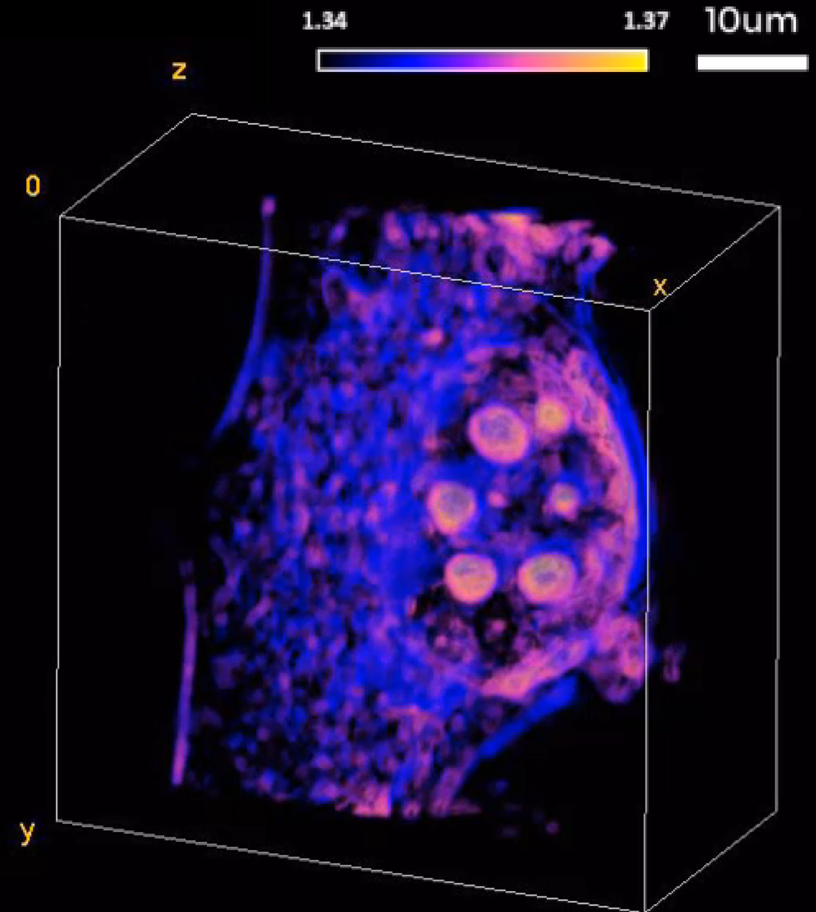

3D rendering of Hela cell

1.4 NAill + 1.4 NAobj 100X MO; Lateral resolution 200nm; axial resolution 650 nm.

J Li, et. al. Biomed. Opt. Express 9, 2526-2542 (2018)

High-speed *in vitro* intensity diffraction tomography

- Brief review of IDT （intensity diffraction tomography）

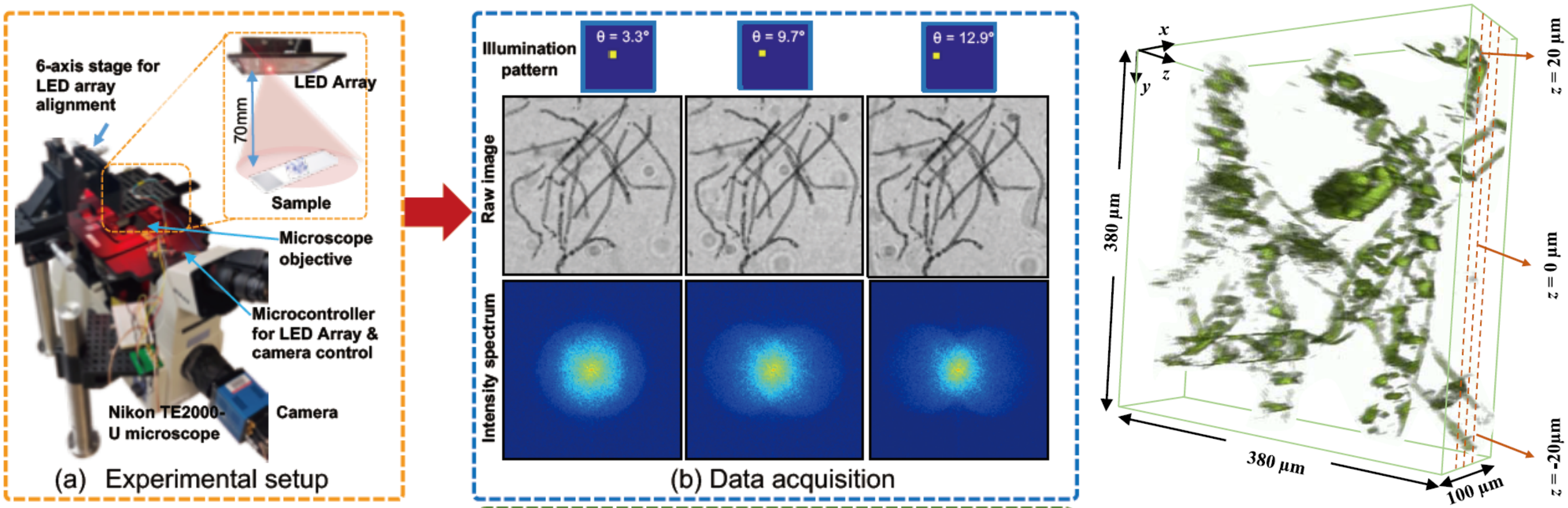

System illumination unit

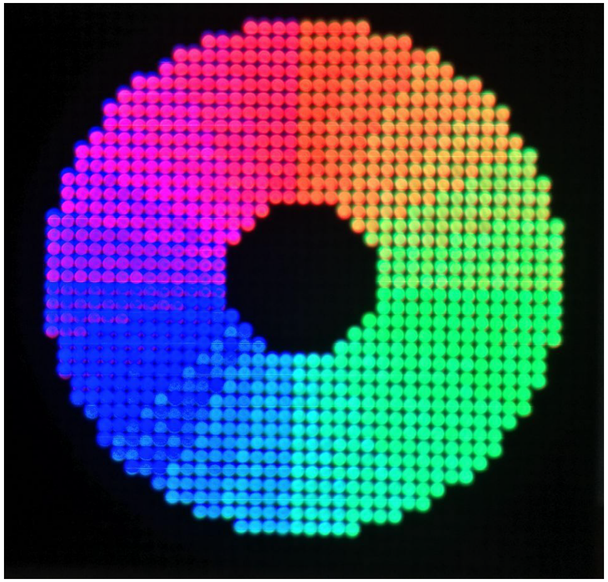

Programmable Square
LED array (1.25mm)
~100$

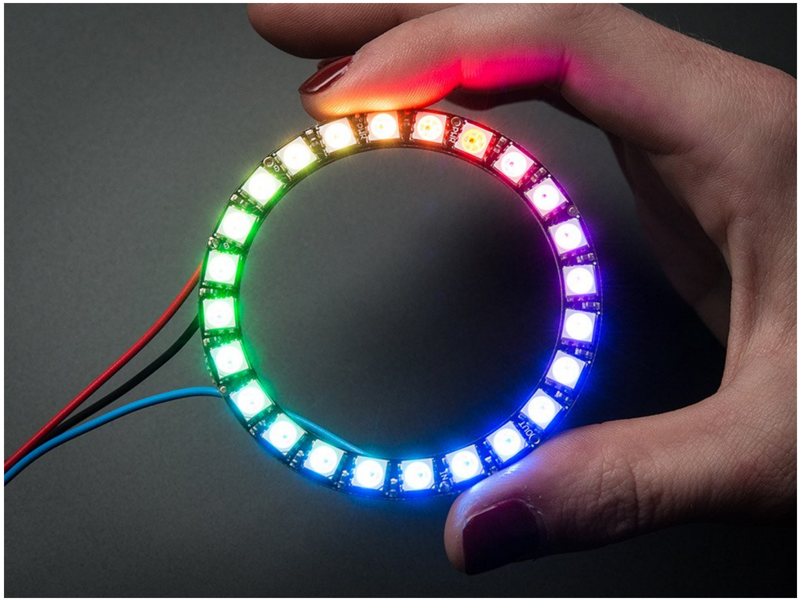

Bright annular LED
from adafruit
~10$

System setup (System illustration of aIDT)

a

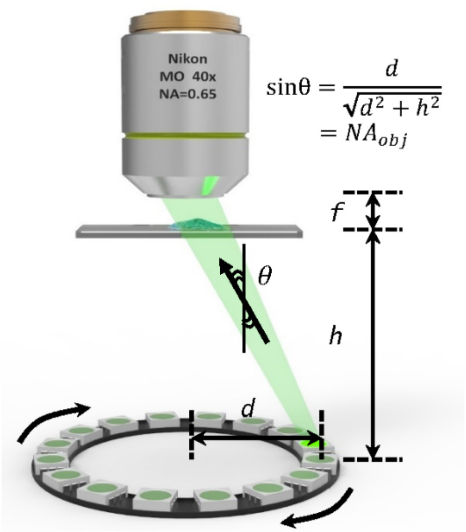

illustration of setup

d

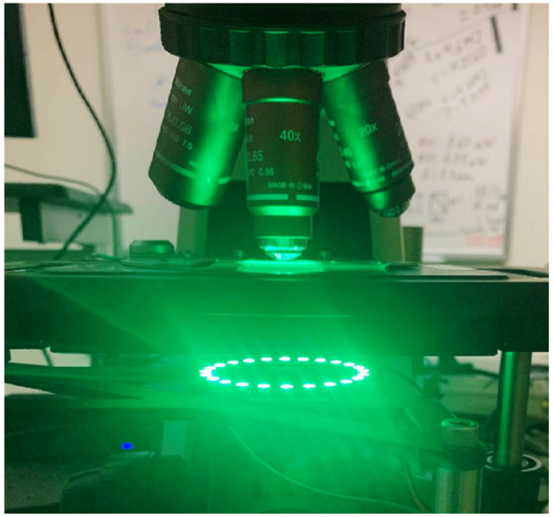

Photography of setup

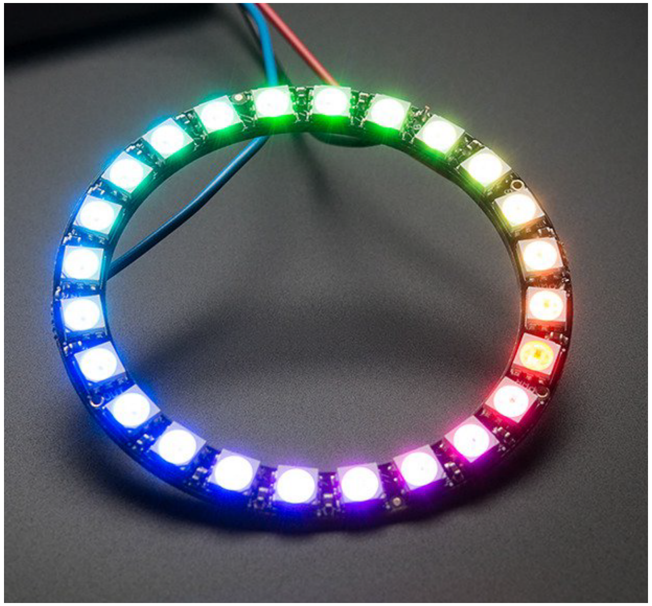

Illumination unit

Key parameters about illumination unit

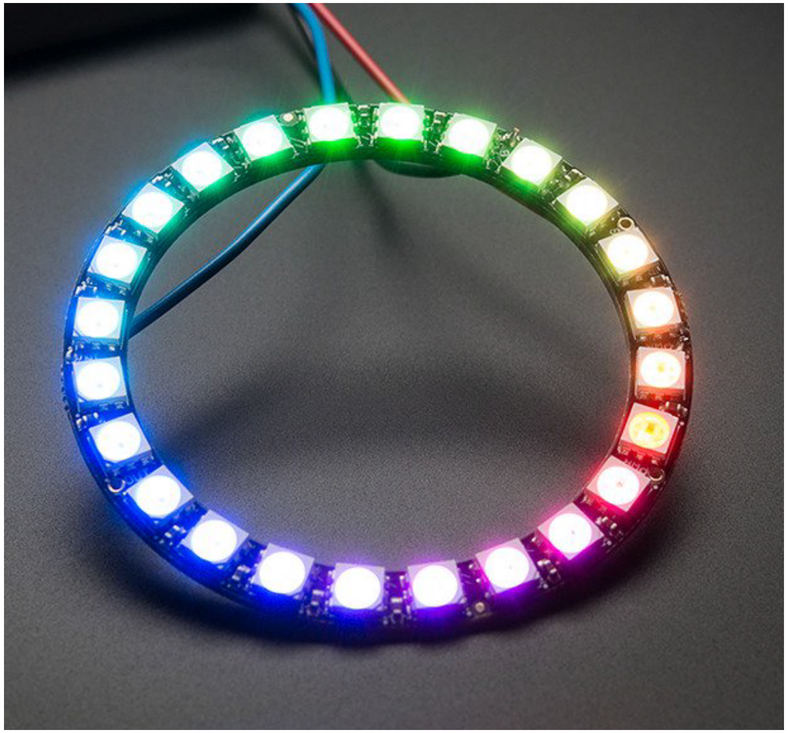

24 Frames or 12 Frames or
8 Frames
(More different size is available)

Maximum speed 800Kbps
(33KHz for each LED
also depends on Microcontroller)

Adjustable for objective with
different NA

Demonstration of aIDT

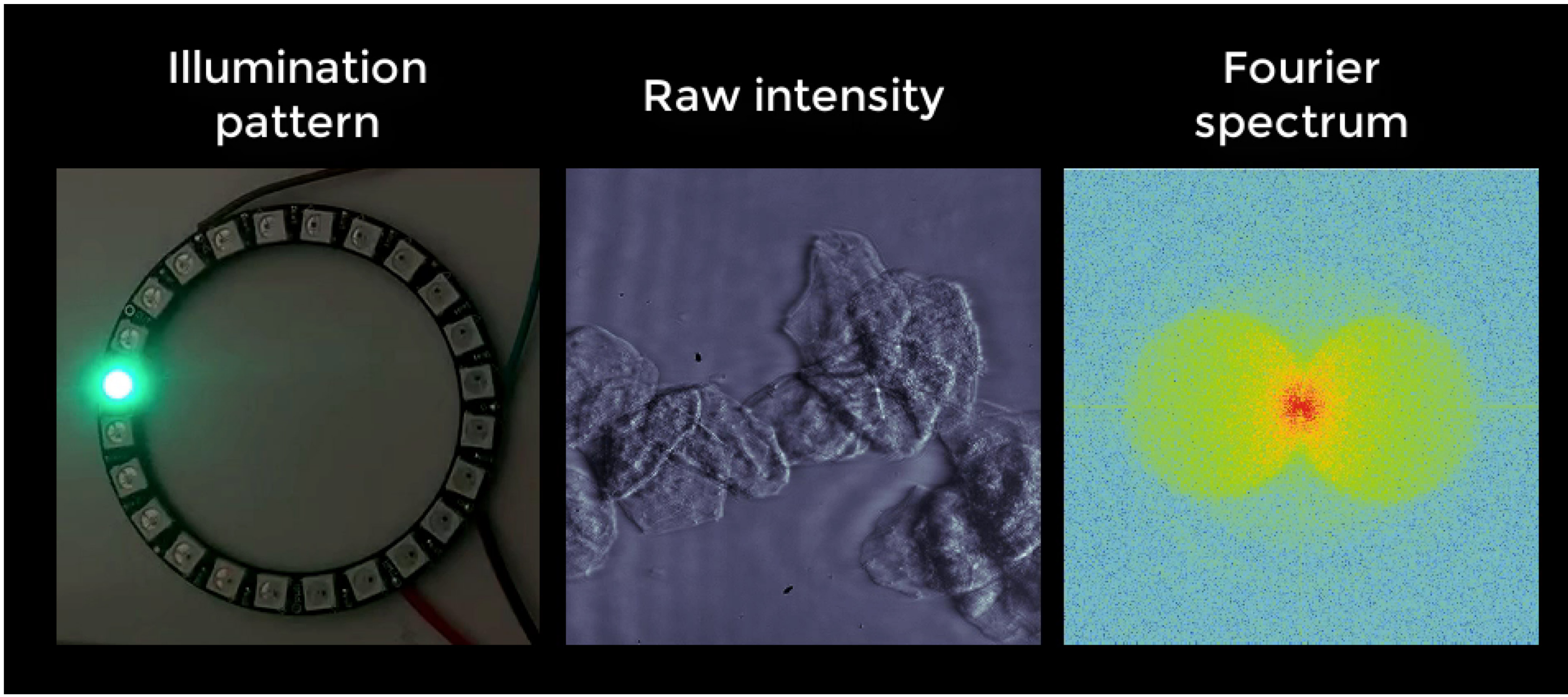

10Hz for each imaging volume

Experimental result of stained Algae

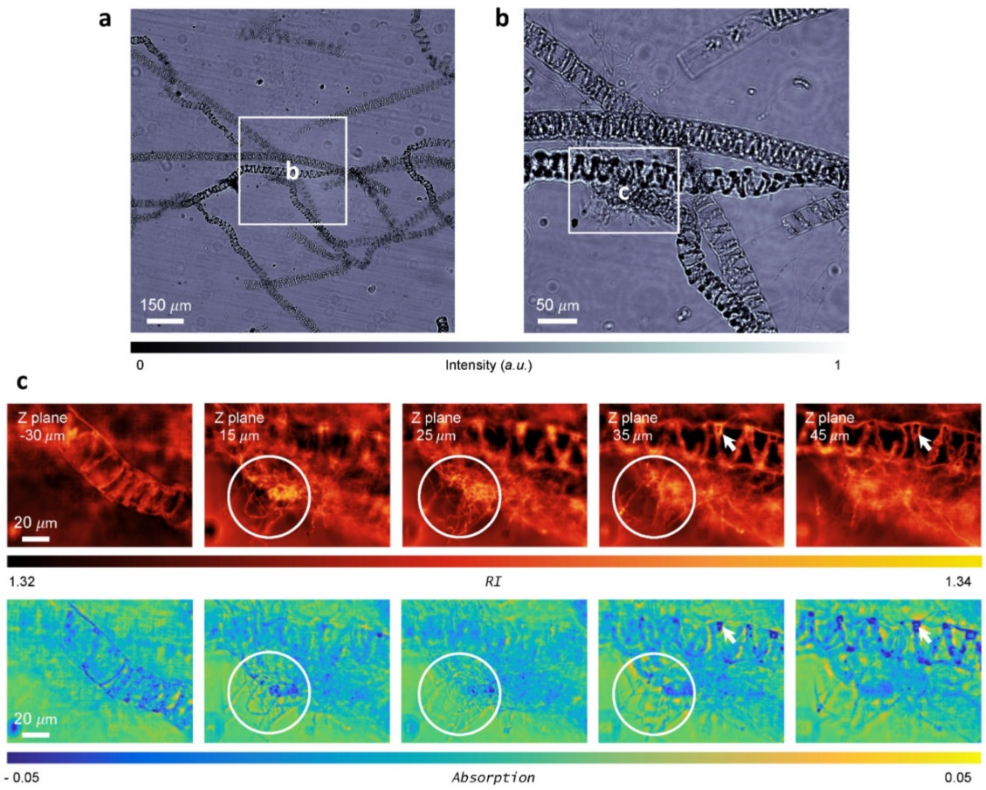

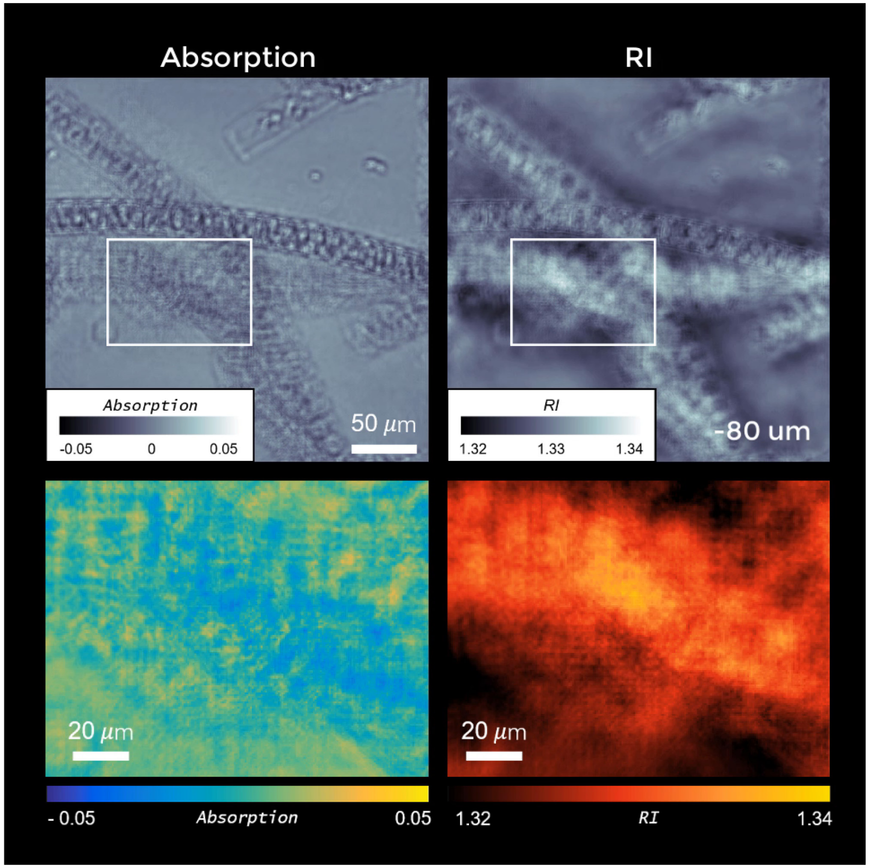

LED illumination calibration and comparative result of diatom

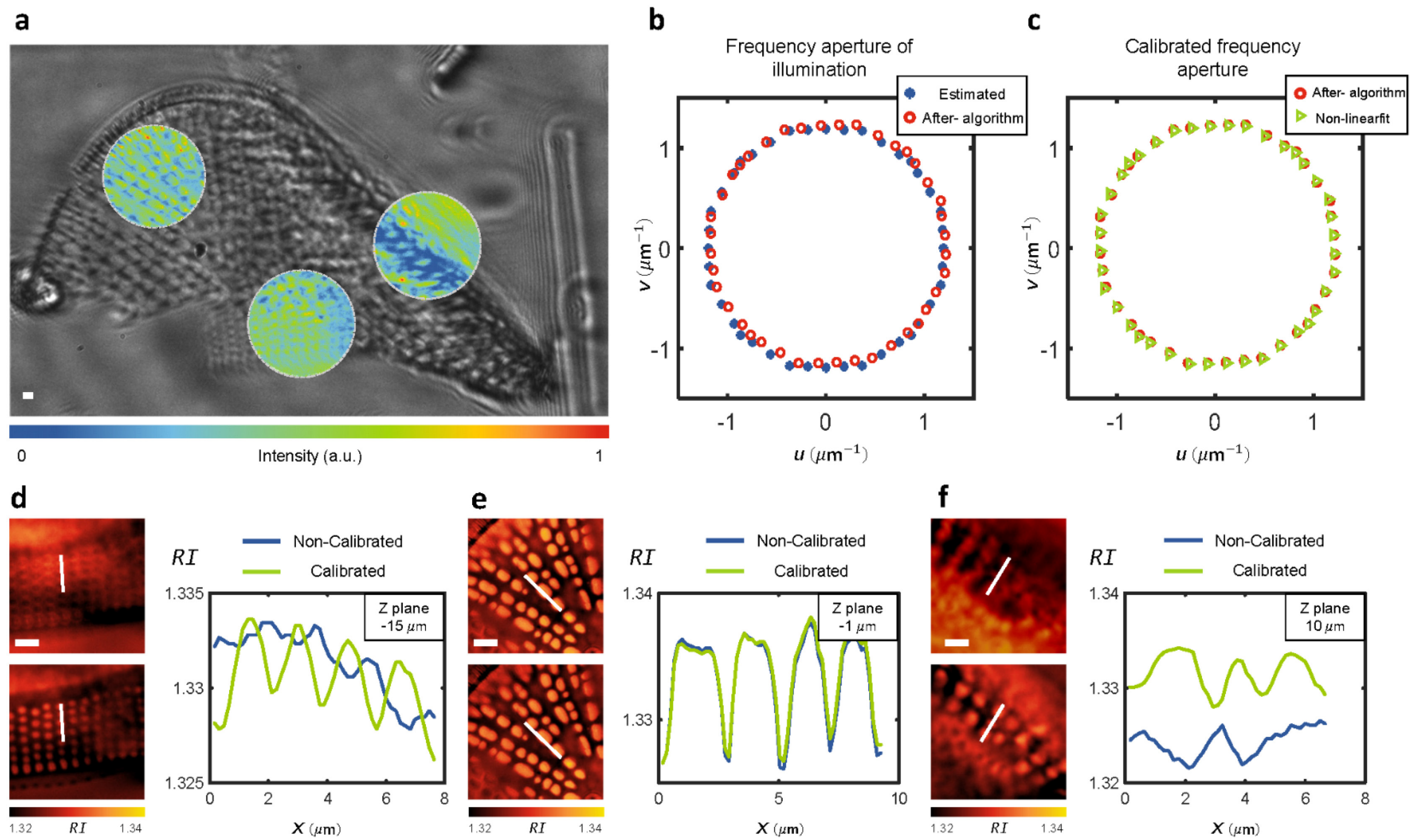

3D Reconstruction results

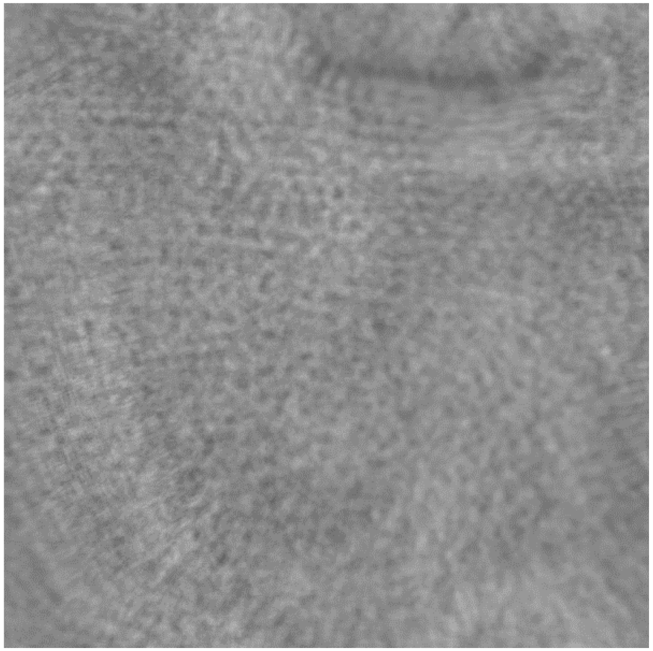

Diatom region1

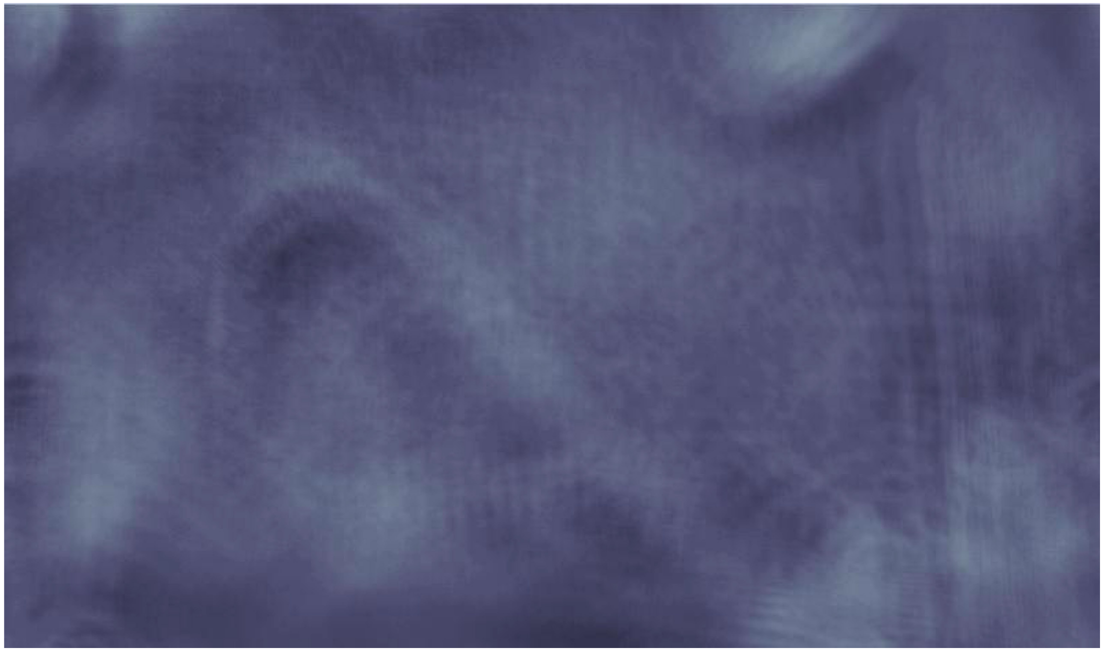

Diatom region2

RI tomography of Surirella spiralis

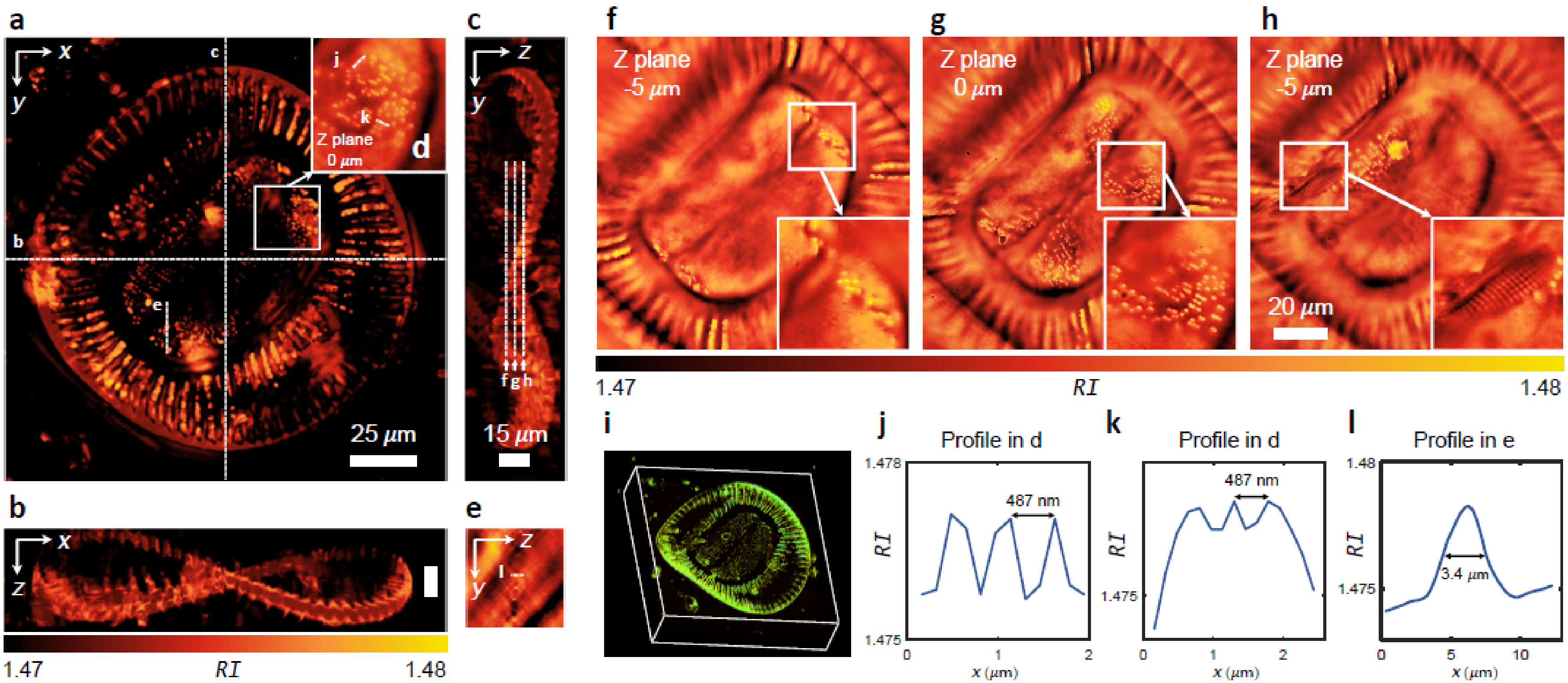

3D reconstruction of diatom

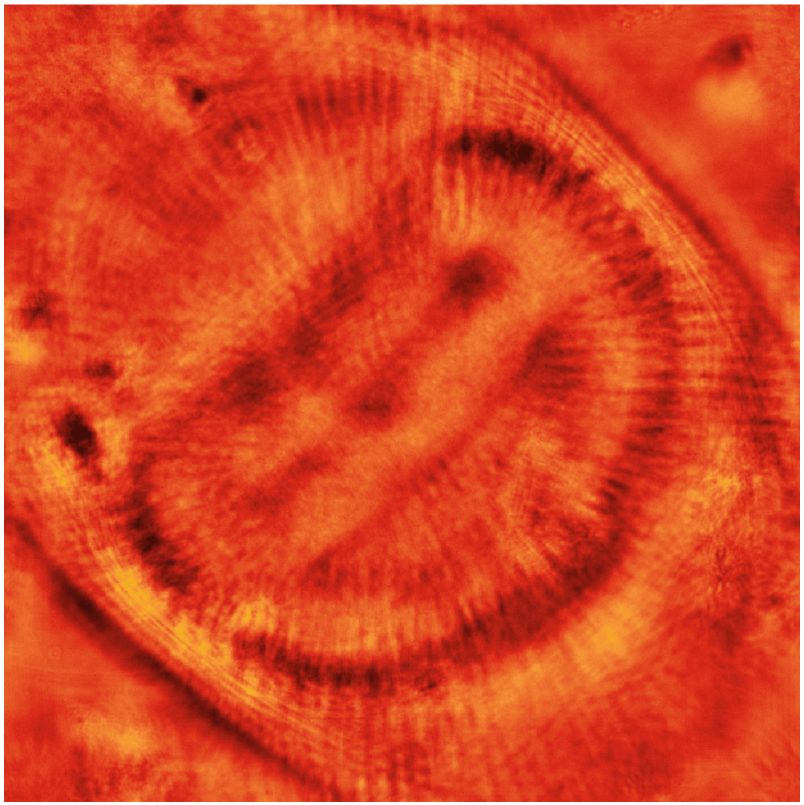

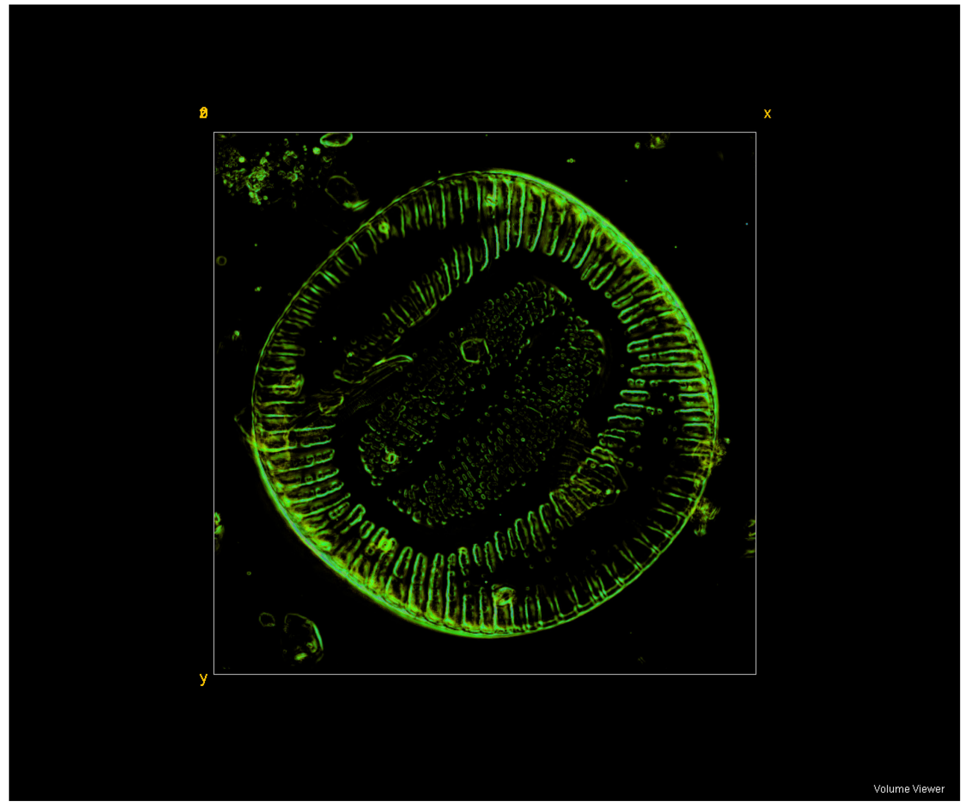

Fixed cheek cell

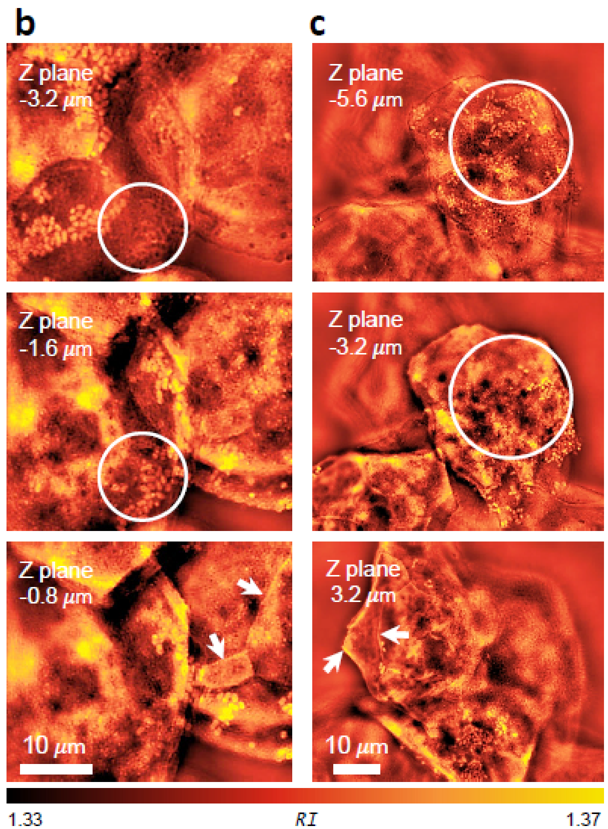

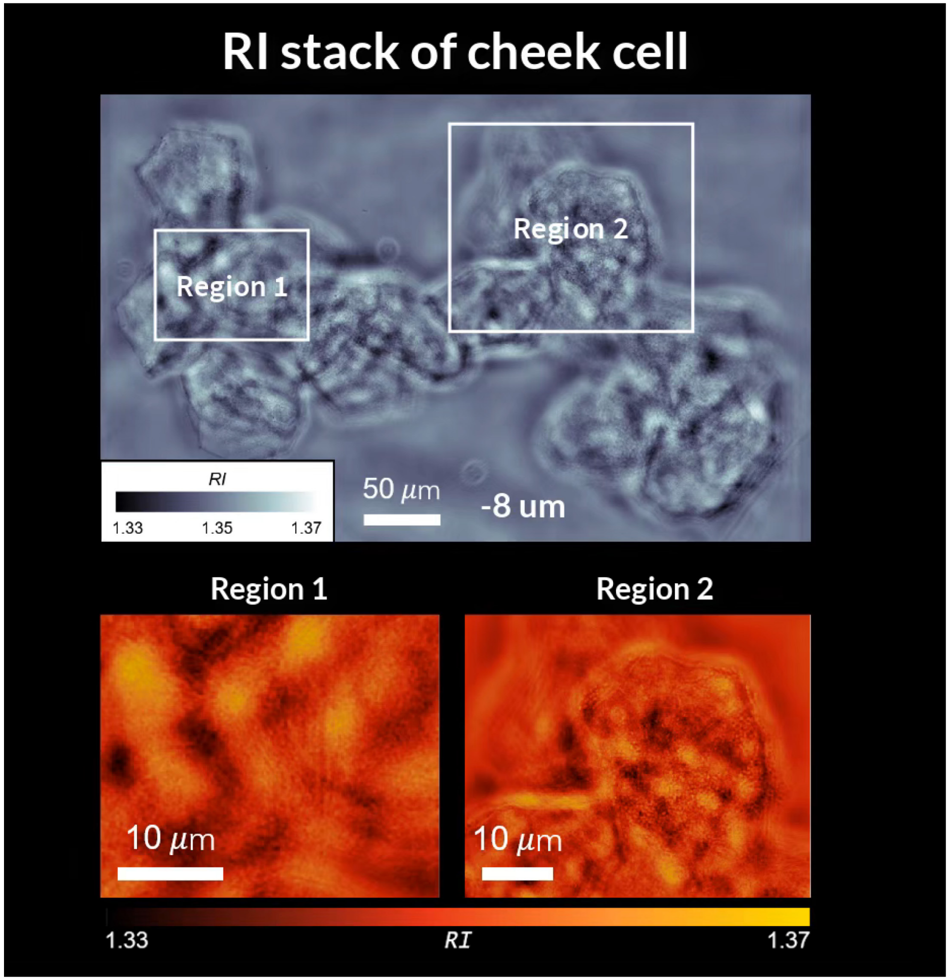

Fixed C. Elegant results

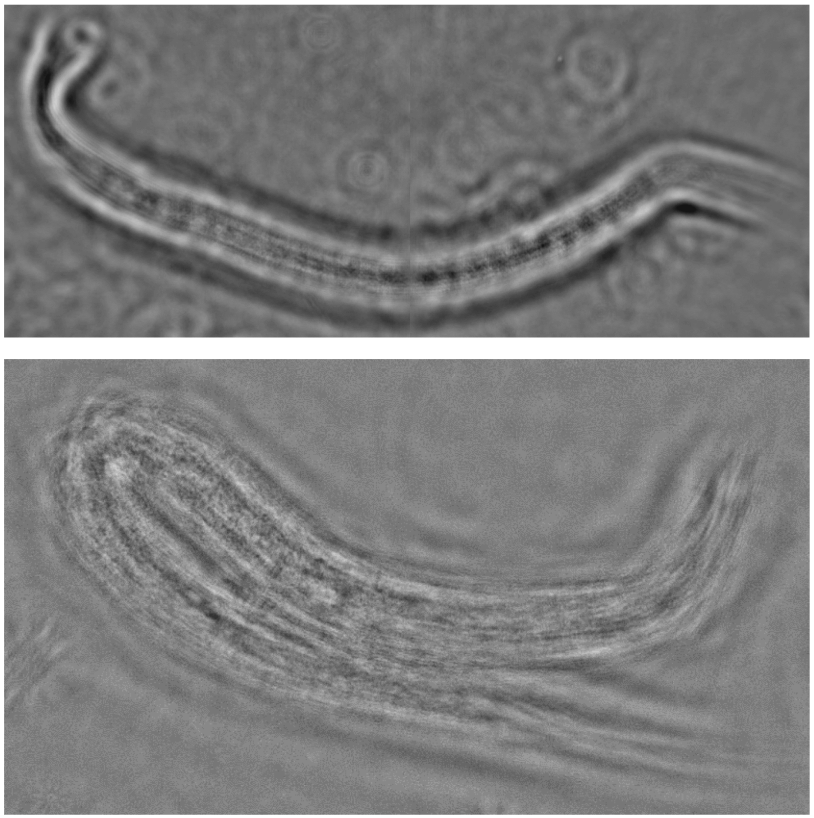

Refractive index stacks

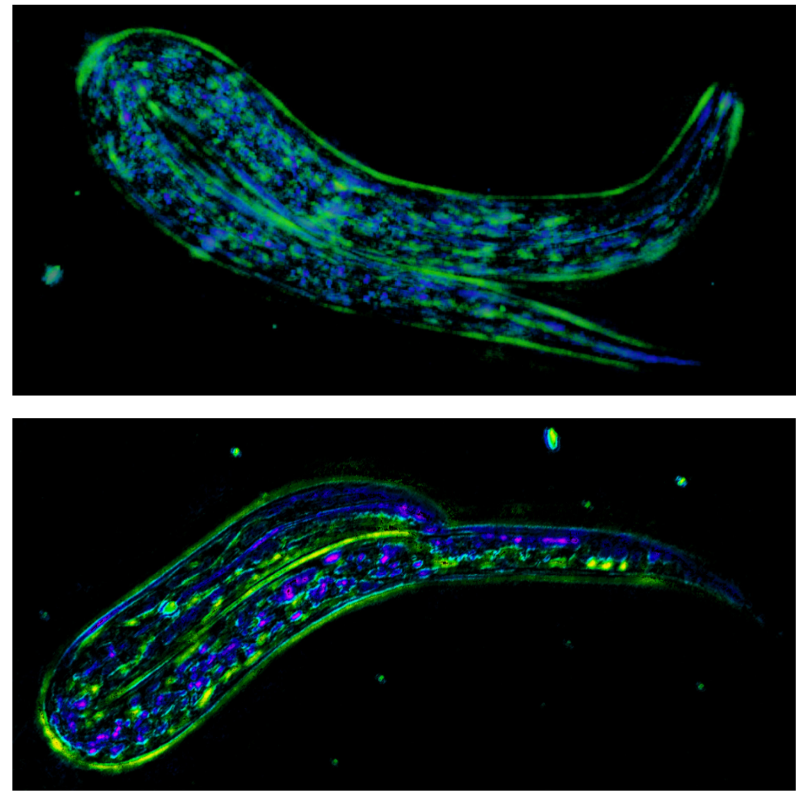

Depth color coding

Morphological analysis of C. elegans

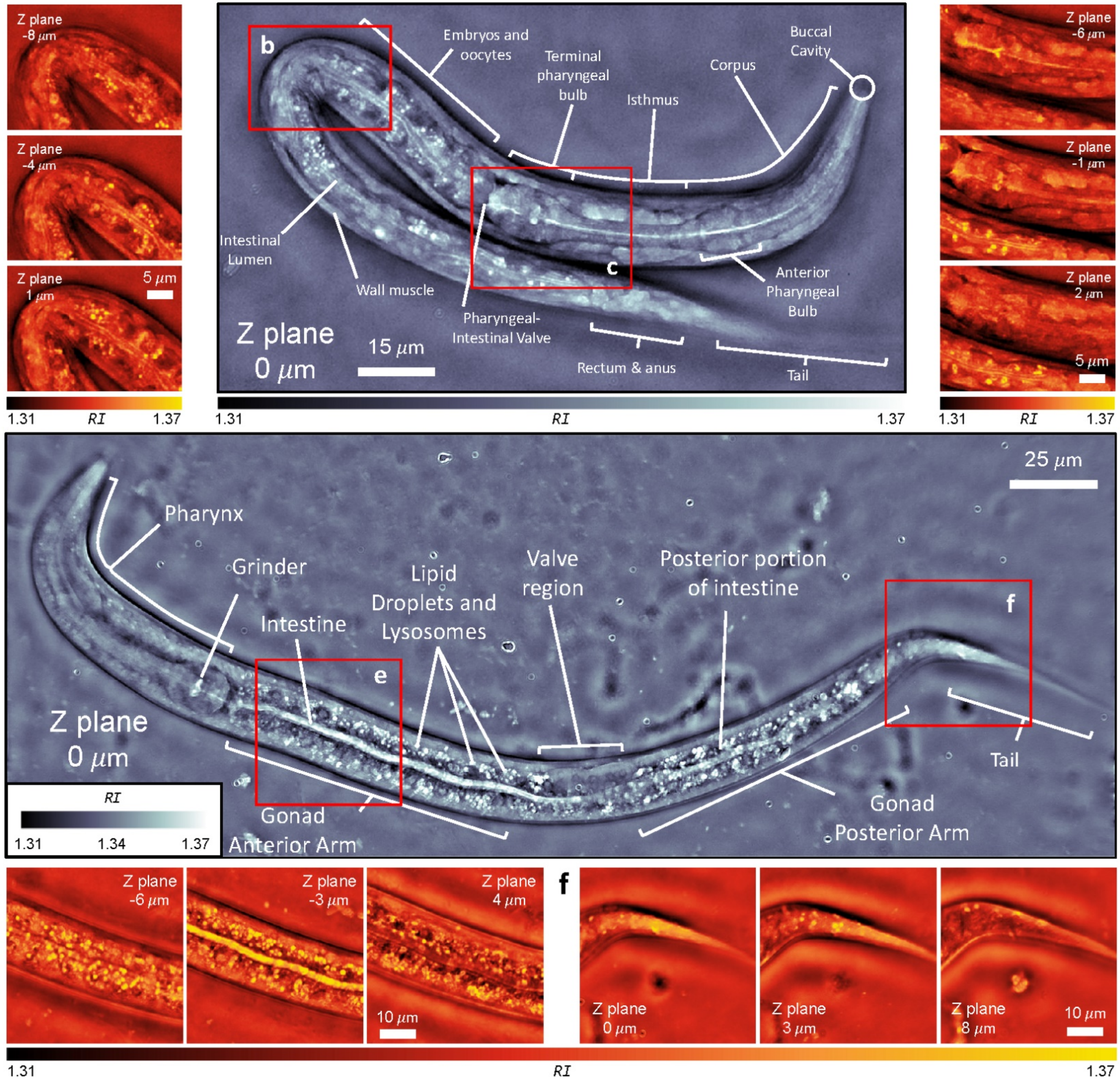

C. Elegans RI slice

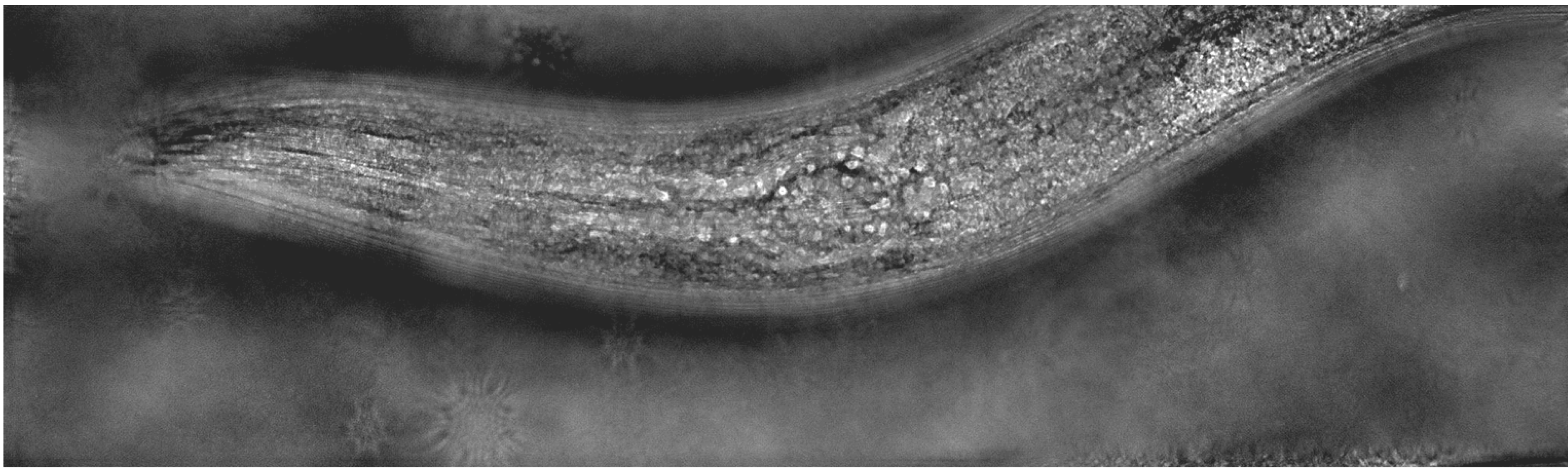

RI slice of sample at $t = 0$ sec

Depth color rendering of C. Elegans

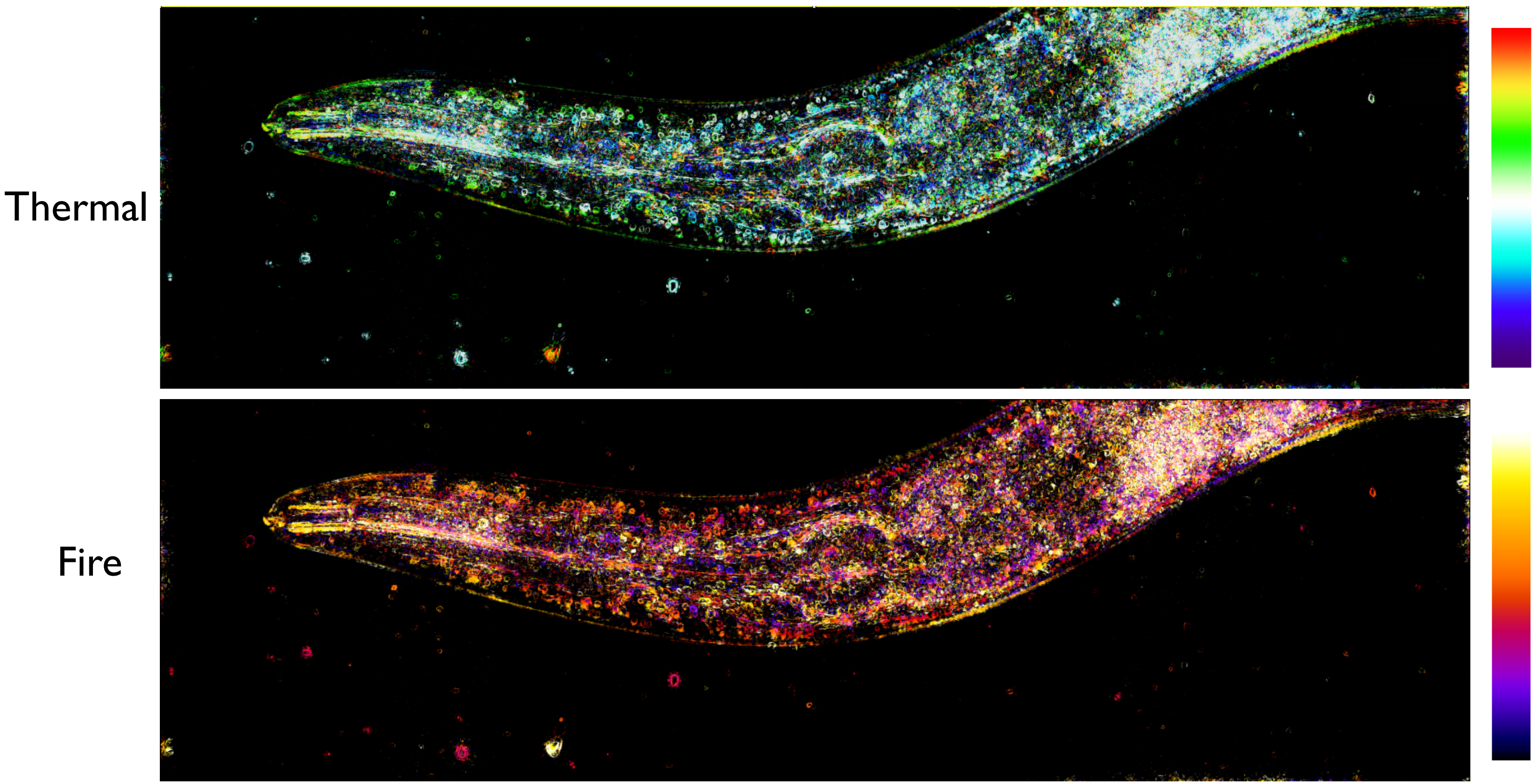

Time lapse results of *C. Elegans*

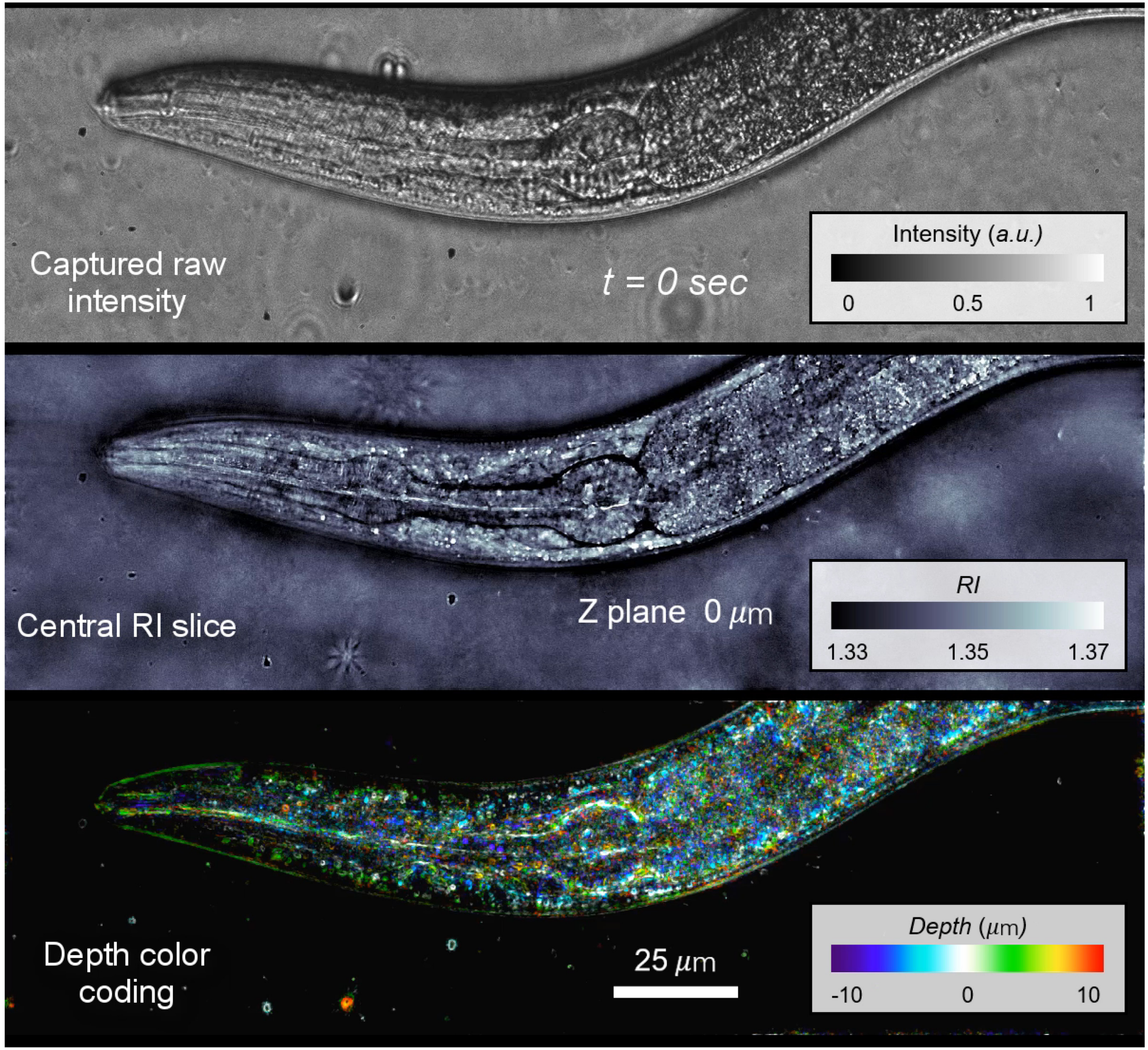

Transport of intensity equation

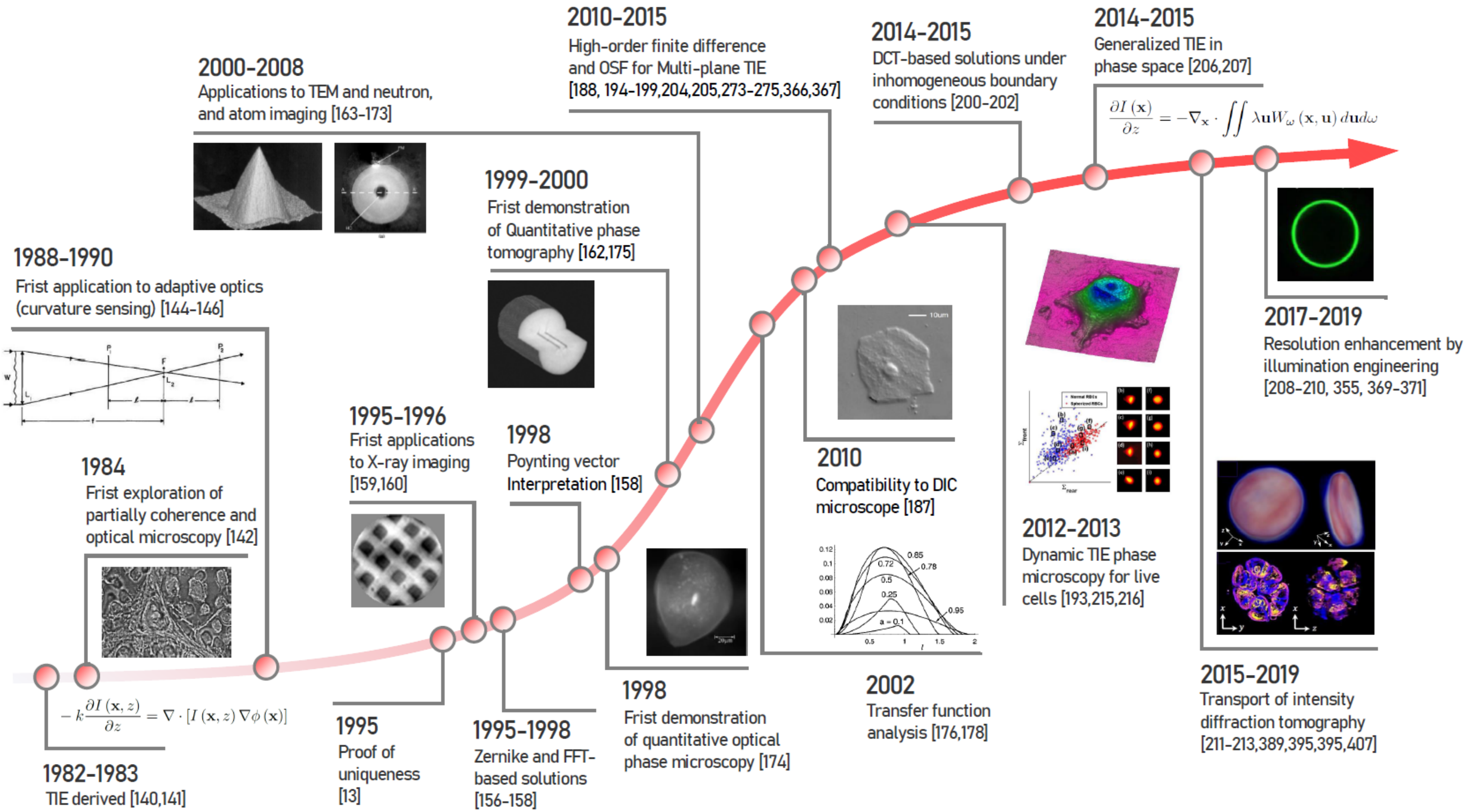

For further details, please refer to:

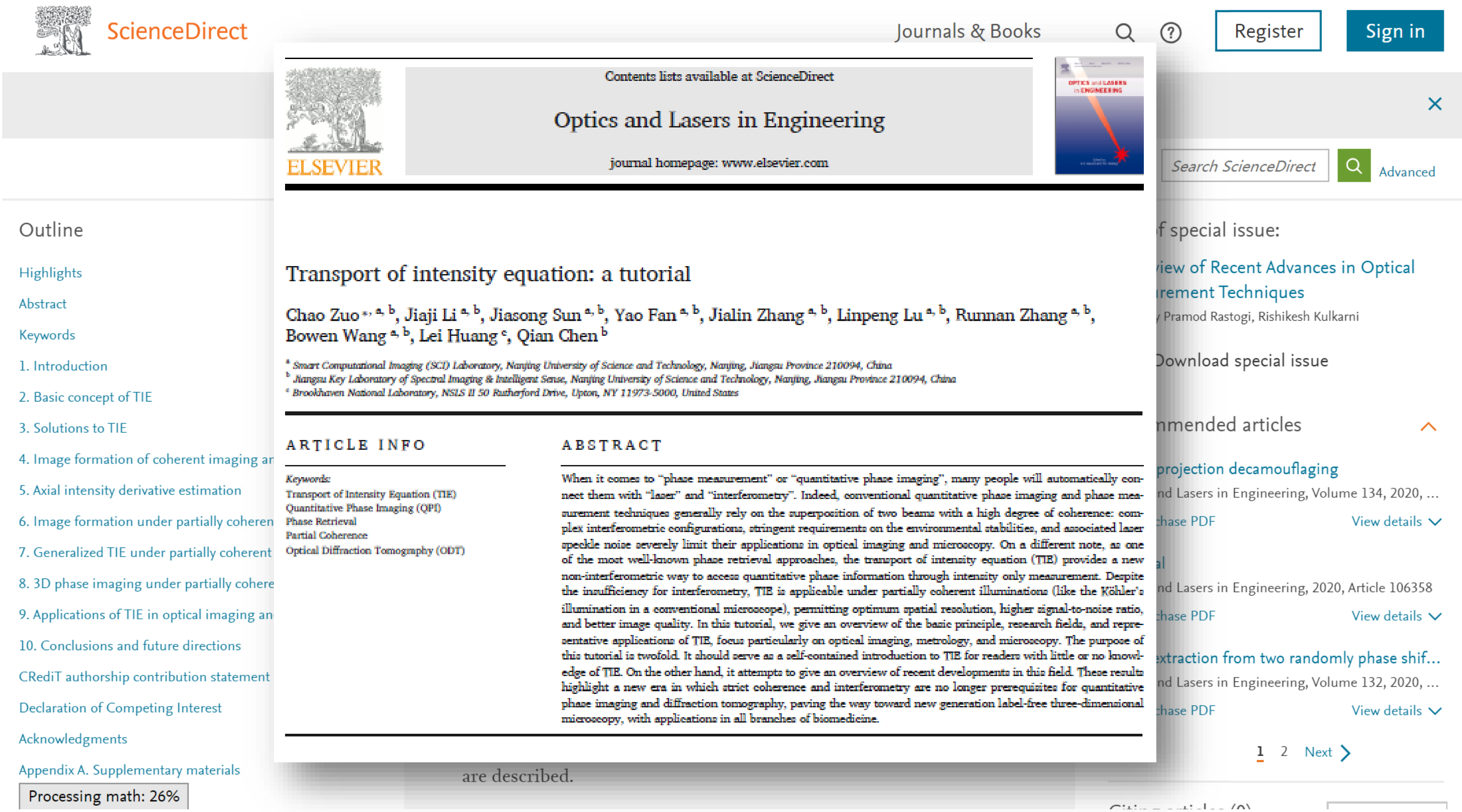

Contents lists available at ScienceDirect

Optics and Lasers in Engineering

journal homepage: www.elsevier.com

Transport of intensity equation: a tutorial

Chao Zuo[*, a, b], Jiaji Li[a, b], Jiasong Sun[a, b], Yao Fan[a, b], Jialin Zhang[a, b], Linpeng Lu[a, b], Runnan Zhang[a, b], Bowen Wang[a, b], Lei Huang[c], Qian Chen[b]

[a] Smart Computational Imaging (SCI) Laboratory, Nanjing University of Science and Technology, Nanjing, Jiangsu Province 210094, China
[b] Jiangsu Key Laboratory of Spectral Imaging & Intelligent Sense, Nanjing University of Science and Technology, Nanjing, Jiangsu Province 210094, China
[c] Brookhaven National Laboratory, NSLS II 50 Rutherford Drive, Upton, NY 11973-5000, United States

ARTICLE INFO

Keywords:
Transport of Intensity Equation (TIE)
Quantitative Phase Imaging (QPI)
Phase Retrieval
Partial Coherence
Optical Diffraction Tomography (ODT)

ABSTRACT

When it comes to "phase measurement" or "quantitative phase imaging", many people will automatically connect them with "laser" and "interferometry". Indeed, conventional quantitative phase imaging and phase measurement techniques generally rely on the superposition of two beams with a high degree of coherence: complex interferometric configurations, stringent requirements on the environmental stabilities, and associated laser speckle noise severely limit their applications in optical imaging and microscopy. On a different note, as one of the most well-known phase retrieval approaches, the transport of intensity equation (TIE) provides a new non-interferometric way to access quantitative phase information through intensity only measurement. Despite the insufficiency for interferometry, TIE is applicable under partially coherent illuminations (like the Köhler's illumination in a conventional microscope), permitting optimum spatial resolution, higher signal-to-noise ratio, and better image quality. In this tutorial, we give an overview of the basic principle, research fields, and representative applications of TIE, focus particularly on optical imaging, metrology, and microscopy. The purpose of this tutorial is twofold. It should serve as a self-contained introduction to TIE for readers with little or no knowledge of TIE. On the other hand, it attempts to give an overview of recent developments in this field. These results highlight a new era in which strict coherence and interferometry are no longer prerequisites for quantitative phase imaging and diffraction tomography, paving the way toward new generation label-free three-dimensional microscopy, with applications in all branches of biomedicine.

Transport of intensity equation: a tutorial

C Zuo, J Li, J Sun, Y Fan, J Zhang, L Lu, R Zhang, B Wang, L Huang, Q Chen

Optics and Lasers in Engineering, 106187, 2020

Computational imaging

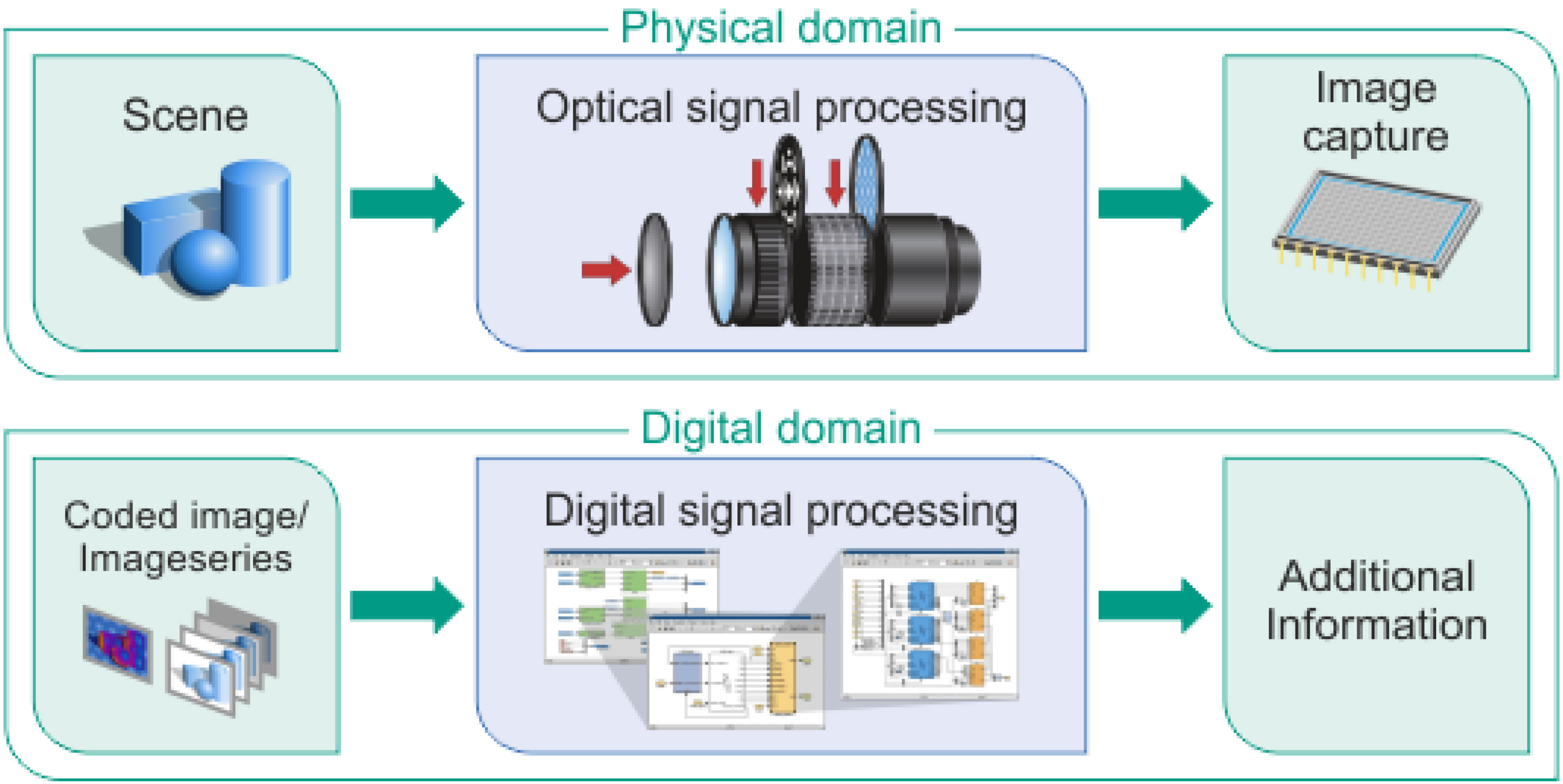

第 40 卷 第 1 期
2020 年 1 月
光 学 学 报
Acta Optica Sinica
Vol. 40, No. 1
January, 2020

·特邀综述·

深度学习下的计算成像:现状、挑战与未来

左超[1,2], 冯世杰[1,2], 张翔宇[1,2], 韩静[2], 陈钱[2]*
[1]南京理工大学电子工程与光电技术学院,智能计算成像实验室(SCILab), 江苏 南京 210094;
[2]南京理工大学江苏省光谱成像与智能感知重点实验室, 江苏 南京 210094

摘要 近年来,光学成像技术已经由传统的强度、彩色成像发展进入计算光学成像时代。计算光学成像基于几何光学、波动光学等理论对场景目标经光学系统成像再到探测器采样这一完整图像生成过程建立精确的正向数学模型,再求解该正向成像模型所对应的“逆问题”,以计算重构的方式来获得场景目标的高质量图像或者传统技术无法直接获得的相位、光谱、偏振、光场、相干度、折射率、三维形貌等高维度物理信息。然而,计算成像系统的实际成像性能也同样极大程度地受限于“正向数学模型的准确性”以及“逆向重构算法的可靠性”,实际成像物理过程的不可预见性与高维病态逆问题求解的复杂性已成为这一领域进一步发展的瓶颈问题。近年来,人工智能与深度学习技术的飞跃式发展为计算光学成像技术开启了一扇全新的大门。不同于传统计算成像方法所依赖的物理驱动,深度学习下的计算成像是一类由数据驱动的方法,它不但解决了许多过去计算成像领域难以解决的难题,还在信息获取能力、成像的功能、核心性能指标(如成像空间分辨率、时间分辨率、灵敏度等)上都获得了显著提升。基于此,首先概括性介绍深度学习技术在计算光学成像领域的研究进展与最新成果,然后分析了当前深度学习技术在计算光学成像领域面临的主要问题与挑战,最后展望了该领域未来的发展方向与可能的研究方向。

关键词 成像系统; 计算成像; 深度学习; 光学成像; 光信息处理
中图分类号 O436　　**文献标志码** A　　**doi**: 10.3788/AOS202040.0111003

Computational imaging

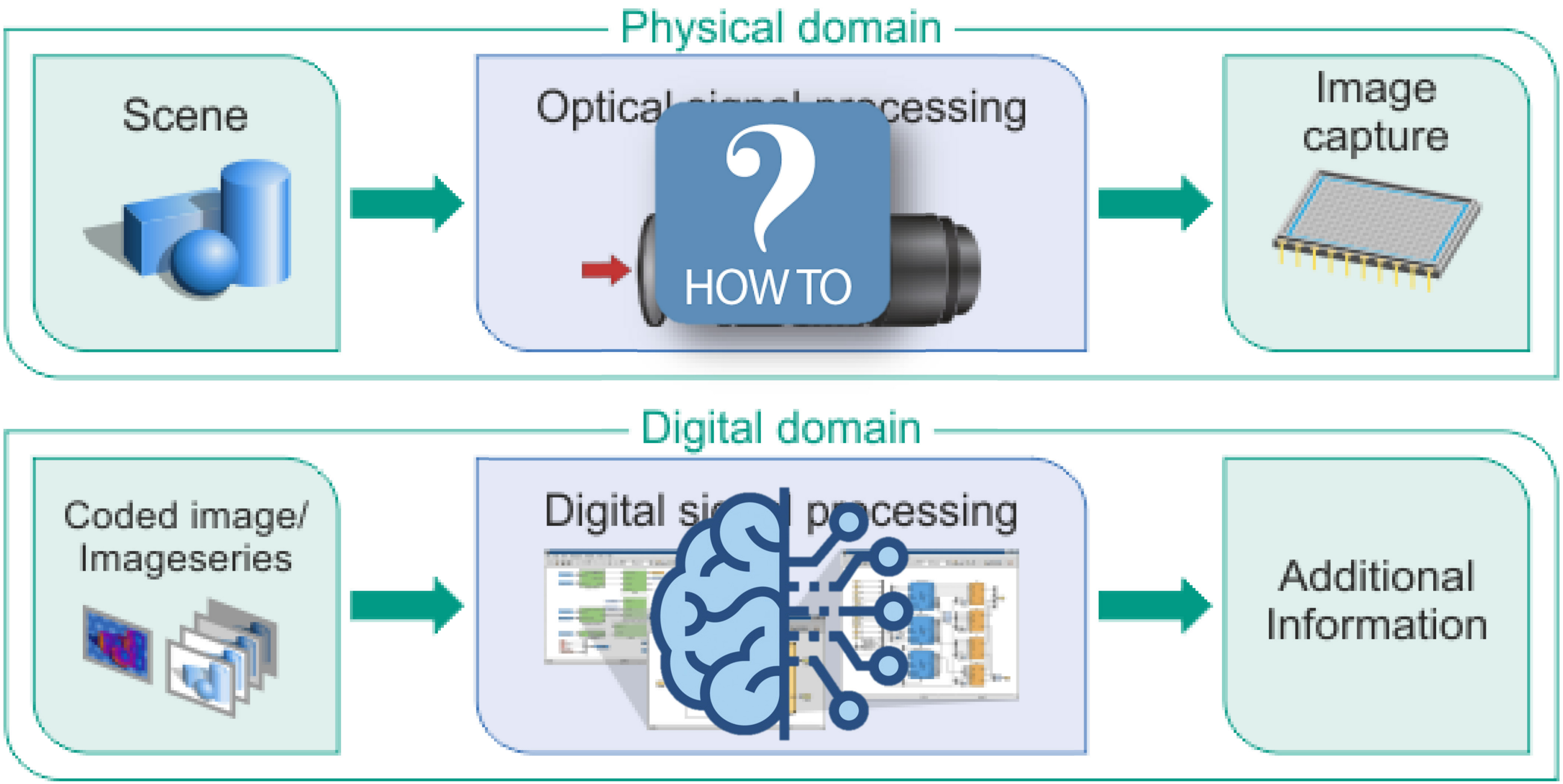

出国留学情况简介

- PostDoc@SCILab 智能计算成像实验室
- 2018-2019国家留学基金委（CSC）资助
- 为期12个月
- 美国波士顿大学（Boston University，BU）
- 电子工程学院-计算成像系统实验室（CISL）

美国 马萨诸塞州

维多利亚
Victoria
西雅图
Seattle
华盛顿
波特兰
Portland
蒙大纳
北达科他州
明尼苏达州
明尼阿波利斯
Minneapolis
威斯康星
魁北克市
Québec
渥太华
Ottawa
蒙特利尔
Montréal
佛蒙特州
新罕布什尔州
麻萨诸塞州
康涅狄格
纽约州
多伦多
Toronto
密歇根州
底特律
Detroit
芝加哥
Chicago
爱荷华
南达科他州
俄勒冈州
爱达荷州
怀俄明州
内布拉斯加州
宾夕法尼亚州
新泽西州
马里兰州
特拉华
华盛顿
Washington
伊利诺伊州
印第安纳州
印第安纳波利斯
Indianapolis
俄亥俄州
西弗吉尼亚州
弗吉尼亚州
肯塔基州
丹佛
Denver
美国
内华达
犹他州
科罗拉多州
堪萨斯城
Kansas City
堪萨斯
密苏里州
旧金山
San Francisco
圣荷西
San Jose
加利福尼亚州
拉斯维加斯
Las Vegas
纳什维尔
Nashville
田纳西州
夏洛特
Charlotte
北卡罗来纳州
俄克拉何马
阿肯色州
洛杉矶
Los Angeles
亚利桑那州
新墨西哥州
菲尼克斯
Phoenix
圣地亚哥
San Diego
图森
Tucson
埃尔帕索
El Paso
达拉斯
Dallas
密西西比州
亚拉巴马州
亚特兰大
Atlanta
南卡罗来纳州
乔治亚州
德克萨斯州
下加利福尼亚
索诺拉
奇瓦瓦
奥斯汀
Austin
休斯敦
Houston
路易斯安那州
新奥尔良
New Orleans
杰克逊维尔
Jacksonville
圣安东尼奥
San Antonio
科阿韦拉
奥蘭多
Orlando
坦帕
Tampa
佛罗里达

波士顿大学

哈佛大学
Harvard University
麻省理工大学
Massachusetts Institute of Technology
波士顿大学
Boston University
SOMERVILLE
PROSPECT HILL
剑桥
Cambridge
RIVERSIDE
哈佛商学院
Harvard Business School
摇滚天堂俱乐部
Paradise Rock Club
ALLSTON
OAK SQUARE
PACKARD'S CORNER
BRIGHTON
ST. ELIZABETH'S
波士顿学院
Boston College
栗树山
CHESTNUT HILL
布鲁克莱恩
Brookline
传教山
MISSION HILL
Fenway Park
Museum of Fine Arts, Boston
Isabella Stewart Gardner Museum
Harvard Medical School
SOUTH END
DUDLEY SQUARE
后湾
BACK BAY
Beehive
Boston Park Plaza
波士顿
Boston
The Paul Revere House
邦克山纪念碑
Bunker Hill Monument
CENTRAL-MAVERICK SQUARE / PARIS STREET
EAST BOSTON
公园
Piers Park Sailing Center
The Institute of Contemporary Art
波士顿会展中心
Boston Convention and Exhibition Center
Blue Hills Bank Pavilion
SOUTH BOSTON
COLUMBUS PARK / ANDREW SQUARE
乔-莫克利公园
Joe Moakley Park
国家公园
Castle Island
肯尼迪总统图书馆暨博物馆
John F. Kennedy
The Country Club
Massachusetts Turnpike
Soldiers Field Rd
Tremont St
Columbus Ave

Welcome to Computational Imaging Systems Lab at Boston University!

What's new →

[Benjamin Wong wins UROP award](#)
September 27, 2019

[Joe, Hao, and Jiabei join CISL for PhD, Welcome!](#)
August 30, 2019

[Joe defended MS thesis](#)
August 16, 2019

[Yunzhe presents at SPIE Defense + Commercial Sensing Congress](#)
April 25, 2019

[Alex, Waleed present at OSA Biophotonics Congress](#)
April 24, 2019

Boston生活照片

第一次踏上踏上美利坚
的土地，内心充满着对
未知的恐慌，也充满了
对未来的期待

无处不在的名校印记


Tang Hall
Massachusetts
Institute of
Technology


VE RI
TAS
VE RI
TAS

身体是革命
的本钱


BU
AMERICA EAST
CHAMPIONS
AMERICAN
ARMY
BUCKNELL
COLGATE
HOLY CROSS
LAFAYETTE
LEHIGH
LOYOLA
NAVY
BOSTON
BU
AMERICA EAST
CHAMPIONS
UMASS

秋风扫落叶

Boston
雪景

春天来了

夏天
到了

SCI Lab@ NJUST

- **Qian Chen(Advisor)**
- **Chao Zuo**

CISL @ Boston University

- **Lei Tian (Advisor)**

Funding

BOSTON UNIVERSITY

Thank you

zuochao@njust.edu.cn